Geometric models and applications to material media with defects

van Hoi Nguyen

UNIVERSITÉ DE RENNES 1

THESE DE DOCTORAT DE

L'UNIVERSITE DE RENNES 1

ECOLE DOCTORALE N° 601
Mathématiques et Sciences et Technologies de l'Information et de la Communication
Spécialité : *Mathématiques et leurs interactions*

Par
Van Hoi NGUYEN

Geometric models and applications to material media with defects

Thèse présentée et soutenue à Université de Rennes 1, le 14 décembre 2021
Unité de recherche : IRMAR, UMR CNRS 6625 Institut de Recherche Mathématique de Rennes
Thèse N° :

Rapporteurs avant soutenance :

Patrizio NEFF	Professeur, Université de Duisburg-Essen
Vladimir SALNIKOV	Chercheur CNRS LASIE, La Rochelle

Composition du Jury :
Attention, en cas d'absence d'un des membres du Jury le jour de la soutenance, la composition du jury doit être revue pour s'assurer qu'elle est conforme et devra être répercutée sur la couverture de thèse

Président:	Emmanuelle ROUHAUD	Professeur, Université de technologie de Troyes
Examinateurs	Lalaonirina R. RAKOTOMANANA	Professeur IRMAR, Université de Rennes 1
	Emmanuelle ROUHAUD	Professeur, Université de technologie de Troyes
	Boris KOLEV	Directeur de Recherche CNRS, LMT ENS Paris Saclay
	Nicolas AUFFRAY	Maître de conférences MSME, Université Gustave Eiffel
	Patrick VEROVIC	Maître de conférences LAMA, Université de Chambéry
	Patrizio NEFF	Professeur, Université de Duisburg-Essen
	Vladimir SALNIKOV	Chercheur CNRS LASIE, La Rochelle
Dir. de thèse	Loïc LE MARREC	Maître de conférences IRMAR, Université de Rennes 1

UNIVERSITÉ DE RENNES 1

DOCTORAL THESIS

Geometric models and applications to material media with defects

---

Tuesday 14th December 2021

"As far as the laws of mathematics refer to reality, they are not certain;
and as far as they are certain, they do not refer to reality."

Albert Einstein (1879–1955)

Acknowledgements

No words can express my sincere wishes and thanks to those who directly or indirectly support and encourage me to complete this thesis successfully. They all deserve my gratitude and appreciation.

I wish to express my gratitude most strongly to my supervisors, Professor Loïc LE MARREC and Professor Guy CASALE, for guiding me here to do the work I love and have unforgettable memories. They have taught me the methodology to do the research and present it professionally and understandably. Principally, they provided invaluable guidance, encouraged me during the darkest moments throughout this research, and shared their exciting moments with their great sense of humour. It was a great privilege and honour to work and study under their guidance.

It is an occasion to express my gratitude to Professor DUONG Minh Duc, who helped me become more confident in pursuing my dreams. Through his teaching method, most problems have become naturally simple, coherent and concise. I learnt a lot from him, not only the methodology but also the humility and sympathy. I am incredibly grateful for what he has offered me.

I greatly appreciate Professor Patrizio NEFF and Professor Vladimir SALNIKOV - the reviewers of the thesis, who have been so kindly spend time to read my thesis. Their comments and remarks are helpful to improve the manuscript. It is my pleasure to thank Professor Lalaonorina R.RAKOTOMANANA, Professor Emmanuelle ROUHAUD, Professor Boris KOLEV, Professor Patrick VEROVIC and Professor Nicolas AUFFRAY, who accepted to be on my thesis committee.

I would like to acknowledge the Institute of Mathematical Researcher of Rennes (IRMAR) and Center Henri Lebesgue (CHL) and the staff therein. A special thank goes to Xhenxila Lachambre, Marie-Aude Verger and Chantal Halet for all their administrative supports to complete this thesis successfully. By the way, my sincere thanks to the French-Vietnam Master in Applied Mathematics Program for being a bridge for "us" to studying and researching in France.

My sincere thanks go to Professor Lalaonorina R.RAKOTOMANANA, who has always been interested in our research, for his careful and thoughtful comments. I also want to thank Professor Ilya M. PESHKOV. His kindness has left me with unforgettable memories. Thanks to my colleagues Nguyen Dinh Duong and Marwan Hariz, who share the experience of PhD life with me. A special mention goes to the Vietnamese community in France. Thank all of you for your caring, sharing Vietnamese foods with me and especially our friendship. A special thanks go to Nguyen Thi Minh Phuong, who is always willing to help everyone.

Last but not least, I wish to give all my heart to my family, particularly my parents for their love and sacrifices for my future. I am very much thankful for my passion, "Minh Chau" and my lovely cat "Happy/Pi", who stand by and constantly encourage me during the darkest moments. The thesis is dedicated to my Dad and Mom.

Nguyen Van Hoi, Rennes, France (December 2021)

Contents

To my parents
Nguyen Mui et Do Thi Chau

Résumé

Cette thèse porte sur un modèle géométrique de transformations mécaniques de milieux matériels possédant une micro-structure.
Ce type de matériaux est courant dans la nature. La modélisation du comportement de ces milieux est un vaste sujet qui englobe l'homogénéisation, les théories de milieux effectifs, ou encore les théories multi-échelles. Ces approches sont souvent efficaces en petites déformations mais des difficultés géométriques apparaissent pour des grandes déformations.
Une alternative consiste à interpréter le milieu continu comme une variété, dite matérielle, $\mathscr{M}$ fibrée sur une variété, dite spatiale, $\mathscr{B}$. Cette dernière est plongée dans l'espace ambiant euclidien. Dans ce cas, le type de variété illustre certaines caractéristiques du matériau. En mécanique des milieux continus, les variétés spatiales permettent de modéliser le comportement macroscopique de domaines matériels ; ici sa configuration est modélisée à travers le choix d'une connexion et d'une métrique sur la variété matérielle $\mathscr{M}$.
Nous ne considérons dans cette thèse que des défauts de type mécanique, c'est-à-dire provenant d'incohérence dans les placements et orientations des micro-éléments. Ce placement induit sur la variété matérielle une connexion et une métrique tirées en arrière des connexion et métrique de l'espace euclidien. Les défauts sont alors mesurés à travers la torsion, la courbure et la non-métricité de la connexion. Le choix de la cinématique du plongement est donc un élément crucial pour la construction du modèle.
Dans ce texte plusieurs types de plongements seront abordés et chaque fois la variété matérielle induite sera étudiée et comparée aux modèles classiques ou plus modernes de la littérature. Il s'avère que si l'on considère le plongement d'une variété spatiale et de son espace tangent, la variété induite possède des caractéristiques d'une variété de Riemann-Cartan déjà exploitées pour l'étude des matériaux à défauts cristallins ou à dislocations. La connexion n'a pas de courbure mais possède une torsion qui s'interprète comme une densité de dislocations.

Une des contributions principales de cette thèse est d'introduire une nouvelle approche des transformations de matériaux micro-structurés. Les transformations sont définies sur l'espace tangent à la variété matérielle $T\mathscr{M}$. On construit ainsi une connexion et une métrique obtenues par tiré-en-arrière. Cette construction permet une grande liberté dans la description de la structure induite. Elle permet naturellement de distinguer les notions de connexion et de métrique à diverses échelles. Cela confère au modèle la possibilité d'avoir une interprétation physique des résultats.
La variété ainsi construite possède des propriétés très riches car elle possède une connexion munie de torsion et de courbure et la métrique n'est plus forcément compatible avec la connexion. L'ensemble de ces propriétés qui se distinguent d'une variété de Riemann classique permet de modéliser une large classe de défauts de microstructures. Les applications en mécanique des milieux continus sont larges : de la mécaniques des fluides à l'écrouissage en passant par la plasticité ; mais ces thèmes ne seront pas abordés dans cette thèse.

La seconde contribution majeure consiste en le choix de ce morphisme de fibré. Il est en effet obtenu en n'introduisant qu'une nouvelle quantité scalaire (un facteur d'échelle). Les autres

ingrédients (ou degrés de libertés du modèle) utilisés sont associés à la cinématique du micro-élément et existent de longue date dans d'autres modèles. On dispose donc d'une modélisation contrôlable par un nombre réduit de variables indépendantes ce qui permet une discussion exhaustive et rigoureuse. En particulier la notion de facteur d'échelle est relativement explicite à la lecture des résultats.

La troisième contribution de cette thèse est relative à la mise en pratique de ces modèles à travers des simulations numériques. Ces simulations permettent d'illustrer les propriétés microscopiques et macroscopiques du matériau après transformation. Les effets de ces connexions sont illustrés en simulant numériquement le transport parallèle de directeurs le long d'un chemin de longueur finie. Cela a permis d'interpréter macroscopiquement des phénomènes qui sont souvent illustrés sur des lacets infinitésimaux. Dans le cadre d'une modélisation multi-échelle, ces lacets infinitésimaux ne fournissent en effet qu'une information partielle (car ils sont relatifs par construction à des interprétations microscopiques). Afin d'élargir et de compléter ce type d'interprétation d'autres transports ont été élaborés afin de fournir des outils originaux aux mécaniciens : transport par roulement sans glissement, transport le long d'un circuit de Burger de dimension finie. L'ensemble de ces simulations permet une analyse exhaustive des propriétés du modèle sur des variables scalaires ou vectorielles, dont le support peut être macroscopique ou microscopique.

Ce texte est composé de cinq chapitres. Le premier chapitre décrit les types de défauts étudiés dans cette thèse et présente rapidement les différentes approches mises en place dans la littérature pour modéliser mathématiquement la présence de ces types de défauts dans un matériau. La plupart des travaux précédents utilisent des transformations multi-valuées ce qui crée des difficultés tant théoriques que lors de la mise en place d'une analyse numérique. Ces points faibles sont la motivation de ce travail visant à une description de ces phénomènes en utilisant des transformations uni-valuées.
Dans le second chapitre, nous examinons les matériaux soumis à des transformations du type:

$$\Upsilon \ : \ T\mathscr{B} \to T\mathbb{E}^3, \qquad (X, V) \mapsto (\phi(X), \Psi(X)V). \tag{0.0.1}$$

En général ces transformations vérifient $\Psi \neq D\phi$, ce qui correspond à une incompatibilité des placements des particules macroscopiques avec les placements des particules microscopiques créant des défauts dans le matériaux. Ce type de transformation permet une reformulation de la description donnée par Eringen des micro et macro-déformations en théorie micromorphique (ERINGEN, 1999). Le pull-back de la connexion de Levi-Civita et de la métrique euclidienne par Υ font de $\mathscr{B}$ une variété de Riemann-Cartan d'un type spécial appelé variété de Weitzenböck : la connexion n'a pas de courbure, est compatible à la métrique, seule la présence de torsion témoigne de la présence de défauts.
Dans le chapitre 4, nous présentons les concepts de variétés fibrés, de connexions de Ehresmann, de formes de soudure et de métriques de Sasaki ainsi que les notions de torsions et courbures généralisées pour ces objets. Nous traitons plus particulièrement le cas de microstructures linéaires "canoniques" : la macro-particule en $p \in \mathscr{B}$ est interprétée comme une portion microscopique de

matériau et modélisé mathématiquement par l'espace tangent $T_p\mathscr{B}$.
Le chapitre 5 se restreint au cas de microstructure linéaire canonique : $\mathscr{M}$ est $T\mathscr{B}$ et la forme de soudure est l'application identité. Dans un premier temps, nous autorisons notre matériau à subir des transformations non-linéaires à l'échelle microscopique, c'est-à-dire représentées par :

$$\Upsilon \ : \ T\mathscr{B} \to T\mathbb{E}^3 \qquad (X,Y) \mapsto (\phi(X), \Psi(X,Y)). \tag{0.0.2}$$

La connexion obtenue par tiré-en-arrière n'est plus linéaire et la métrique est remplacée par une métrique de Sasaki. Malheureusement ce type de transformation ne permettent pas de construire une connexion avec de la courbure. Afin de généraliser le raisonnement, l'idée a été d'introduire un modèle de matériaux dits "dimensionné" considérant que la matrice jacobienne de la transformation macroscopique $F = D\phi$ définie la déformation (transformation linéaire tangeante) d'un macro-élément dV alors que Ψ contrôle la déformation d'un micro-élément δV à une sous échelle. Le type de transformation considérée est alors le suivant.
Considérons un vecteur Y dans $T_X\mathscr{B}$ et un vecteur Z à l'échelle microscopique, c'est-à-dire dans $VT_X\mathscr{B}$, nos transformations sont données par

$$\Upsilon^v : VT\mathscr{B} \to VT\mathbb{E}^3, \quad (X,Y,Z) \mapsto (\phi(X), F(X)Y, \Theta(X)Z), \tag{0.0.3}$$

avec $\det F = D\phi > 0$ et $\det \Theta > 0$. Nous construisons une connexion de Ehresmann induite par une telle transformation en étendant Υ^v à l'espace total du double tangent i.e., en considérant Υ: $TT\mathscr{B} \to TT\mathbb{E}^3$ tel que

$$\Upsilon(X,Y,Z) = \Upsilon^v(X,Y,Z) \qquad \forall\, (X,Y,Z) \in VT\mathscr{B}. \tag{0.0.4}$$

A priori, la forme de $\Upsilon : TT\mathscr{B} \to TT\mathbb{E}^3$ est

$$(X,Y,Z) \mapsto (\phi(X), F(X)Y, \Omega(X,Y)Z),$$

avec $X \in \mathscr{B}$, $Y \in T_X\mathscr{B}$, $Z \in T_{(X,Y)}T\mathscr{B}$. Par analogie avec la formule du gradient total d'une application $T\mathscr{B} \to T\mathbb{E}^3$, $(X,Y) \mapsto (\phi(X), \Psi(X,Y))$, nous posons Ω de la forme suivante :

$$\Omega = F^a_A \partial_a \otimes dX^A + \Omega^i_A \partial_i \otimes dX^A + \Theta^i_J \partial_i \otimes dY^J, \tag{0.0.5}$$

où le choix de Ω^i_A est a priori libre mais doit être spécifié pour définir totalement Υ. Dans ce travail nous introduisons un facteur d'échelle ζ et posons

$$\Omega^i_A(X,Y) = \Big((1-\zeta)\partial_A F^i_I + \zeta \partial_A \Theta^i_I \Big) Y^I$$

où $0 < \zeta \leq 1$ est un paramètre libre controllant les interactions d'échelles. Il peut être défini comme $\zeta = \ell/L$ où L and ℓ sont les échelles macroscopiques et microscopiques caractéristiques. Ce modèle "dimensionné" décrit donc la cinématique à deux échelles à travers les quantités F et Θ et deux métriques associées à chaque échelle sont obtenues: $\mathsf{G}^h_{AB} = F^a_A \mathsf{g}_{ab} F^b_B$ et $\mathsf{G}^v_{IJ} = \Theta^i_I \mathsf{g}_{ij} \Theta^j_J$

respectivement. Le facteur d'échelle n'intervient pas à ce niveau mais à travers la connexion:

$$\Gamma^I_{AJ} = \Theta^I_i \Big((1-\zeta)\partial_A F^i_J + \zeta \partial_A \Theta^i_J \Big) \,. \tag{0.0.6}$$

et donc les tenseurs associés de torsion, courbure et non-métricité.
Cette dichotomie est illustrée par de nombreux exemples numériques. Ainsi dans la Figure 1 une illustration relativement standard est fournie. Cette illustration est obtenue en imposant un

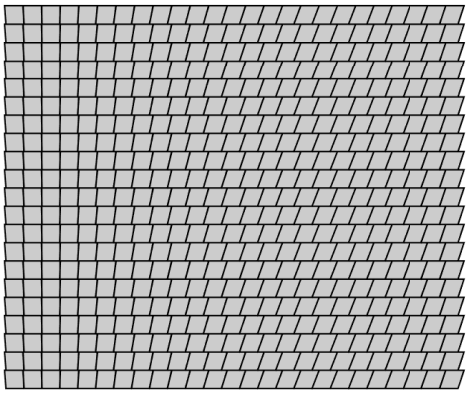

FIGURE 1: Plongement dans l'espace ambiant de la variété matérielle. Ici la déformation macroscopique est nulle mais les micro-éléments ont subi un glissement non-uniforme.

déplacement nul $F = I$ mais un glissement non-uniforme des micro-éléments. Dans le modèle proposé cette describtion cinématique ne préfigure pas de la présence ou non de défauts (à savoir ici de dislocation). En effet la connexion n'est pas complètement déterminée par ces déformations locales mais dépend également du facteur ζ qui *relie* le deux échelles. En fonction du paramètre ζ la transformation Υ induit (par tiré en arrière) sur la variété $\mathscr{M}$ une torsion nulle ou non-triviale. La présence de torsion ou courbure n'est révélée que par intégration. Sur une courbe fermée définie sur un domaine macroscopique, plusieurs procédés d'intégration permettent d'exhiber ces indicateurs. Que cela soit par roulement sans-glissement ou par transport parallèle, la présence de torsion ou courbure apparait par la non-fermeture de la quantité intégrée. Cette approche permet de généraliser la notion de circuit de Burger sur un domaine macroscopique sous la forme d'une courbe intégrale dans un domaine matériel munie de torsion ou courbure.

Le modèle proposé permet d'interpréter les transformations de matériaux micro-structurés en controllant le lien entre les phénomènes à deux échelles distinctes. Ce modèle est basé sur une formulation géométrique qui est particulièrement dédiée aux grandes transformations et aux simulations numériques. Les applications à des matériaux réels nécessitent cependant des travaux supplémentaires qui sont listés en conclusion.

Chapter 1

Introduction

"Write down all things we have and we want.
Observe the same and different factors, break down the problems and take the simplest step first.
It takes us further than we are."

DUONG Minh Duc (translated by NVH)

1.1 General introduction

A crystalline structure, in practice, always has a great number of defects. These may be chemical, electrical or structural involving foreign atoms. Most of physical properties of a medium, such as plasticity, melting, growth, etc., depend on crystalline structure defects. Accordingly, the study of defects becomes an essential research field. Comprehensive experimental and theoretical investigations of defects in crystals began in the 1930s ("Zur Theorie der Elastizitätsgrenze und der Festigkeit kristallinischer Körper"). It continues to be of interest until nowadays (Cordier et al., 2014). There are many different kinds of defects, that are classified depending on their space dimensionality. The simplest one is a point defect occurring if an atom is missing from its regular lattice site (vacancy), or there may be an excess atom (interstitial). Suppose a more extensive set of vacancies comes to lie side by side, forming an entire disc of missing atoms. The boundary line forms a line-like defect. Certainly, line-like defects can also arise in an opposite process of clustering of interstitial atoms. Line-like defects of this type are called dislocation lines. A dislocation line may also result from several discs of missing or excessive atoms stacked on top of each other. If many discs of missing or added atoms come to lie close together, defects in such a case say a disclination (Kleinert, 2008). Dislocations and disclinations play a central discussion in this thesis.

The experiment process leading to all kinds of defects from an ideal crystal is the Volterra process (Volterra, 1907), in which layers of matter are cut from a perfect crystal, with a subsequent smooth rejoining of the cutting surfaces; for a shortcut, the sketch of the process is presented in Figure 1.6. In this context, dislocations are obtained by a (local) discontinuity translation from ideal crystalline to perturbed one, and hence dislocations are so-called translational defects; similarly disclinations are underlined as rotational defects.

One possible way to model a continuum with a large number of defects is to consider it in a continuum framework. The most promising approach, concerned by such a point of view, is to model a continuum with defects in the framework of differential geometry. Indeed, since the

1950s it has been noticed by several authors (Bilby, Bullough, and Smith, 1955; Kondo, 1955; Eshelby, 1956; Kröner, 1960; Nye, 1953) and others that the Riemann-Cartan (RC) manifolds exhibit some close relations with the continuum with defects, in which dislocations and disclinations densities are interpreted as torsion and curvature tensors, respectively, of a material connection. These seminal works have their roots in Cartan's approach (Cartan, 1922) where the author insists on the crucial interpretation of lack of closure of a parallelogram supported by a moving frame after a parallel transport along an infinitesimal loop. The paper was arisen from the Cosserat brothers who introduced a continuum model involving an independent field of rotation in addition to the standard displacement field (Cosserat and Cosserat, 1909).

The limitation of these theories is that even though these authors laid down the crucial interpretation of dislocations as the sources of torsion, none of them identified the geometric origin for the relevance of torsion and then curvature as well. From what is said above, it should be clear that the problem of determining the material connection and the metric as well is important for the theory of defects. Among them, Lee and his co-worker (Le and Stumpf, 1996a; Le and Stumpf, 1996c) starting with the ideas from Noll, 1967/68; Wang, 1967/68 and the multiplicative decomposition of the deformation gradient $\mathbb{F} = \mathbb{F}_e\mathbb{F}_p$ (which was initially proposed by (Bilby, Bullough, and Smith, 1955) and (Lee and Liu, 1967)), they obtained some relations between torsion of the crystal connection and the elastic and plastic deformation gradients. In this approach,the material connection is metric compatible, with torsion but vanishing curvature. Yavari and Goriely, 2012a were inspired by this approach and had introduced the slightly different method in which they identified the plastic deformation gradients as Cartan's moving frames to construct the appropriate material manifolds. In this seminal work, they equipped that the material manifold with an evolving connection (compatible with the metric) such that the frame field is everywhere parallel. Nevertheless, from a mathematical viewpoint, this requirement is not trivial.

Another popular approach consists in focusing on the discontinuity of scalar and vector fields (Rakotomanana, 1998) by invoking multivalued fields (Kleinert, 2008). Such approach is a microscopic alternative interpretation of the non-holonomy supported by geometrical quantities (scalar or tensorial) at a scale for which the material may be interpreted as a continuum (Rakotomanana, 2018). Even if this approach was inspired by elastoplastic transformation of crystals, its applications has a wider range including relativity and quantum mechanics (Kleinert, 2000; Katanaev, 2005). In this modeling, the global smooth transformation is replaced by a multivalued map, and hence the global coordinates transformation is replaced by a local ones $dx^a = \mathbf{e}^a_A dX^A$ where the triads $\mathbf{e}^a_A$ may be multivalued too. Such a map carries a flat space to spaces with curvature and torsion. The connection and metric are not induced by a smooth and single-valued transformation but the multivalued triads may cause some difficulties.

The aim of this thesis: From the foregoing, we aim to consist of mathematical modeling of material with defects, which is represented by the appropriated Rieman-Cartan (RC) manifold derived from a true transformation (single-valued map). Our idea is driven by the reformulation of the Eringen-Mindlin approach (Suhubi and Eringen, 1964; Mindlin, 1964) in terms of RC geometry. Even if it relates to the theories, but its root is to introduce an additional degree of freedom, for which macroscopic mapping is still diffeomorphism, whereas the additional field

modifies the topology of the continuum at another scale, meaning that neighbours of microcells are changed. Soon, we realize that the fiber geometry (Epstein, 2010; Epstein, 2014) is a satisfactory mathematical framework where these intuitive considerations, that are the microcontinuum field theories (Eringen, 1999; Mindlin, 1964) and RC approach, would fit naturally. By the way, it is reasonable to begin this thesis with the introduction of RC geometry and some applications in mechanics.

In this chapter, we remind a synthesis of some definitions on Riemann-Cartan geometry (RC manifold). A global overview on generalized continuous media for medium with distributions of defects is presented, too. Particular attention is addressed on models using mathematical supports associated with RC manifold: a development of the Cosserat continuum is presented and several more modern approaches to construct such a manifold are given. Finally, this chapter ends with a description of the objectives of this dissertation regarding previous works and the plan of the study.

1.2 Riemann-Cartan geometry

Riemann (1826-1866) aimed to introduce the notion of a manifold and its structures. The first used in this thesis is a Riemannian metric, a quadratic field that plays the role of a natural generalization of the inner product between two vectors in Euclidean space. A second is a connection what will then be called the Levi-Civita connection, which is derived from the metric. By definition, the associated torsion of the Levi-Civita connection is null. Briefly, the resulting geometry is Riemannian geometry. Later, Cartan (1869-1951) enriched Riemann's geometry by introducing connection with a non-vanishing torsion. The connection is now independent of the metric. Riemannian geometry is renamed by Riemann-Cartan geometry regarding the contribution of Cartan.

In the present section, we will review the principal properties on Riemann-Cartan geometry. Readers can find more details on Nakahara, 2003; Epstein, 2010; Epstein, 2014; Choquet-Bruhat, DeWitt-Morette, and Dillard-Bleick, 1982; Rakotomanana, 2018 and references therein.

1.2.1 Affine connection and covariant derivative

Let $\mathscr{B}$ be an arbitrary manifold, we denote that $T\mathscr{B}$ is the tangent bundle space of the manifold, $T^*\mathscr{B}$ is its dual bundle space, and $\mathfrak{X}(\mathscr{B})$ is the set of vector fields on $\mathscr{B}$. On the manifold, two vectors defined at different points cannot be naively compared with each other. So far, there is no directional derivative acting on vector fields or more general tensors fields. Hence, one needs a tool, called a connection, which specifies how a vector is transported along a curve.

Definition 1.2.1 (Affine connection). *A linear (affine) connection on $\mathscr{B}$ is an operation*

$$\begin{array}{rccc} \nabla : & \mathfrak{X}(\mathscr{B}) \times \mathfrak{X}(\mathscr{B}) & \to & \mathfrak{X}(\mathscr{B}) \\ & (u, v) & \mapsto & \nabla_u v \end{array}$$

which satisfies the following conditions,

$$\begin{aligned} \nabla_u(v+w) &= \nabla_u v + \nabla_u w, & \nabla_{(fu)} v &= f\nabla_u v, \\ \nabla_{u+v} w &= \nabla_u w + \nabla_v w, & \nabla_u(fv) &= u[f]v + f\nabla_u v, \end{aligned} \tag{1.2.1}$$

where $f \in \mathscr{C}^\infty(\mathscr{B})$ and $u[f]$ is the directional derivative of f along a vector field u. Employing (x^a) as coordinates system on $\mathscr{B}$, we deduce that $u[f] = u^a \partial_a f$[1] *and*

$$\nabla_{\partial_a} \partial_b = \Gamma^c_{ab} \partial_c, \tag{1.2.2}$$

where Γ^c_{ab} are the connection coefficients or so-called Christoffel symbols and $\partial_a = \partial/\partial x^a$ is the natural base for the tangent bundle corresponding to coordinates (x^a) (sometimes e_a will be used instead of ∂_a). The connection coefficients specify how the basis vectors change from a point to its neighbor.

The connection must not depend on the chosen coordinate. In practice, under a coordinate transformation $x^a \mapsto \tilde{x}^j = \tilde{x}^j(x^a)$, the connection coefficients transform as

$$\widetilde{\Gamma}^k_{ij} = \frac{\partial x^b}{\partial \tilde{x}^i} \frac{\partial x^c}{\partial \tilde{x}^j} \frac{\partial \tilde{x}^k}{\partial x^a} \Gamma^a_{bc} + \frac{\partial^2 x^a}{\partial \tilde{x}^i \partial \tilde{x}^j} \frac{\partial \tilde{x}^k}{\partial x^a}. \tag{1.2.3}$$

Hereafter, to verify that an object is an affine connection, we only need to confirm that it is a set of smooth functions satisfying this transformation rule (1.2.3).

Having the tool in hand that measures the variation of a vector field from a point to its neighborhood, one may first extend this notion along any general curve on $\mathscr{B}$.

Definition 1.2.2 (Curves). *Let σ be a curve in $\mathscr{B}$:*

$$\begin{aligned} \sigma : \quad [0,1] &\to \mathscr{B} \\ t &\mapsto \sigma(t) = (x^a(t)) \end{aligned} \tag{1.2.4}$$

For such coordinate system, the velocity field of the curve $\dot{\sigma}(t) = u(t)$ is a vector field defined along this curve:

$$u(t) = \frac{\mathrm{dx^a(t)}}{\mathrm{dt}} \partial_a$$

In particular, one may control the transport of a vector along a curve without changing or losing information. The following definition performs it. The one-to-one correspondence between the connection and parallel transport is pictorially given in Figure 1.1.

Definition 1.2.3 (Parallel transport). *Let*

$$\sigma : \ [0,1] \to \mathscr{B} \ t \mapsto \sigma(t) = (x^a(t)) \tag{1.2.5}$$

be a curve in $\mathscr{B}$, its velocity field $u(t) = \dot{\sigma}(t) = \dot{x}^a(t) e_a$, and let v be a vector field defined (at least) along this curve. The vector field v is said to be parallel transported along σ if and only if it satisfies

$$\nabla_u v = 0 \tag{1.2.6}$$

[1] when an index variable appears twice in a single term and is not otherwise defined, it implies summation of that term over all the values of the index. This convention is called Einstein summation.

In terms of the components, (1.2.6) *reads as ((Nakahara, 2003))*

$$\frac{\mathrm{d}v^a}{\mathrm{d}t} + \Gamma^a_{bc}\frac{\mathrm{d}x^b(\sigma(t))}{\mathrm{d}t}v^c = 0. \tag{1.2.7}$$

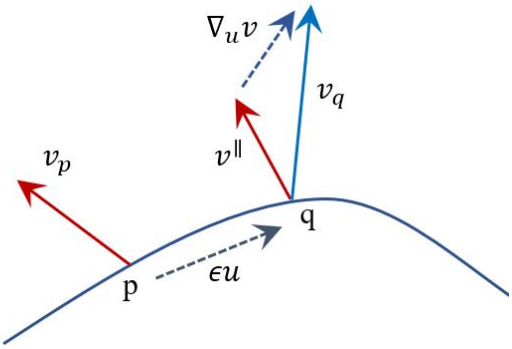

FIGURE 1.1: The relationship between the connection and parallel transport: The vector u defines a path of length ϵ. Let $v^{\parallel}$ denote a vector v_p "parallel transported" to q.

Since ∇_u has the meaning of a derivative, it is natural to define the covariant derivative of $f \in \mathscr{C}^\infty(\mathscr{B})$ by the ordinary directional derivative: $\nabla_u f = u[f]$. Furthermore, it can generalize the derivative of tensor fields on a manifold. In particular, the covariant derivative of a vector field v and of a 1-form field ω are respectively given by

$$\nabla_{\partial_b}(v^a\partial_a) = \left(\partial_b v^a + \Gamma^a_{bc}u^c\right)\partial_a \tag{1.2.8}$$

$$\nabla_{\partial_b}(\omega_a dx^a) = \left(\partial_b\omega_a - \Gamma^c_{ba}\omega_c\right)dx^a. \tag{1.2.9}$$

One may write that $\nabla v = \nabla_{\partial_b}(v^a\partial_a)\otimes dx^b$ and $\nabla\omega = \nabla_{\partial_b}(\omega_a dx^a)\otimes dx^b$.
More generally, we can say that the covariant derivative of a type (p,q) tensor is a type $(p,q+1)$ tensor as follows. We require that for any product of arbitrary tensors, we should have

$$\nabla(\mathsf{t}_1\otimes\mathsf{t}_2) = \nabla\mathsf{t}_1\otimes\mathsf{t}_2 + \mathsf{t}_1\otimes\nabla\mathsf{t}_2. \tag{1.2.10}$$

This allows us to define the components of the covariant derivative of any tensor field as

$$\begin{aligned}\nabla_{\partial_b}\mathsf{t}^{a_1..a_p}_{1...c_q} = \partial_b\mathsf{t}^{a_1..a_p}_{c_1...c_q} + \Gamma^a_{bd}\mathsf{t}^{d..a_p}_{c_1...c_q} + ... + \Gamma^a_{bd}\mathsf{t}^{a_1..d}_{c_1...c_q}\\ - \Gamma^d_{bc_1}\mathsf{t}^{a_1..a_p}_{d...c_q} - ... - \Gamma^d_{bc_1}\mathsf{t}^{a_1..a_p}_{c_1...d}.\end{aligned} \tag{1.2.11}$$

1.2.2 Torsion and curvature

Now the manifold $\mathscr{B}$ is always supposed to be endowed with the affine connection ∇. It must be emphasized that the connection is not a tensor, it cannot have an intrinsic geometrical meaning as a measure of how much a manifold is curved. Torsion and curvature tensors are introduced for that purpose (Nakahara, 2003).

Definition 1.2.4 (Torsion). *Denote $[u, v]$ the Lie bracket of vector fields given by*

$$[u, v] = (u^a \partial_a v^b - v^a \partial_a u^b) e_b. \tag{1.2.12}$$

The torsion tensor of the connection is a map

$$\begin{array}{rccl} \mathsf{T} : & \mathfrak{X}(\mathscr{B}) \times \mathfrak{X}(\mathscr{B}) & \to & \mathfrak{X}(\mathscr{B}) \\ & (u, v) & \mapsto & \mathsf{T}(u, v) = \nabla_u v - \nabla_v u - [u, v]. \end{array} \tag{1.2.13}$$

This map satisfies the tensorial property. Then, we can write $\mathsf{T} = \mathsf{T}^a{}_{bc} dx^b \otimes dx^c \otimes \partial_a$ with

$$\mathsf{T}^a{}_{bc} = \Gamma^a{}_{bc} - \Gamma^a{}_{cb}. \tag{1.2.14}$$

The tensor measures the failure of the closure of the parallelogram made up of the small displacement vectors and their parallel transports, a visual representation is formed in Figure 1.2.

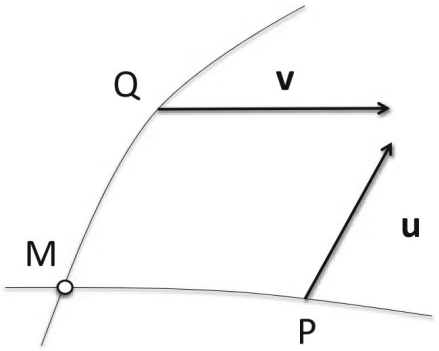

FIGURE 1.2: Geometrical meaning of the the torsion tensor: Cartan parallelogram. Let M be a point on the manifold $\mathscr{B}$, and (MP) and (MQ) be two sets of curves intersecting at M. Both MP and MQ are assumed infinitesimal and then constitutes two vectors of the tangent bundle $T_M\mathscr{B}$. Vectors u and v are the images of MQ and MP by parallel transport along (MP) an (MQ) respectively. The torsion measures the lack of closure of the parallelogram made up of infinitesimal vectors MP and MQ and their parallel transport v and u (Rakotomanana, 2018).

Definition 1.2.5 (Curvature). *The curvature tensor is a map*

$$\begin{array}{rccl} \mathsf{R} : & \mathfrak{X}(\mathscr{B}) \times \mathfrak{X}(\mathscr{B}) \times \mathfrak{X}(\mathscr{B}) & \to & \mathfrak{X}(\mathscr{B}) \\ & (u, v, w) & \mapsto & \mathsf{R}(u, v)w = \nabla_u \nabla_v w - \nabla_v \nabla_u w - \nabla_{[u,v]} w. \end{array} \tag{1.2.15}$$

It is a tensor field of type (1, 3). Writing $\mathsf{R} = \mathsf{R}^a{}_{bcd} \partial_a$, with

$$\mathsf{R}^a{}_{bcd} = \partial_c \Gamma^a{}_{db} - \partial_d \Gamma^a{}_{cb} + \Gamma^a{}_{ce} \Gamma^e{}_{db} - \Gamma^a{}_{de} \Gamma^e{}_{cb}, \quad \textit{then} \qquad \mathsf{R}^a{}_{bcd} = -\mathsf{R}^a{}_{bdc}. \tag{1.2.16}$$

This tensor measures the difference between two vectors: an initial one and a final one obtained by parallel transport the initial vector along a loop, a pictorial representation is formed in Figure 1.3.

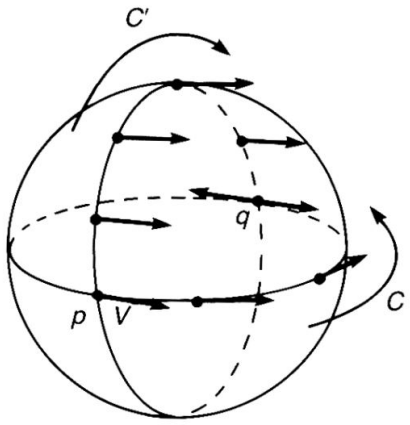

FIGURE 1.3: Geometrical meaning of the curvature tensor: It is natural to define V parallel transported along a great circle if the angle V makes with the great circle is kept fixed. If V at p is parallel transported along great circles C and C', the resulting vector at q points in opposite directions (Nakahara, 2003).

1.2.3 Metric tensor and metric-compatible connection

A manifold is a topological space that locally looks like Euclidean space. Calculus on a manifold is assured by the existence of smooth local coordinate systems. A structure - called a metric tensor - is a natural generalization to an arbitrary manifold of the inner product between two vectors in the Euclidean space. It is defined as follows.

Definition 1.2.6. *A Riemannian metric* g *on the manifold is a type* $(0,2)$ *tensor field which satisfies the following axioms at each point* $p \in \mathscr{B}$ *and for* $u, v \in T_p\mathscr{B}$ *-the tangent space at the point* $p \in \mathscr{B}$

- $\mathrm{g}_p(u,v) = \mathrm{g}_p(v,u)$
- $\mathrm{g}_p(u,u) \geq 0$, *the equality holds if and only if* $u = 0$.

Locally, the tensor can be read in the coordinate system as

$$\mathrm{g} = \mathrm{g}_{ab}(x) dx^a \otimes dx^b. \tag{1.2.17}$$

Definition 1.2.7. *On a manifold with a connection and a metric,* $(\mathscr{B}, \nabla, \mathrm{g})$, *the connection* ∇ *is said metric-compatible if and only if*

$$\nabla \mathrm{g} = 0\,.$$

In terms of coordinates, one gets

$$\nabla_{\partial_c} \mathrm{g}_{ab} - \Gamma^d_{ca} \mathrm{g}_{db} - \Gamma^d_{cb} \mathrm{g}_{da} = 0. \tag{1.2.18}$$

Equivalently, the metric-compatible condition is $\nabla_v \mathrm{g}(u,w) = 0$ *for arbitrary vector fields* u, v, w *on* $\mathscr{B}$. *It can be read as*

$$\nabla_v \mathrm{g}(u,w) = \mathrm{g}(u, \nabla_v w) + \mathrm{g}(\nabla_v u, w).$$

Theorem 1.2.8 (Levi-Civita connection)**.** *It can be shown that on any Riemannian manifold* $(\mathscr{B}, \mathrm{g})$, *there is a unique linear connection that is compatible with* g *and is torsion-free. This connection is the*

Levi-Civita connection and denoted $\overline{\nabla}$ *(Nakahara, 2003) with the connection coefficients:*

$$\mathsf{L}^{a}_{\ bc} = \frac{1}{2}\mathsf{g}^{ad}\left(\frac{\partial \mathsf{g}_{cd}}{\partial x^{b}} + \frac{\partial \mathsf{g}_{db}}{\partial x^{c}} - \frac{\partial \mathsf{g}_{cb}}{\partial x^{d}}\right). \tag{1.2.19}$$

For an arbitrary connection ∇ satisfying metric-compatible condition, the connection coefficients can be decomposed by (Nakahara, 2003)

$$\Gamma^{a}_{\ bc} = \mathsf{L}^{a}_{\ bc} + \mathsf{K}^{a}_{\ bc}. \tag{1.2.20}$$

where the second term of right-hand side term of (1.2.20) is called contorsion, denoted by

$$\mathsf{K}^{a}_{\ bc} = \frac{1}{2}\left(\mathsf{T}^{a}_{\ bc} + \mathsf{g}^{ad}\mathsf{T}^{e}_{\ dc}\mathsf{g}_{db} + \mathsf{g}^{ad}\mathsf{T}^{e}_{\ db}\mathsf{g}_{dc}\right). \tag{1.2.21}$$

As a consequence, the curvature tensor R can be written in terms of curvature of the Levi-Civita connection $\overline{\mathsf{R}}$ and the contorsion tensor K as (Yavari and Goriely, 2012a)

$$\mathsf{R}^{\ell}_{\ abc} = \overline{\mathsf{R}}^{\ell}_{\ abc} + \overline{\nabla}_{\partial_b}\mathsf{K}^{\ell}_{\ ca} - \overline{\nabla}_{\partial_c}\mathsf{K}^{\ell}_{\ ba} + \mathsf{K}^{\ell}_{\ bs}\mathsf{K}^{s}_{\ ca} - \mathsf{K}^{\ell}_{\ cs}\mathsf{K}^{s}_{\ ba}, \tag{1.2.22}$$

where the covariant derivatives of the contortion tensor are given with respect to the Levi-Civita connection $\overline{\nabla}$.

We last summarize the classification of manifold with connection and metric

Definition 1.2.9. *If the manifold* $\mathscr{B}$ *endowed with connection* ∇*, and a metric* g*, one gets*

- *If* $\nabla\mathsf{g} = 0$; $\mathsf{T} = 0$ *and* $\mathsf{R} = 0$*, the manifold is a flat (Euclidean) manifold.*
- *If* $\nabla\mathsf{g} = 0$; $\mathsf{T} \neq 0$ *and* $\mathsf{R} = 0$*,* $(\mathscr{B}, \nabla, \mathsf{g})$ *is a Weitzenböck manifold.*
- *If* $\nabla\mathsf{g} = 0$; $\mathsf{T} \neq 0$ *and* $\mathsf{R} \neq 0$*,* $(\mathscr{B}, \nabla, \mathsf{g})$ *is a Riemann–Cartan manifold.*
- *If* $\nabla\mathsf{g} \neq 0$*,* $(\mathscr{B}, \nabla, \mathsf{g})$ *is sometimes (in mechanical litterature) called a Weyl manifold.*

Remark 1.2.10. *Trivial geometry of the Euclidean space:*
Denote $\mathbb{E}^n$ *the n-dimensional Euclidean space. It admits a natural Riemannian metric tensor (still denote* g*) and a canonical affine connection* γ*, which is nothing else than the Levi-Civita connection of the metric. In particular, when Cartesian systems are used on* $\mathbb{E}^n$*, the metric coincides with Kronecker delta, i.e.* $\mathsf{g} = \delta$ *and the connection* γ *vanishes identically.*

1.3 Generalized material continuum

1.3.1 Transformation

Basically, a body $\mathscr{B}$ is a set of particles. The mean role of B is to label each material element p. In a physical configuration, each element $p \in \mathscr{B}$ is identified with the position x in the space that it occupies. This space is usually called the ambient space and corresponds to this work to the Euclidean space $\mathbb{E}^3$. Such identification may define a notion of differential manifold $\mathscr{B}$. In this

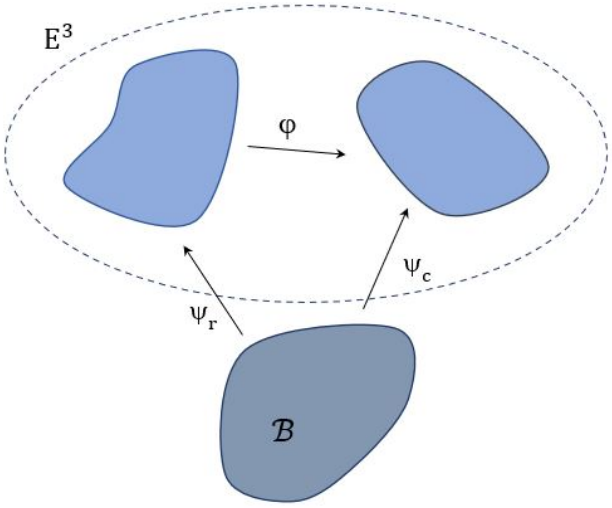

FIGURE 1.4: Transformation of a continuum (Rakotomanana, 2018).

context, we will suppose that the material body is a three-dimensional differentiable manifold $\mathscr{B}$ with boundary such that there exists a global orientation-preserving diffeomorphism

$$\psi \ : \mathscr{B} \to \mathbb{E}^3. \tag{1.3.1}$$

Such a map depends on time in general. The image of $\mathscr{B}$ is assumed to be a connected subset of the Euclidean space. In that sense, a configuration of the continuum is the pair$(\psi, \psi(\mathscr{B}))$ (Rakotomanana, 2018). Let us consider two configurations of the continuum matter: a so-called reference configuration $(\psi_r, \psi_r(\mathscr{B}))$ and a so-called current configuration $(\psi_c, \psi_c(\mathscr{B}))$. A transformation of the body concerning the reference state to the current state is a mapping $\mathbb{E}^3 \to \mathbb{E}^3$ (see Figure 1.4)

$$\varphi = \psi_c \psi_r^{-1}. \tag{1.3.2}$$

This description is the limits of Noll, 1967/68. In most studies, ones thinks of the body as an ideal initial state that is brought into a deformed final state. In other words, it assumes that $\mathscr{B}$ and $\psi_r(\mathscr{B})$ are merged. Hereafter, we call transformation and denote φ for either (1.3.1) and (1.3.2).

Definition 1.3.1. *Deformation gradient:*
Let us consider a transformation $\psi \ : \mathscr{B} \to \mathbb{E}^3$. Most of studies of transformations are based on the local analysis on infinitesimal area located around $X \in \mathscr{B}$. As the small piece, the transformation of neighboring points surrounding X can be represented by a linear mapping $F(X) : \ T_X\mathscr{B} \to T_{\varphi(X)}\mathbb{E}^3$ which is called deformation gradient at X. Let (X^A) and (x^a) denote coordinate systems on $\mathscr{B}$ and $\mathbb{E}^3$, respectively. Then, the deformation gradient with respect to the coordinate bases is given by

$$F(X) = F^a_A(X)\partial_a \otimes dX^A \qquad \textit{with} \qquad F^a_A(X) = \frac{\partial \varphi^a(X)}{\partial X^A}. \tag{1.3.3}$$

Sometimes, we denote $F = D\varphi$ or $F = \varphi_*$ or even $F = d\varphi$. Its inverse $F^{-1} = \varphi^*$ is given by $\varphi^*(x) = F_a^A \partial_A \otimes dx^a$ satisfying the completeness relationships:

$$F_A^a(X)F_a^B(\varphi(X)) = \delta_A^B \qquad F_A^a(X)F_b^A(\varphi(X)) = \delta_b^a. \tag{1.3.4}$$

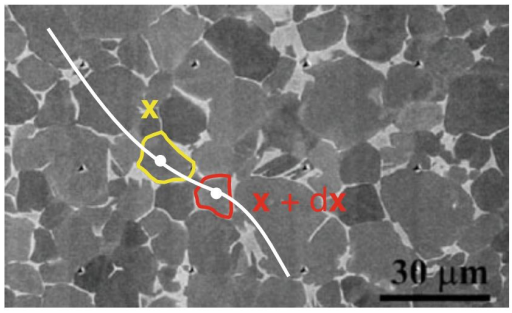

FIGURE 1.5: Two connected material points x and $x + dx$ along a material line. At a length scale $30\mu m$, the metric alone is not sufficient for modeling the shape change due to relativistic motions of grains. Grain interfaces are source of dislocations during plastic flow of poly-crystalline solids. (Rakotomanana, 2018).

As an arbitrary manifold, $\mathscr{B}$ can be equipped with a connection ∇ and a metric G. Technically, the transformation ψ is used to carry the geometry of the Euclidean ambient space onto $\mathscr{B}$ to obtain a connection and a metric on $\mathscr{B}$. These quantities (expressed in the reference coordinates) contain all the relevant informations to describe the state of the configuration, at least in the case of this study. More precise, the metric tensor provides a suitable tool for measuring angles and distances, whereas the connection specifies a way to identify an element to another in its neighbourhood. As a consequence, the structure of the medium can be characterized by the induced manifold $(\mathscr{B}, \nabla, \mathsf{G})$. As if $\varphi \in \mathscr{C}^\infty$, the induced manifold is equivalent to the ambient Euclidean space $\mathbb{E}^3$ (Marsden and Hughes, 1994). Such a map captures a pure elastic solid.

Nevertheless, the smooth mapping does not capture a wide type of material, for instance, a defective continuum. Besides, the plastic behaviour of the solids also yields that such a transformation does not exist. The smooth transformation is again not sufficient to deal with the evolution of a microstructure, see Figure 1.5.

To go further, some approaches have been introduced. With respect to the scope of this thesis, there is a considerable breakthrough dealing with a non-smooth and/or multivalued transformation rather than the previous smooth and single-valued one. Such a map - namely nonholonomic map - does not preserve the topology of the body (Kleinert, 2000). The method concerns such a map is known as the nonholonomic principle. We refer the reader to the books Kleinert, 2008; Rakotomanana, 2018 and references therein.

Following the nonholonomic principle, the material manifold $\mathscr{B}$ is then equipped with a metric and a connection (that is metric compatible) and may have both torsion and curvature. The nonholonomic mappings enable to exhibit the Volterra process (Volterra, 1907). This process is describe as follows. To simplify the problem, let a hollow cylinder composed of an elastic material, then cut it, thereby destroying its multiple connectedness. Then take the two lips that the cut has separated, translate and rotate them against each other. Finally, after eventually removing superfluous or adding missing material, we weld the two planes together again. The

pictorial representation is given in Figure 1.6. The Volterra process, by construction, yields two different kinds of defects : dislocations or translational defects and disclinations or rotational defects (Kleinert, 2008; Puntigam and Soleng, 1997; Katanaev, 2005).

Employing such a nonholonomic mapping, different cases may occur: we first consider that the current configuration is defect-free in the sense that the mapping ψ_r is a diffeomorphism ensuring that the reference configuration has zero torsion $\mathsf{T}_r = 0$ and zero curvature $\mathsf{R}_r = 0$. In such a case, if φ is a diffeomorphism, the current configuration is defect-free too. Conversely, defects may appear during the transformation by meant of the non-zero torsion and/or curvature ($\mathsf{T}_r \neq 0$ and $\mathsf{R}_r \neq 0$). Now, let us assume the reference configuration is not defect-free in the sense that ψ_r is not a diffeomorphism, then the induced connection may have torsion and/or curvature. If the current configuration is prescribed by diffeomorphism φ, no additional defects are created, and hence $\mathsf{T}_c = \mathsf{T}_r$ and $\mathsf{R}_c = \mathsf{R}_r$; but if ψ_r is not a diffeomorphism, the current configuration may not have the same internal defects as before, and hence $\mathsf{T}_c \neq \mathsf{T}_r$ and $\mathsf{R}_c \neq \mathsf{R}_r$.

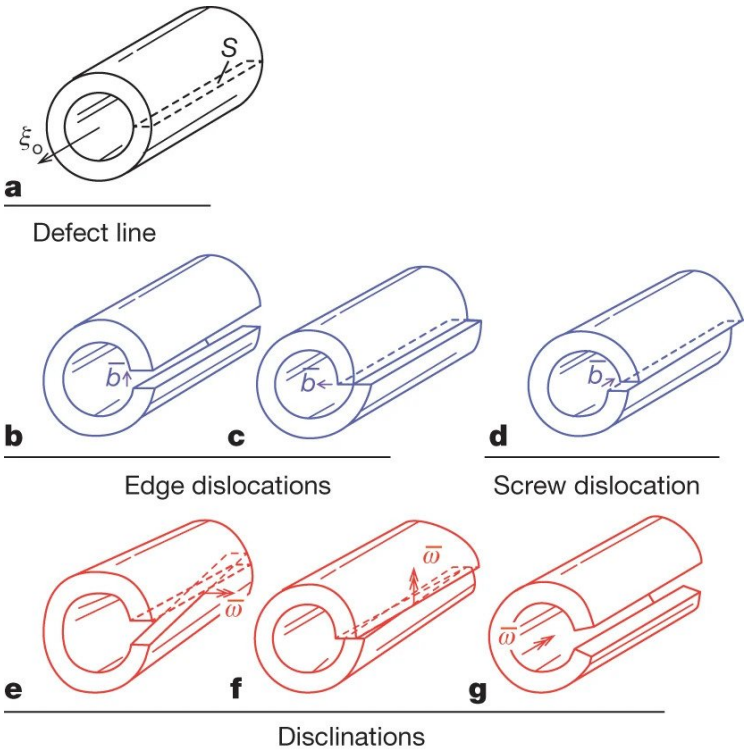

FIGURE 1.6: The sketch of the Volterra process: (a): Reference cylinder with defect line ξ_0 and cut surface S. (b,c) Edge dislocations with Bürgers vector $\overline{b}$. (d) Screw dislocation. (e,f) Twist disclinations with Frank vector $\overline{\omega}$. (g) Wedge disclination (Cordier et al., 2014).

1.3.2 Defective medium

The description of dislocations and disclinations in terms of the differential geometry of manifolds has a long history. The connection between a continuum mechanics of solids with a distribution of defects and RC geometry follows from the fact that the dislocation density is equivalent to the torsion of the differential geometric space. This point of view has been initiated by

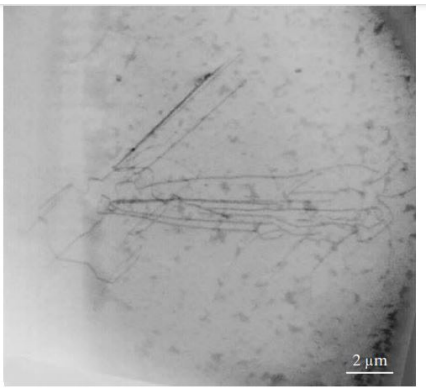

FIGURE 1.7: Transmission electron microscopy (TEM) picture of dislocations in a steel (Cordier et al., 2014).

(Kondo, 1955; Bilby, Bullough, and Smith, 1955). A related idea has been developed to formulate disclinations in terms of the curvature tensor. It is attributed to (Kröner, 1960). Since the 1950s, numerous researchers have working on the connections between the mechanics of solids with distributed defects and (non-)Riemannian geometries, see for example Katanaev, 2005; Puntigam and Soleng, 1997.

Methodologically speaking, these theories were perhaps spurred by the realization that certain objects of differential geometry, already provided on a path, may give intuitively graspable pictures to generalize the presence of defects in the medium. In particular, the so-called Burger vector exhibiting the lack of closure of a Burgers' circuit enclosing an edge dislocation in two dimensions and the lack of commutativity of two vector fields in case of the presence of torsion (see Figure 1.8):

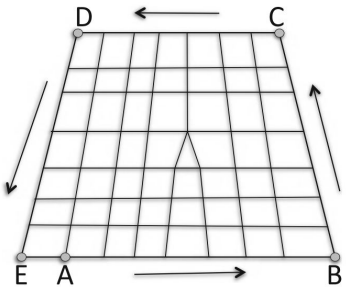

FIGURE 1.8: Burger circuit is considered as a discrete version of the Cartan parallelogram. The non closure of the path $ABCDE$ measures the number of defect inside the parallelogram. Only one defect (triangle) is represented here. The opening EA define the so-called Burgers vector (Rakotomanana, 2018).

More precisely, let M be a point on the manifold $\mathscr{B}$ and (MP) and(MQ) two sets of curves intersecting at M. Both MP (whose components $(d_1x^a(M))$) and MQ (whose components $(d_2x^a(M))$) are assumed infinitesimal and then regarded as two vectors of the tangent bundle $T_M\mathscr{B}$. Vectors $u = d_2x^a(P)e_a$ and $v = d_1x^a(Q)e_a$ are the images of MQ and MP by parallel transport along

(MP) an (MQ) respectively (Figure 1.2):

$$\begin{aligned} d_2x^a(P) &= d_2x^a(M) - \Gamma^a_{\ bc} d_2x^c d_1x^b \\ d_1x^a(Q) &= d_1x^a(M) - \Gamma^a_{\ bc} d_1x^c d_2x^b. \end{aligned} \tag{1.3.5}$$

Then , $\vec{MQ} + v$ and $\vec{MP} + u$ do not agree and the difference is

$$(\vec{MQ} + v) - (\vec{MP} + u) = \Gamma^a_{\ bc} dS^{bc} = \frac{1}{2}(\Gamma^a_{\ bc} - \Gamma^a_{\ cb}) dS^{bc} = \frac{1}{2}\mathsf{T}^a_{\ bc} dS^{bc}, \tag{1.3.6}$$

where $dS^{bc} = d_1x^b d_2x^c - d_1x^c d_2x^b$ has been identified as the surface area element. On the other hand, if we denote db^e a resulting Burgers vector of all dislocation which pierces through the area element, the dislocation density is then obtained by (Kröner, 1981)

$$db^e = \frac{1}{2}\alpha^{ea}\epsilon_{abc} dS^{bc}, \tag{1.3.7}$$

where the anti-symmetric tensor ϵ:

$$\epsilon_{amn} = \begin{cases} 1 & \text{if } (amn) \text{ is an even permutation of } (123) \\ -1 & \text{if } (amn) \text{ is an odd permutation of } (123) \\ 0 & \text{otherwise.} \end{cases} \tag{1.3.8}$$

Therefore, the identification of the dislocations density (1.3.7) and Cartan circuit (1.3.6) suggests that the dislocation density can be given by

$$\mathsf{T}^e_{\ bc} = \alpha^{ea}\epsilon_{abc} \qquad\qquad \alpha^{ea} = \frac{1}{2}\mathsf{T}^e_{\ bc}\epsilon^{abc}. \tag{1.3.9}$$

In another way, the dislocation density can be exposed as

$$\Gamma^e_{\ bc} = \frac{1}{2}\alpha^{ea}\epsilon_{abc} \qquad\qquad \alpha^{ea} = \Gamma^e_{\ bc}\epsilon^{abc}. \tag{1.3.10}$$

If the connection is compatible with the metric g, then $\Gamma^e_{\ bc} = \mathsf{L}^e_{\ bc} + \mathsf{K}^e_{\ bc}$; and hence

$$\alpha^{ea} = \mathsf{K}^e_{\ bc}\epsilon^{abc}. \tag{1.3.11}$$

Since $\mathsf{K}^a_{\ bc}$ is antisymmetric in the indices b, c, it is useful to introduce a tensor of second rank κ, so-called Nye' contortion tensor, by

$$\kappa^{ec} = \frac{1}{2}\mathsf{K}^e_{\ bd}\epsilon^{cbd} \qquad\qquad \mathsf{K}^e_{\ bc} = \kappa^{ea}\epsilon_{abc}. \tag{1.3.12}$$

Inserting (1.3.12) into (1.3.11), one deduces

$$\alpha^{ea} = \kappa^{ed}\epsilon_{dbc}\epsilon^{abc} = \kappa^{ea} - \delta_{ea}\kappa^{bb}. \tag{1.3.13}$$

These equations are similar to Nye's equations of the classical dislocation mechanics (Nye, 1953).

We also refer the survey papers Kröner, 1960; Kröner, 1981 for a more discussion.

A crucial observation as follows shows that the curvature tensor is a measurement of disclinations densities. If we parallel transport a vector at a given point along a loop or transport it to another point along two different curves, the resulting vectors at the end-point are generally different Figure 1.3. We expect that this non-integrability of parallel transport characterizes the intrinsic notion of curvature. On the other hand, it was recognized that disclinations might be generated by cutting a section of matter out of an ideal medium. In this sense, the missing area line-like the properties of the curvature tensor. In conclusion, this identity defines a foundation of the differential geometrical statement of the defective continuum theory and says that the disclinations densities and the curvature torsion represent precisely the same phenomenon.

1.4 Cosserat continuum

1.4.1 Linear Cosserat continuum

In Cosserat and Cosserat, 1909, Cosserat brothers introduced a continuum model involving an independent field of infinitesimal rotation ω of the geometric structure (in the case of crystals: of the lattice structure) in addition to the standard (elastic) displacement field u. A crystalline body is a field of applications of the theory. Especially, one can easily illustrate dislocated crystals whose building blocks had indeed been made by rotations (which varies from one element to another) but by not translations. In Kröner, 1960, Kröner outlined the development of the Cosserat theory (in which an elastic distortion and a (lattice) structure field (see later) are generally not derived from the displacement and rotation fields). Follow the ideas developed by (Kondo, 1955) and (Bilby, Bullough, and Smith, 1955), the general theory was shown to be identical to a medium whose geometrical state is described by Riemann-Cartan geometry. Briefly, the Levi-Civita connection represents the elastic deformations, and a contortion represents the (lattic) structure field. In linear version , force field and torque field are identical with Einstein and torsion tensors, respectively (Kröner, 1981).

It is reasonable to make a presentation of the Cosserat continuum. The (static) linear continuum theory is represented as follows. The rotation angle can be replaced by the equivalent (axial) vector $\vec{\omega}$ where its components are given by

$$\omega_a = \frac{1}{2}\epsilon_{bca}\omega_{bc}. \tag{1.4.1}$$

Instead of displacements and rotations one can also use the elastic deformations and the structure fields. Indeed, the displacement field and rotation field uniquely define the elastic distortion tensor β and the structure tensor ξ (it is called Nye's curvature in the case of the lattice structure (Nye, 1953), it is described by RC geometry, torsion tensor (Kröner, 1960)) which are respectively defined by (Katanaev, 2005)

$$\beta_{ab} = \partial_a u_b - \omega_{ab} \tag{1.4.2}$$

$$\xi_{ab} = \partial_a \omega_b. \tag{1.4.3}$$

In the case of the crystal structure, the latter implies that the lattice structure field (Nye's tensor) has precisely the characteristics that described by the Cosserats. Let Ξ be an internal energy function of β and ξ :

$$\Xi(\beta, \xi). \tag{1.4.4}$$

We define an associated force stresses tensor σ (this is an analogy to the stress that uses in elasticity theory) and a (Cosserat) torque-stresses tensor τ (these are defined as the torque that a surface element is endowed with when no rotations take place) by

$$\varsigma = \frac{\partial \Xi}{\partial \beta} \qquad\qquad \tau = \frac{\partial \Xi}{\partial \xi}. \tag{1.4.5}$$

The linear (static) Cosserat medium is in equilibrium if the forces and the torques balanced at every point are valid in Eulerian notation: (a very nice introduction to the Cosserat continuum theory is supplied in the note of Kröner, 1960, see also (Katanaev, 2005))

$$\partial_b \varsigma^{ba} + f^a = 0 \tag{1.4.6}$$

$$\epsilon^a_{bc} \varsigma^{bc} + \partial_b \tau^{ba} + m^a = 0 \tag{1.4.7}$$

where f^a and m^a mean the densities of external forces and torques. The stress tensor is symmetric if and only if the condition $\partial_b \tau^{ba} + m^a = 0$ is satisfied. Consequently, the fundamental static systems reduces to the elasticity theory (Gonzalez and Stuart, 2008; Marsden and Hughes, 1994).

1.4.2 Generalization of Cosserat continuum

Inspired by the work's Cosserat brothers (Cosserat and Cosserat, 1909), Élie Cartan developed an extended continuum model based on the Riemann-Cartan manifold. It is endowed with not only a Riemannian metric (measuring the shape change) but also an affine connection ∇, replacing the classical partial derivative operator "∂", incorporating torsion and curvature (Cartan, 1922). Cartan published a series of articles Cartan, 1923; Cartan, 1924; Cartan, 1925 (English translation is in Cartan, 1986), where he presented a theory of generalized relativity in the framework of his formulation of affine geometry.

Following the same spirit, to generalize Navier equation with respect to the presence of defects in a medium (Futhazar, Le Marrec, and Rakotomanana, 2014) proposed that the reference state is modeled by a RC manifold in order to take into account the presence of defects. In their work, the authors focused on a small elastic perturbation superimposed on the medium. To simplify problem, the superimposed transformation is assumed to be a diffeomorphism. Hence, no additional defects are created. Therefore, the connection is a fixed parameter in the Lagrangian function, so that we do not consider its variation during the superimposed transformation. We employ the same conservation equations as in the classical elasticity (Marsden and Hughes, 1994) but "∂" is replaced by the material connection ∇ with respect to the defected reference state.
Let u, ε, and σ be respectively the superimposed displacement field, the small-strain tensor, and the (symmetric) stress tensor. Then, the conservation laws are (Rakotomanana, 1998):

- Mass conservation

$$\rho = \rho_0 \det(\mathbf{e}) \tag{1.4.8}$$

where ρ_0 is a mass density at the time $t = 0$, and $\mathbf{e}$ is so-called triads that will be defined later in *Section*-1.5.2.2.

- Momentum conservation without external force:

$$\rho_0 \partial_t^2 u = \nabla \cdot \sigma. \tag{1.4.9}$$

Next, one assumes a linear Hooke's constitutive law for an homogeneous isotropic elastic medium to obtain

$$\sigma = \lambda \mathrm{Tr}(\varepsilon)\mathbb{I} + 2\mu\varepsilon \tag{1.4.10}$$

with λ and μ are Lamé constant coefficients, and $\mathbb{I}$ is the identity tensor. However, the two definitions of the strain ε can be proposed with the help of the Levi-Civita connection $\overline{\nabla}$ and the material connection ∇ (Futhazar, Le Marrec, and Rakotomanana, 2014):

$$\bar{\varepsilon} = \frac{1}{2}\left(\overline{\nabla} u + \overline{\nabla} u^T\right) \qquad \text{and} \qquad \varepsilon = \frac{1}{2}\left(\nabla u + \nabla u^T\right). \tag{1.4.11}$$

The two different options are available: firstly, according to the RC geometry of the reference state, it seems more rigorous to use the covariant derivative with respect to the material connection for calculating the strain tensor, which illustrates how the continuum is locally modified. But on the other hand, we could suppose that the superimposed deformation is only sensible to the metric; hence, the influence of defects on the strain definition would be neglected: each infinitesimal volume is deformed without further restrictions due to the defected arrangement within matter.

These two options presented in Futhazar, Le Marrec, and Rakotomanana, 2014 show how physical considerations may be invoked in order to develop mechanical model based on RC geometry. In particular, the methodology is not unique and is subject of interesting debates (in this paper as in most of other works).

1.5 Overview on continuum theory of defects

Even if it has been shown that RC manifolds can be used to describe a medium with distributions of defects, a crucial point still arises. Indeed, one need to construct a connection and metric of the manifold.

Before going into details of the proposed theory, let us briefly and critically review the classical linearized, non-linear dislocation mechanics and existing geometrical theories. This will help us to fix more clearly ideas and notations. It will help to see the parallel between the existing methods and at the end the approach proposed in this manuscript.

1.5.1 Classical dislocation mechanics

1.5.1.1 Linearized dislocation mechanics

Following the textbook we used, we use the previous notations for different objects in this subsection. We must be careful that they are not the same, even if they may reveal identical meanings.

We start with classical linearized dislocation mechanics. In the linearized setting, the total distortion can be additively decomposed into elastic and plastic parts (Kröner, 1960, English translation (Kröner, 1981))

$$\beta = \beta_e + \beta_p \tag{1.5.1}$$

(Be careful that β is distinct from (1.4.2)). The difference between the elastic and plastic distortions is a change in the internal state of the infinitesimal domain dV (for instance, particles, atoms,...place inside the domain dV). The elastic distortion always means the same distortion of the domain and its internal state, whereas this is not the case with the corresponding plastic distortion β_p in the sense of Kröner, 1981. The total distortion must be integrable:

$$\text{curl } \beta = \epsilon_{amn}\partial_m\beta_{bn} = 0, \tag{1.5.2}$$

implying that

$$\alpha = \text{curl } \beta_p = -\text{curl } \beta_e. \tag{1.5.3}$$

Here, α is interpreted as a tensor of dislocation density. An immediate consequence of the definition of α is the equation

$$\text{div } \alpha = \partial_c\alpha_{ab} = 0. \tag{1.5.4}$$

This equation shows that dislocations cannot end inside the medium. In addition, the vanishing of α implies the existence of an elastic displacement u such that $\beta_e = \nabla u$.

In the nineteenth century, St. Venant found that the elastic distortion can lead to a smooth u if and only if the elastic strain

$$\varepsilon = \frac{1}{2}(\beta_e + \beta_e^T) \tag{1.5.5}$$

satisfies the differential equations

$$\text{inc } \varepsilon = \nabla \times \varepsilon \times \nabla = 0 \qquad (-\epsilon_{cam}\epsilon_{dbn}\partial_b\partial_a\varepsilon_{mn} = 0), \tag{1.5.6}$$

which is called compatibility condition. It suggests to introduce second order incompatibility law of the form

$$\eta = \text{inc } \varepsilon. \tag{1.5.7}$$

The incompatibility tensor η measures the deviation from compatibility. Furthermore, its appearance or disappearance describes whether the body has internal stresses. Then, this tensor can be considered as the source tensor for a kind of internal stresses (Kröner, 1981).

The relation between the incompatibility tensor η and the dislocation density tensor α is obtained as the following: the equation $\alpha = -\text{curl}\, \beta_e$ can be rewritten as follows

$$\epsilon_{acd}\partial_c\omega_{db} = -\epsilon_{acd}\partial_c\varepsilon_{db} - \alpha_{ab}, \tag{1.5.8}$$

where

$$\omega = \frac{1}{2}(\beta_e - \beta_e^T) \tag{1.5.9}$$

is the antisymmetric part of the elastic distortion tensor. It interpreters as a rigid rotation of the volume element dV. The tensor can be replaced by the equivalent (axial) vector $\vec{\omega}$ whose components are given by

$$\omega_a = \frac{1}{2}\epsilon_{bca}\omega_{bc} \qquad \omega_{bc} = \epsilon_{bca}\omega_c. \tag{1.5.10}$$

Straightforward computations give

$$\partial_b\omega_a = \epsilon_{acd}\partial_c\varepsilon_{db} + \alpha_{ab} - \frac{1}{2}\alpha_{cc}\delta_{ba}, \tag{1.5.11}$$

The lattice rotation is can be rewritten by using the elastic strain and the distribution from the dislocations.

Now, we define Nye tensor κ

$$\kappa_{ab} = \alpha_{ab} - \frac{1}{2}\alpha_{cc}\delta_{ab}. \tag{1.5.12}$$

It is identical to (1.3.13). Inserting the above equation into (1.5.10) and then applying the curl operation, one obtains (Kröner, 1960)

$$\text{inc}\, \varepsilon - \text{curl}\, \kappa = 0. \tag{1.5.13}$$

As a consequence, we may find some examples of zero-stress dislocations distributions in the linearized setting (Head et al., 1993) or in geometric approach (Yavari and Goriely, 2012b).

1.5.1.2 Non-linear dislocation mechanics

A standard starting point in many theories of non-linear plasticity is to assume a decomposition $\mathbb{F} = \mathbb{F}_e\mathbb{F}_p$ (their coordinates expression follows in F_e and F_p, respectively), which was initially proposed by Bilby, Bullough, and Smith, 1955 and Lee and Liu, 1967. Physically, $\mathbb{F}_p$ represents the plastic distortion due to the flow of defects through the material structure, whereas $\mathbb{F}_e$ is the local deformation due to the stretch and the rotation of the material structure. However, they are not defined as the gradients of a continuous one-to-one mapping. Using this decomposition, one can introduce an intermediate configuration as shown in Figure 1.9: $\mathbb{F}_p$ may be interpreted

as a local deformation from the initial configuration to the intermediate one, and $\mathbb{F}_e$ relates the intermediate state to the current state. As usual, it is assumed that the reference and the final deformed bodies are embedded in a Euclidean space.

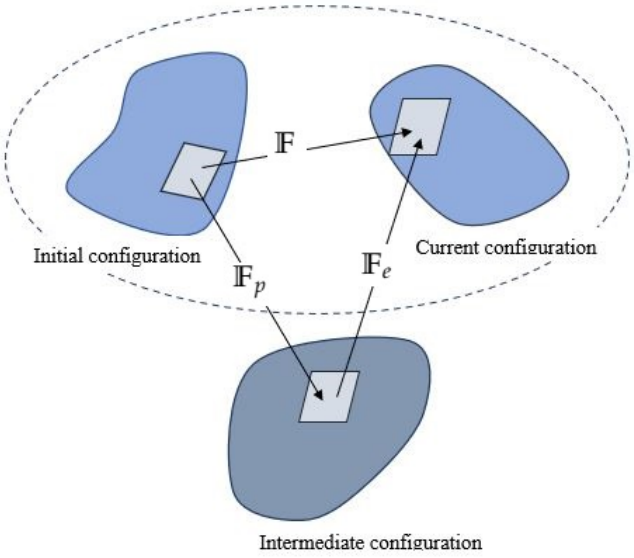

FIGURE 1.9: Pictorial representation of Kröner-Lee-decomposition.

Let us consider an arbitrary circuit c in the current configuration, Burger vector of dislocation is defined by Le and Stumpf, 1996b

$$\mathbf{b}^{\alpha} = -\oint_c (F_e^{-1})^{\alpha}_b dx^b. \tag{1.5.14}$$

Here, it is assumed that (x^a) and (z^{α}) are coordinates of current and intermediate configurations, respectively. Thanks to Stokes' theorem, one gets

$$\mathbf{b}^{\alpha} = \frac{1}{2}\int_A \left(\frac{\partial (F_e^{-1})^{\alpha}_c}{\partial x^b} - \frac{\partial (F_e^{-1})^{\alpha}_b}{\partial x^c}\right) dx^b \wedge dx^c, \tag{1.5.15}$$

where A is a surface area surround by the circuit. For infinitesimal circuits, a Burger vector is given as a two-form

$$\mathbf{b}^{\alpha} = \frac{1}{2}\left(\frac{\partial (F_e^{-1})^{\alpha}_c}{\partial x^b} - \frac{\partial (F_e^{-1})^{\alpha}_b}{\partial x^c}\right) dx^b \wedge dx^c. \tag{1.5.16}$$

The indices α in $\mathbf{b}^{\alpha}$ are used to describe the Burgers vector in the intermediate configuration. Equivalently, we can push this vector forward to the current configuration as

$$\mathbf{b}^{a} = (F_e)^{a}_{\alpha}\left(\frac{\partial (F_e^{-1})^{\alpha}_b}{\partial x^c} - \frac{\partial (F_e^{-1})^{\alpha}_c}{\partial x^b}\right) dx^b \wedge dx^c. \tag{1.5.17}$$

It is the occasion to define the dislocation density tensor, or, in a differential-geometric interpretation, the torsion tensor t

$$\mathsf{t}^{a}_{\ bc} = (F_e)^{a}_{\alpha}\left(\frac{\partial (F_e^{-1})^{\alpha}_{b}}{\partial x^c} - \frac{\partial (F_e^{-1})^{\alpha}_{c}}{\partial x^b}\right). \tag{1.5.18}$$

One can equivalently write the dislocation density tensor in terms referred to the initial configuration

$$\mathsf{T}^{A}_{\ BC} = (F_p^{-1})^{A}_{\alpha}\left(\frac{\partial (F_p)^{\alpha}_{B}}{\partial X^C} - \frac{\partial (F_p)^{\alpha}_{C}}{\partial X^B}\right). \tag{1.5.19}$$

Here, (X^A) is a chart respect to the initial configuration. Nevertheless, in this approach the coordinate on the intermediate configuration (z^α) is not explicit.

1.5.2 Geometric theories of defects

1.5.2.1 Dislocation mechanics and Cartan's moving frames

Mechanics of solids with distributed dislocations can be formulated as a classical non-linear elasticity problem (Yavari and Goriely, 2012b). The idea behind this theory is to define the appropriate material manifold by considering Lee-Kröner decomposition as a Cartan's moving frame. The same idea has been previously applied to the mechanics of growing solids (Yavari, 2010). More precisely, the authors showed that in multiplicative plasticity, one could combine the reference and intermediate configurations into a parallelizable material manifold (i.e. the manifold with connection has torsion but no curvature, this connection is metric compatible) by identifying the plastic part to Cartan's moving frames: let (X^A) coordinates in the manifold $\mathscr{B}$, consider a moving frame defined by

$$e_\alpha = (F_p^{-1})^{A}_{\alpha}\partial_A. \tag{1.5.20}$$

We assume that this frame is orthogonal i.e. the metric tensor has a simple representation:

$$\mathsf{G}_{\alpha\beta} = \delta_{\alpha\beta} e^\alpha \otimes e^\beta. \tag{1.5.21}$$

Denote e^α the corresponding coframe of the frame e_α. One requires that this frame is everywhere parallel, and hence back to the natural frame ∂_A the connection has the form

$$\Gamma^{A}_{BC} = (F_p^{-1})^{A}_{\alpha}\frac{\partial (F_p)^{\alpha}_{C}}{\partial X^B}. \tag{1.5.22}$$

Accordingly, the torsion 2-form is

$$\mathsf{T}^{A}_{\ BC} = (F_p^{-1})^{A}_{\alpha}\left(\frac{\partial (F_p)^{\alpha}_{C}}{\partial X^B} - \frac{\partial (F_p)^{\alpha}_{B}}{\partial X^C}\right) dX^B \wedge dX^C. \tag{1.5.23}$$

It is identical to (1.5.19).
The material metric is

$$\mathsf{G}_{AB} = (F_p^{-1})^{\alpha}_{A}(F_p^{-1})^{\beta}_{B}\delta_{\alpha\beta}. \tag{1.5.24}$$

Note that by construction, the connection is metric-compatible, has torsion but has vanishing curvature. The connection and the metric are, in general, time-dependent.

As the manifold is flat (zero curvature), one gets (see Yavari and Goriely, 2012b for details)

$$\operatorname{div} \alpha = 0, \tag{1.5.25}$$

where

$$\alpha^{AB} = \frac{1}{2}\mathsf{T}^{A}_{CD}\epsilon^{BCD} \tag{1.5.26}$$

is the dislocation density tensor.

Following this approach, the intermediate configuration is not necessarily needed. The important thing is that the reference material manifold is now described by a Weitzenböck manifold, which generally depends on time. At the same time, the authors constructed the material manifold for several examples of bodies with distributed dislocations and presented non-trivial examples of zero-stress dislocation distributions. Extension of this geometric approach to distributed disclinations is given in (Yavari and Goriely, 2013).

1.5.2.2 Nonholonomic principle

In this section, we show how the nonholonomic transformations change the intrinsic geometry of matter. This new geometry is interpreted as a material manifold with defects (Kleinert, 2000; Kleinert, 2008). In this context, the continuum is assumed to be a differential manifold $\mathscr{B}$ undergoing a material transformation (a map from $\mathscr{B}$ into $\mathbb{E}^3$) $X \mapsto x$, which may be non-smooth and maybe a multivalued map (to simplify problem we assume (x^a) is Cartesian). However, it is possible to map the points surrounding X defined by the tangent vector dX to dx via an infinitesimal transformation thanks to the triads $\mathbf{e}^a_A$ such that

$$dx^a = \mathbf{e}^a_A dX^A. \tag{1.5.27}$$

Their reciprocal triads are introduced by

$$\mathbf{e}^a_A \mathbf{e}^A_b = \delta^a_b \qquad \text{and} \qquad \mathbf{e}^a_A \mathbf{e}^B_a = \delta^B_A. \tag{1.5.28}$$

Remark 1.5.1. *The notion of the triads $\boldsymbol{e}$ is sometimes introduced with other name (distortion field Peshkov and Romenski, 2016) or as micro-deformation field in the microcontinuum theories Mindlin, 1964; Eringen, 1999 or a Cartan's moving frame in geometrical model Yavari and Goriely, 2012a. It may be the support for analysis of static and dynamics of defects under name vielbein Katanaev, 2005.*

It is therefore usual to define metric-components, as extension of the usual definitions

$$\mathsf{G}_{AB} = \mathsf{g}(\mathbf{e}^a_A e_a, \mathbf{e}^b_B e_b) = \mathbf{e}^a_A \mathsf{g}_{ab} \mathbf{e}^b_B, \tag{1.5.29}$$

where g is the metric tensor of the Euclidean space $\mathbb{E}^3$.

On the other hand, we can differentiate the vector base, and implicitly define an affine connection coefficients

$$\nabla_B e_C = \frac{\partial e_C}{\partial X^B} = \frac{\partial \mathbf{e}^c_C}{\partial X^B} e_c = \mathbf{e}^A_c \frac{\partial \mathbf{e}^c_C}{\partial X^B} e_A := \Gamma^A_{BC} e_A. \tag{1.5.30}$$

The connection may have both torsion and curvature. Furthermore, the multivalued triads form a basic of parallel fields

$$\nabla_A \left(\mathbf{e}^b_B dX^B \right) = \left(\frac{\partial \mathbf{e}^b_B}{\partial X^A} - \Gamma^C_{AB} \mathbf{e}^b_C \right) dX^B = \left(\frac{\partial \mathbf{e}^b_B}{\partial X^A} - \mathbf{e}^C_c \frac{\partial \mathbf{e}^c_B}{\partial X^A} \mathbf{e}^b_C \right) dX^B = 0. \tag{1.5.31}$$

Consequently, the induced metric is also a parallel tensor

$$\nabla_A \mathsf{G} = \nabla_A \left(\mathsf{g}_{bc} \mathbf{e}^b_B dX^B \otimes \mathbf{e}^c_C dX^C \right) = \mathsf{g}_{bc} \nabla_A \left(\mathbf{e}^b_B dX^B \right) \otimes \mathbf{e}^c_C dX^C + \mathsf{g}_{bc} \mathbf{e}^b_B dX^B \otimes \nabla_A \left(\mathbf{e}^c_C dX^C \right) = 0. \tag{1.5.32}$$

However, the connection and metric are, in general, multivalued. It could cause difficulties in performing consistent length measuring and parallel transport. To overcome this difficulty, one has to require that the induced connection and the induced metric are smooth and single-valued. The multivalued fields are driven by mathematical requirements and physical motivations, for instance used to describe magnetic monopoly (Kleinert, 1990; Kleinert, 1992; Kleinert, 2000) and many other systems also described by multivalued fields (Kleinert, 1989; Kleinert, 2008). In addition, even if multi-valuation of some fields may introduce some difficulties, numerical simulations can be performed and lead to applications in solid and fluid mechanics (Dumbser, Peshkov, and Romenski, 2018).

As the construction, several cases may occur, it permits us to highlight the role of torsion and curvature tensors on the classification of continuum transformation:

Holonomic transformation:
If the mapping $X \mapsto x$ is smooth and single-valued, the triads are usually the deformation gradient of the map with

$$\mathbf{e}^a_A = \frac{\partial x^a}{\partial X^A}. \tag{1.5.33}$$

Since the transformation is smooth and single valued, it is integrable i.e. its second derivative commutes

$$\frac{\partial \mathbf{e}^a_A}{\partial X^B} - \frac{\partial \mathbf{e}^a_B}{\partial X^A} = \frac{\partial^2 x^a}{\partial X^A \partial X^B} - \frac{\partial^2 x^a}{\partial X^B \partial X^A} = 0. \tag{1.5.34}$$

Then it is straightforward to check that the torsion is equal to zero undergoing an holonomic transformation:

$$\mathsf{T}^{A}_{BC} = \mathbf{e}^{A}_{a}\left(\frac{\partial \mathbf{e}^{a}_{C}}{\partial X^{B}} - \frac{\partial \mathbf{e}^{a}_{B}}{\partial X^{C}}\right) = 0. \tag{1.5.35}$$

Nonholonomic transformation and torsion:
If $\mathbf{e}$ is single-valued but are not the deformation gradient of a mapping $X \mapsto x$. Then (1.5.34) is not satisfied showing that the torsion tensor is not equal to zero for such a nonholonomic transformation. The induced manifold is a Weitzenböck manifold. This transformation captures translational dislocations of Volterra.

Typical examples of torsion corresponding to edge dislocations are generated by a Volterra process in which a layer of atoms is added or removed Figure 1.10, is given by (Kleinert, 2000)

$$\begin{cases} dx^{1} = dX^{1} \\ dx^{2} = dX^{2} + b\left(\dfrac{\partial}{\partial X^{A}} \arctan \dfrac{X^{2}}{X^{1}}\right) dX^{A}. \end{cases} \tag{1.5.36}$$

The only non-zero component of torsion is $\mathsf{T}^{2}_{12}(X) = \dfrac{b}{2}\delta^{(2)}(X)$ where $\delta^{(2)}$ is a Dirac distribution.

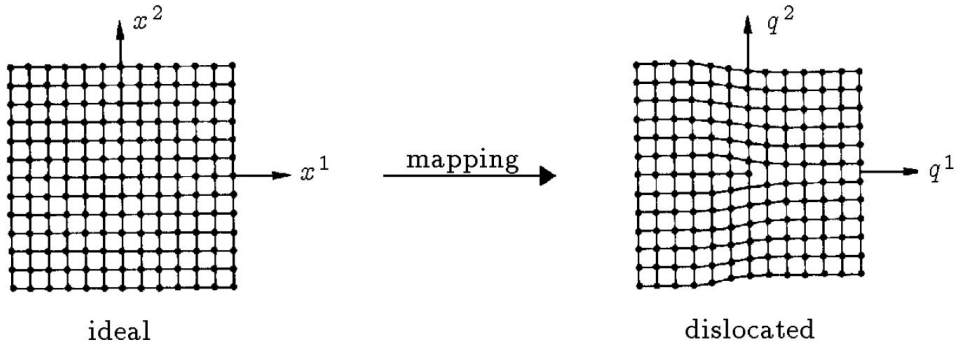

FIGURE 1.10: Here, the letter q is used to replace X. Edge dislocation associated with a missing semi-infinite plane of atoms are created by the multivalued mapping from the ideal (Kleinert, 2000; Kleinert, 2008).

Nonholonomic transformations and curvature:
It is known that the preceeding mapping is not sufficient to describe all topological defects. To go further, we must also add the multivaluedness of the triads. As a consequence, (1.5.34) is still not satisfied. Furthermore, the multivaluedness of the triads lead its second-order derivatives do not commute. It yields that the curvature tensor is not equal to zero (Rakotomanana, 2018)

$$\frac{\partial}{\partial X^{A}}\left(\frac{\partial e_{C}}{\partial X^{B}}\right) - \frac{\partial}{\partial X^{B}}\left(\frac{\partial e_{C}}{\partial X^{A}}\right) = \frac{\partial}{\partial X^{A}}(\Gamma^{D}_{BC} e_{D}) - \frac{\partial}{\partial X^{B}}(\Gamma^{D}_{AC} e_{D}) = \mathsf{R}^{D}_{ABC} e_{D} \neq 0. \tag{1.5.37}$$

We can also calculate the curvature in terms of the triads to give

$$\mathrm{R}^{D}{}_{ABC}e_{D} = \mathbf{e}^{D}_{a}\left(\frac{\partial^2 \mathbf{e}^{a}_{C}}{\partial X^{A}\partial X^{B}} - \frac{\partial^2 \mathbf{e}^{a}_{C}}{\partial X^{A}\partial X^{B}}\right) \neq 0. \tag{1.5.38}$$

Such a transformation may be related to the process of rotational dislocations or some plastic deformations of matter. A typical example corresponding to an edge disclinations is associated with an infinitesimal angle Ω adding in an ideal atomic array Figure 1.11, is defined (Kleinert, 2000; Kleinert, 2008)

$$x^{a} = \delta^{a}_{A}\left(X^{A} - \frac{\Omega}{2\pi}\epsilon^{A}_{B}X^{B}\arctan\frac{X^{2}}{X^{1}}\right). \tag{1.5.39}$$

Here, we remind that

$$\epsilon^{A}_{B} = \begin{cases} 1 & \text{if } (A,B) = (1,2) \\ -1 & \text{if } (A,B) = (2,1) \\ 0 & \text{if } A = B. \end{cases}$$

The only non-zero component of curvature is $\mathrm{R}^{1}_{212}(X) = \Omega\delta^{(2)}(X)$.

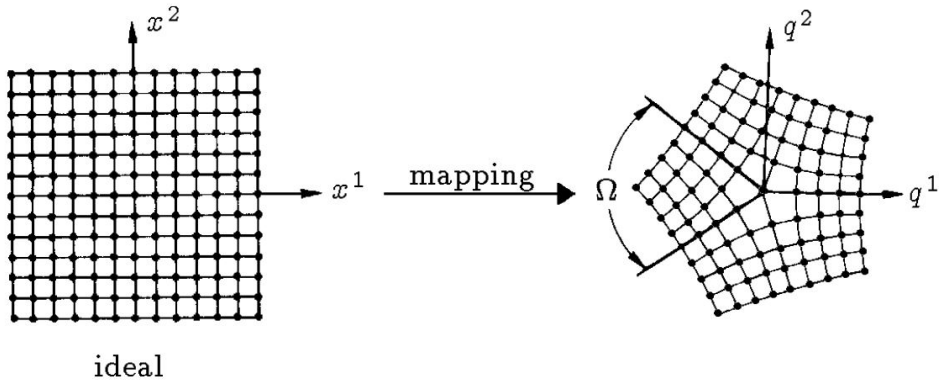

FIGURE 1.11: Edge disclination associated with an adding semi-infinite section of atoms of angle Ω is formulated by the nonholonomic mapping (Kleinert, 2000; Kleinert, 2008).

1.5.2.3 Spin connection

As it has been underlined just before, connection having both torsion and curvature cannot be obtained with single-valued triads. Another method consists in introducing an additional field

$$\omega^{c}{}_{Ba} = S^{c}_{C}\partial_{B}(S^{-1})^{C}_{a}, \tag{1.5.40}$$

where S is the rotation matrix, to give a connection (Obukhov, Ponomariev, and Zhytnikov, 1989; Rakotomanana, 2018) by solving the relation (Katanaev, 2005)

$$\nabla_B \mathbf{e}^c_C = \partial_B \mathbf{e}^c_C - \Gamma^A_{BC}\mathbf{e}^c_A + \mathbf{e}^a_C \omega^c_{Ba} = 0. \tag{1.5.41}$$

Consequently,

$$\Gamma^A_{BC} = \mathbf{e}^A_c \partial_B \mathbf{e}^c_C + \mathbf{e}^A_c \omega^c{}_{Ba}\mathbf{e}^a_C, \tag{1.5.42}$$

where the first term reduces to the Weitzenböck connection with non-zero torsion but zero curvature. The second term $\mathbf{e}^A_c \omega^c{}_{Ba}\mathbf{e}^a_C$ has a role of spin connection, with possibly non-zero torsion and/or non-zero curvature. Such a connection is also metric compatible.

1.6 Contribution of this thesis

1.6.1 Motivation: a reformulation of Eringen's description

Following the paradigm of Cosserat's brothers, the attention is mainly paid to new degree of freedom illustrating the versatility of microstructured media. In terms of physical picture, a material body may be seen as a collection of a huge number of small elements containing a large number of small particles that contribute to the macroscopic behavior of the body. Mathematically, material particles are assumed to be geometric objects (point, vector) that possess physical and mathematical properties i.e. mass, charge, deformable directors. The paradigm of such a continuum model accounting for microstructure effect is the micromorphic medium introduced by Suhubi and Eringen, 1964 and Mindlin, 1964 in 1964. Nowadays, the size effects involved in a natural way in this model have received more and more attention both in statics (Polizzotto, 2013; Forest, 2009; Grammenoudis and Tsakmakis, 2009) and dynamics (Ghiba et al., 2015; Madeo et al., 2015; Madeo et al., 2018).

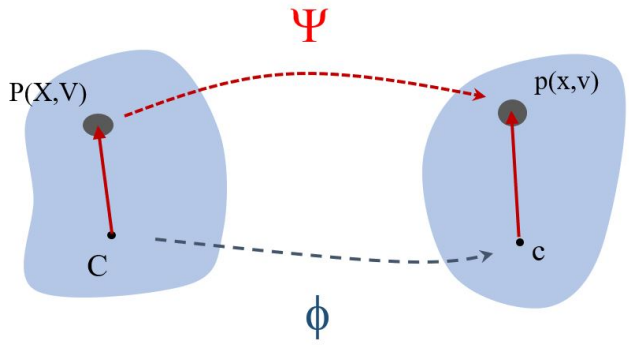

FIGURE 1.12: Deformation of a microelement.

In the micromorphic theory (Eringen, 1999), a material point $P = (X, V) \in T\mathscr{B}$ is characterized by its center of mass C (with coordinates (X^A)) and vector V attached to C. Deformation

carries P to $p = (x, v) \in T\mathbb{E}^3$ in the current state is described by

$$\begin{aligned} X &\mapsto x = \phi(X), \\ V &\mapsto v = \Psi(X)V, \end{aligned} \tag{1.6.1}$$

where $\det F > 0$ and $\det \Psi > 0$. A pictorial interpretation is given in Figure 1.12.

It has been recognized that the evolution of the internal state is the cause of defects in a medium (Kröner, 1981). However, up to the present no connection and metric have been defined illustrating the absence of a geometrical approach related to the micromorphic theories. One of the contributions of this thesis is to fulfil this gap.

Next, we see that even if metric (tensor) and connection are already defined on the manifold $\mathscr{B}$, they actually act on the tangent bundle $T\mathscr{B}$. This suggests that the microcontinuum is then represented by the tangent bundle $T\mathscr{B}$. The material transformation is now a mapping $\Upsilon : T\mathscr{B} \to T\mathbb{E}^3$. Such a map enriches the continuum by an induced geometry pull-backed from the ambient space. The typical example is the transformation (1.6.1):

$$\Upsilon : T\mathscr{B} \to T\mathbb{E}^3, \qquad (X, V) \mapsto (\phi(X), \Psi(X)V), \tag{1.6.2}$$

where Υ is smooth and has an smooth inverse, and preserves orientation, and in general $\Psi \neq D\phi$.

The pull-back of the Levi-Civita connection and the Euclidean metric endow $\mathscr{B}$ with a special type of Riemann-Cartan geometry called Weitzenböck manifold: the connection can have torsion but no curvature. The connection coefficients are exactly the so-called wryness tensor introduced by (Eringen, 1999).

1.6.2 Non scale material modeling: non-linear transformation

Nevertheless, the Weitzenböck manifolds are not suitable to describe all kind of defects since it requires that the connection has both torsion and curvature. A large class of defects can be modelized using connections, this is done by using multivalued triad and multivalued maps in order to encompass disclinations. However, the multivalued fields may cause some difficulties to handle (see Subsection-1.5.2.2).

To overcome this difficulty, several ideas will be proposed: we firstly recognize that fiber bundle manifolds can be used to endow each point on the base manifold additional degrees-of-freedom or internal states, the tangent bundle is the typical example of fiber bundle. In this sense, a microstructured material is modeled by a fiber bundle $\mathscr{M} \xrightarrow{\pi} \mathscr{B}$, the typical example means $\mathscr{M} = T\mathscr{B}$. As an arbitrary fiber bundle manifold, $\mathscr{M}$ can be equipped with a connection-namely Ehresmann connection N and metric tensor G of Sasaki form, in general, these geometric objects and derived quantities (torsion, curvature) may not only depend on position, but also on the internal state. If the bundle is endowed with a connection and a metric, it says fiber geometry (Epstein, 2010; Epstein, 2014; Nakahara, 2003). This extends the Riemann-Cartan geometry for which (relative) position of material points controls all geometric objects. It encompasses various geometries among Euclidean, Riemannian, Weitzenböck, Weyl manifolds (however, the concepts of fiber geometry are out of the scope of *Chapter*-1, we refer the reader to *Chapter*-4 for more details). As usual, the connection and the metric are induced from the Euclidean space by a smooth

transformation represented by a fiber morphism from the bundle $\mathscr{M}$ to the tangent bundle of the Euclidean space.

Hereafter, we restrict ourselves to the linear microstructure case when $\mathscr{M}$ is isomorphic to $T\mathscr{B}$ (to simplify problem $\mathscr{M} = T\mathscr{B}$). Even so, the following methodology may be valid for general cases. Our first idea was to allow non linear transformations of microelements. Such a material transformation is represented by

$$\Upsilon : T\mathscr{B} \to T\mathbb{E}^3, \qquad (X, Y) \mapsto (\phi(X), \Psi(X, Y)). \tag{1.6.3}$$

The connection obtained by pull-back is no longer linear connection and the metric should be replaced by a Sasaki metric. Unfortunately, we proved that even if such connection may have torsion, they never get curvature.

In conclusion, such a bundle map was not sufficient for the intended purpose. One of the main reasons is that the pull-back is performed thanks to the total gradient of Υ. This hypothesis must be relaxed, which we intend to present in the following subsection.

Remark 1.6.1. *Our setting may be interesting to those familiar with (pseudo-)Finsler geometry and its applications. For Finsler space, the connection and its derived quantities (curvature, etc.) are generated by a metric tensor. This geometrical quantity is formed by a fundamental scalar function $L(X, Y)$ that exists at every point except for $Y = 0$, homogeneous of degree one in Y (Bao, Chern, and Shen, 2000). Our theory is more closed to a so-called pseudo-Finsler space (Bejancu, 1990) where the fundamental scalar function with required properties (Bao, Chern, and Shen, 2000), in this context, the components of the metric are obtained by differentiation, does not exist. Accordingly, the connection and metric are completely independent. Application of (pseudo-)Finsler geometry in continuum mechanics and physics have been suggested earlier by Kondo, 1963, later by Saczuk, 1997; Fu, Saczuk, and Stumpf, 1998; Stumpf and Saczuk, 2000, and nowadays by Pfeifer, 2013; Clayton, 2015; Clayton, 2017a; Clayton, 2017b; Yajima and Nagahama, 2020.*

1.6.3 Scaled material model: Higher-order transformations

1.6.3.1 Theoretical analysis

The second idea was to introduce a scaled material model by considering that F defines the stretch of macroelement dV whereas Ψ controls the stretch of a sub-scale micro-element δV. If the material transformation is described by (1.6.2), scaling effects is not directly tractable as F and Ψ are acting on the same space $T\mathscr{B}$. This difficulty can be circumvented in the following way:

Let us consider that a vector Y at a macro-scale belongs to $T_X\mathscr{B}$ and a vector Z at a micro-scale is an element of $VT_X\mathscr{B}$, the transformation may be represented as

$$\Upsilon^v : VT\mathscr{B} \to VT\mathbb{E}^3, \quad (X, Y, Z) \mapsto (\phi(X), F(X)Y, \Theta(X)Z), \tag{1.6.4}$$

with $\det F = |D\phi| > 0$ and $\det \Theta > 0$. Consequently, it is no more redundant since the maps related to each scale act on separated variables. Remark that hereafter, Θ is used instead of Ψ to depict the micro-stretch as these maps are not defined on the same space.

To construct an induced Ehresmann connection, the last idea is to extend Υ^v to the whole space i.e. to find a bundle map Υ: $TT\mathscr{B} \to TT\mathbb{E}^3$ such that

$$\Upsilon(X,Y,Z) = \Upsilon^v(X,Y,Z) \qquad \forall\,(X,Y,Z) \in VT\mathscr{B}. \tag{1.6.5}$$

A priori, $\Upsilon : TT\mathscr{B} \to TT\mathbb{E}^3$ is a map of the form

$$(X,Y,Z) \mapsto (\phi(X), F(X)Y, \Omega(X,Y)Z),$$

with $X \in \mathscr{B}$, $Y \in T_X\mathscr{B}$, $Z \in T_{(X,Y)}T\mathscr{B}$. The extension have to be able to recover the standard model when the material transformation is simply defined by $T\mathscr{B} \to T\mathbb{E}^3$, $(X,Y) \mapsto (\phi(X), \Psi(X,Y))$. In this case, Ω is nothing but the total gradient of such a map. The general-form of Ω should be in the following form:

$$\Omega = F^a_A \partial_a \otimes dX^A + \Omega^i_A \partial_i \otimes dX^A + \Theta^i_J \partial_i \otimes dY^J, \tag{1.6.6}$$

where the choice of Ω^i_A is still free. Let n be the ambient Ehresmann connection derived from the Levi-Civita connection on $T\mathbb{E}^3$. To reduce calculus Without losing any information, we suppose that (x,y) are the Cartesian coordinates, The connection coefficients are equal to zero. The pull-back of n by Υ gives

$$\begin{aligned} N(Y)V &= \Omega^{-1} n(F(X)Y)(\phi_* V) \\ \text{with coefficients} \qquad N^J_A &= \Theta^J_i \Omega^i_A. \end{aligned} \tag{1.6.7}$$

This connection is generally nonlinear. However, as mentioned at the beginning, we need a special hypothesis to ensure the linearity of the connection. It is straightforwardly furnished as follows:

Lemma 1.6.2 (Chapter-5)**.** *The connection is linear i.e.* $N^I_A(X,Y) = \Gamma^I{}_{AJ}(X)Y^J$ *if and only if* $\Omega^i_A(X,Y)$ *is linear i.e.* $\Omega^i_A(X,Y) = \Omega^i_{AJ}(X)Y^J$*. At this context, one gets*

$$\Gamma^I{}_{AJ} = \Theta^I_i \Omega^i_{AJ}.$$

In order to remove this indeterminacy, Ω^i_{AI} is constructed by a linear balance between the stretching variation at each scale:

$$\Omega^i_{AI} = \Big((1-\zeta)\partial_A F^i_I + \zeta \partial_A \Theta^i_I\Big), \tag{1.6.8}$$

where $0 < \zeta \leq 1$ is a free parameter controlling the scaling effect. For example and without loss generality, it can be defined as $\zeta = \ell/L$ where L and ℓ are the macroscopic and microscopic characteristic scales, respectively.
At this stage, one gets

$$\boxed{\Gamma^I{}_{AJ} = \Theta^I_i \Big((1-\zeta)\partial_A F^i_I + \zeta \partial_A \Theta^i_I\Big).} \tag{1.6.9}$$

Usually, an induced metric is obtained by $\mathcal{G} = \Upsilon^* \mathsf{g}$ [2] where is g Riemannian metric of the ambient space. With regarding to the connection N, this metric tensor has a Sasaki structure:

$$\begin{aligned} \mathcal{G}(X,Y) &= \mathsf{G}^h{}_{AB}(X) dX^A \otimes dX^B + \mathsf{G}^v{}_{IJ}(X) \delta Y^I \otimes \delta Y^J \\ \text{with} \qquad \mathsf{G}^h{}_{AB} &= F^a_A \mathsf{g}_{ab} F^b_B \qquad \mathsf{G}^v{}_{IJ} = \Theta^i_I \mathsf{g}_{ij} \Theta^j_J. \end{aligned} \tag{1.6.10}$$

Roughly, this states the existence of two independent mechanisms, the first one is the ordinary dragging of vectors by means of the deformation gradient $F = D\phi$ of the macro-structure. The other mechanism is associated with the transformation Θ of the microstructure.
Their components are functions of the base coordinates X alone. The vertical metric component is explicitly independent of the Ehresmann connection N. More precisely, the components of $\mathcal{G}$ in the proper horizontal and vertical bases are completely specified by Υ^v and independent of the choice of the (possibly non-linear) connection $N(X,Y)$.

The manifold $(\mathscr{M}, \mathcal{G}, \Gamma)$ gives a complete description of the current configuration of the microstructured material. The split structure of the transformation and metrics allows to describe the current state as the superposition of a microscopic and macroscopic processes. The scalar ζ governs such coupling. More precisely, we describe the current configuration on $\mathscr{B}$ by defining a micro-manifold $(\mathscr{B}, \mathsf{G}, \Gamma)$ with $\mathsf{G} \equiv \mathsf{G}^v$ and a macro-manifold $(\mathscr{B}, \mathsf{G}^h, \mathsf{L})$ where L is the Levi-Civita connection of the horizontal metric:

$$\mathsf{L}^C{}_{AB} = \frac{1}{2} \mathsf{G}^{hCD} \Big(\partial_A \mathsf{G}^h{}_{BD} + \partial_B \mathsf{G}^h{}_{AD} - \partial_D \mathsf{G}^h{}_{AB} \Big), \tag{1.6.11}$$

As a consequence, this connection has no torsion and no curvature and is metric-compatible. The property of $(\mathscr{B}, \mathsf{G}, \Gamma)$ is richer.
The following theorem allows us to highlight the classification on the manifolds obtained from the material transformations:

Theorem 1.6.3 (Section-5.2). *If Ω^i_A satisfies lemma-1.6.2, the connection Γ and the metric tensor G construct a large class of manifold $(\mathscr{B}, \Gamma, \mathsf{G})$ where in locally $\mathsf{G}_{AB} = \mathsf{G}^v_{AB}$. In particularly, if Ω^i_A has the form (1.6.8), this manifold is suitable to describe defect-state of the medium and satisfies the following properties*

- *If $\Theta = F$, macro and micro elements behave in the same way. It yields that $\mathsf{T} = 0$; $\mathsf{R} = 0$ and $\nabla \mathsf{G} = 0$. The manifold behaves as an Euclidean space.*
- *If $\zeta = 1$, the scaling effect is no longer considered. In that case the manifold behaves as a Weitzenböck manifold with $\mathsf{T} \neq 0$, $\mathsf{R} = 0$ and $\nabla \mathsf{G} = 0$.*
- *If $\zeta \to 0$, the size of the microsctructure tends to be negligible. Even if $\mathsf{T} \to 0$, one may observe $\mathsf{R} \neq 0$ and $\nabla \mathsf{G} \neq 0$. In particular, if $\nabla \mathsf{G} = 0$, the manifold tends to behaves as Riemann-Cartan manifold.*
- *If $\Theta \neq F$ and $0 < \zeta < 1$, then $\mathsf{T} \neq 0$, $\mathsf{R} \neq 0$ and $\nabla \mathsf{G} \neq 0$. The manifold behaves as a Weyl manifold.*

[2] Υ^* is a pull-back operator or inverse of a gradient of Υ and is defined as the same manner as the definition (1.3.1).

To summarize, our idea is to introduce a new degree of freedom into the material transformations. Hence, even if the macroscopic mapping is still smooth, the additional field does modify the internal topology of the medium. The proposed theory encompasses the macroscopical and microscopical universes as a whole. All the physical quantities that we focused on are single-valued and smooth. Then all geometrical quantities are smooth and single-valued, too, without any "extraordinary" assumption like the nonholonomic principle. Consequently, both theoretical and numerical analysis may be handled without additional difficulties. The general kinematic structure of the theory includes macroscopic and microscopic fields in a multi-scaled approach (represented by the scaling factor ζ), including finite transformations.

To highlight the potential of the new theory, several examples of transformation producing a distribution of material defects are exhibited and analyzed. Particular attention is paid to transports along a finite path to extend the traditional infinitesimal analysis of torsion and curvature to a macroscopical observation.

Last but not least, the new methods could motivate some interesting issues. For example, other extensions Υ and families of scaling factors may exist. They may be chosen in order to treat materials with specific microstructures. Physically and mathematically, the appearance of the scaling factor seems convenient and clear. A mechanical process having the advantage of the scalar factor ζ is, however, still absent at the moment. It promises an interesting mission for further researches. Our geometric setting is consistent with the microcontinuum framework. It is able to reformulate the microcontinuum field in a universal language of differential geometry. The geometrical nature of our approach also indicates that it is able to obtain a relativistic version of the theory, which must conform to the geometrical settings of general relativity.

1.6.3.2 Geometric illustration

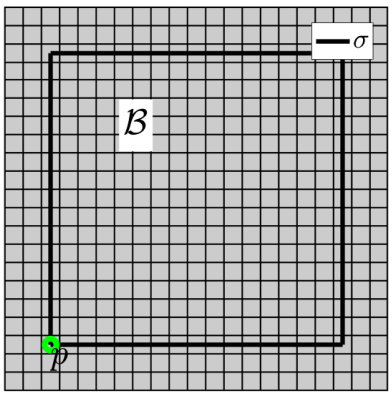

FIGURE 1.13: representation of the body $\mathscr{B}$. Cells are a representation of $VT_p\mathscr{B}$. A closed material loop $\sigma(t)$ is specified.

To give a short presentation but without loss generality, let us consider that $\mathscr{B}$, which is labeled by the two Cartesian coordinates (X^1, X^2), is a subset in the 2D Euclidean space, see

Figure 1.13; and a typical material transformation Υ^v that is completely defined by

$$F = \begin{pmatrix} 1 & 0 \\ 0 & 1 \end{pmatrix} \qquad \text{and} \qquad \Theta = \begin{pmatrix} 1 & \theta(X^1) \\ 0 & 1 \end{pmatrix}. \tag{1.6.12}$$

With these, we can entirely describe the deformation of the body, that is really presented in Figure 1.14 in which the shape of the macroelement is unchanged (since $F = \delta$) but their relative micro-cells change according to Θ. Hence, the transformation induces at the macroscopic level, the initial state Figure 1.13 and the deformed state Figure 1.14 have the same shape, but it includes a perturbation at micro-scale. Such a picture is commonly used to interpret dislocations density.

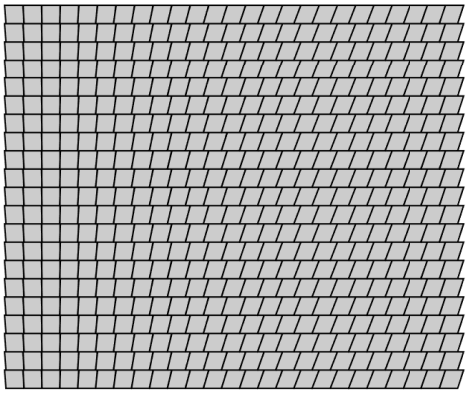

FIGURE 1.14: Representation in the ambient space of the current configuration for the transformations (1.6.12) with $\theta(X^1) = \frac{\pi}{4}\cos(\frac{X^1}{4L}\pi)$.

Now, in order to compare a matter with another, we need a connection to define the parallel transport of vector (fields). The complete transformation Υ has been introduced for that purpose. It has to be ensured that the properties of the connection (i.e. torsion and curvature tensors,...), that are derived from Υ, must coincide with the properties of Υ^v. Accordingly, it allows us to decide whether the material transformation Υ^v creates defects. Last, to measure lengths and angles, metrics tensors have to be defined too.

Suppose that Υ is defined by (1.6.4) with the hypothesis (1.6.8), one gets the induced connection Γ (see (1.6.9)). At the same time, the metrics (see (1.6.10)) are also defined, they are compatible with the deformations of the micro and macro cells undergoing the transformation Υ^v (see Figure 1.14, this picture is useful to illustrate the two metrics). Since we investigate the two different mechanics in a whole, it is useful to express things on a finite domain.First, if we parallel transport a vector along a loop, the resulting vector coincides with the initial one, which means there is no curvature (see Figure 1.15 as an example). Nevertheless, such process is not sufficient to verify the presence of torsion.

In addition to the classical parallel transport, a particular attention is paid to a so-called rolling without slipping transport. Roughly speaking, it allows us to lift a curve in $\mathscr{B}$, passing through a given point $p \in \mathscr{B}$ to the tangent $T_p\mathscr{B}$. The lift of a given curve σ is denoted by $\widetilde{\sigma}$, and named by the developing curve. Conversely, a given $\widetilde{\sigma}$ with the initial point p determines

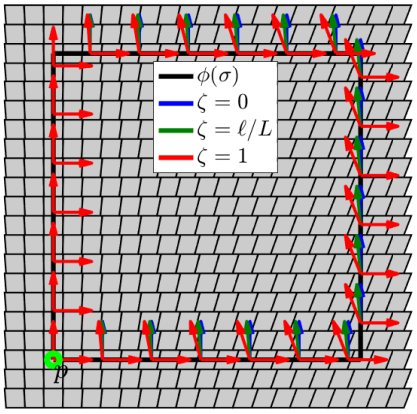

FIGURE 1.15: Representation in the ambient space of the current configuration for the transformations (1.6.12) the developing curve $\widetilde{\sigma}$ obtained for various ζ. There is no curvature but the non-zero torsion: $\mathsf{T}^1_{12} = -\mathsf{T}^1_{21}$, last the metric is not compatible with the induced connection.

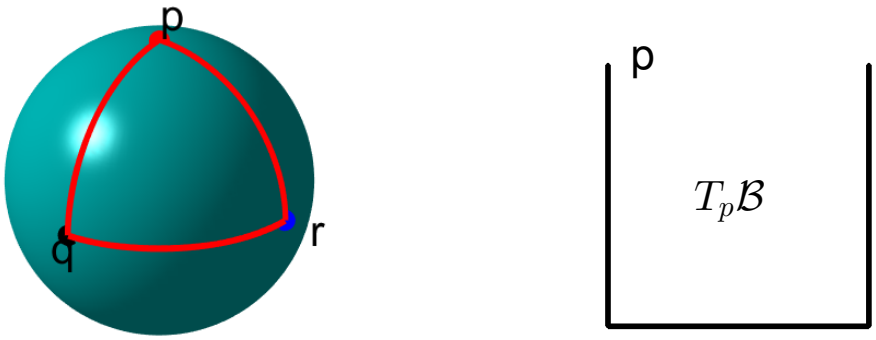

FIGURE 1.16: A pictorial representation of the developing curves: $\mathscr{B}$ is a sphere, a loop σ given on the sphere has an intrinsic curvature of the manifold. Its developing curve $\widetilde{\sigma}$ defined on $T_p\mathscr{B}$ is no more closed, it convinces the presence of the curvature on $\mathscr{B}$.

a unique curve σ (namely the driven curve) in $\mathscr{B}$. Hence, detection of defects can be performed in the tangent bundle $T\mathscr{B}$ or the base manifold $\mathscr{B}$. If the connection has vanishing torsion and curvature, developing curves of a loop in $\mathscr{B}$ still closed. Otherwise, it is no longer true. The gap is a quantifier of dislocation density in the case the curvature is absent. A pictorial representation of the developing curve is given in Figure 1.16. The transformation (1.6.12) is a typical example for which the developing curve is no longer closed (when $\zeta \neq 0$), the resulting gap proves the presence of torsion; moreover, this gap is dependent on ζ Figure 1.17.

Notice that the preceding process does not correspond to the classical (but heuristic) way to define a Burger circuit, over an infinitesimal material loop (the loop in $\mathscr{B}$). Another strategy has been proposed. More precisely, for the given $\widetilde{\sigma}$, a so-called driven curve is obtained suing the connection of the base manifold. This curve is renamed a Burger circuit $\underline{\sigma}$, and it does not coincide with σ in the case of the presence of defects. For example, we consider the example (1.6.12) for which the Burger circuit is not closed, see Figure 1.18.

To sum up, the Burger circuit is not a topological invariant. On the contrary, the developing

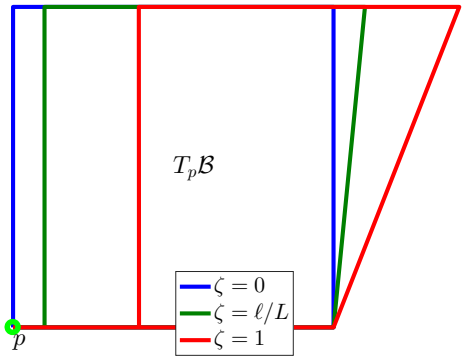

FIGURE 1.17: Representation in the ambient space of the current configuration for the transformations (1.6.12) the parallel transport of the frame along the loop σ obtained for various ζ.

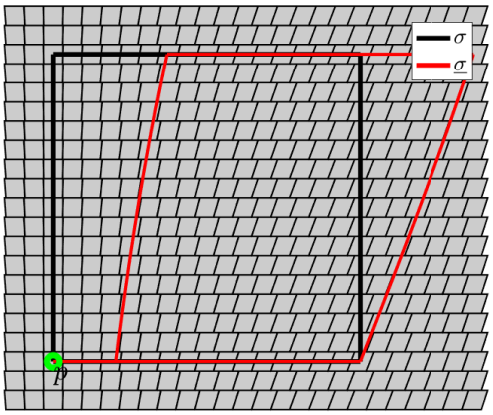

FIGURE 1.18: Burger's circuit $\underline{\sigma}$ obtained for various $\zeta = 1$ and for the transformation (1.6.12) represented in the ambient space.

curve looks more robust for quantification of the density of defects. Moreover, this curve is useful to discriminate the presence of curvature too (see *Chapter*-5).

1.6.4 Outline

1. *Chapter*-2 is devoted to describe how the bundle mapping (1.6.2) induces a material affine connection and metric in the framework of RC geometry. Several physical illustrations are also given to demonstrate that this formalism can simulate the creation of dislocations.

2. In the chapter one, we see how the material transformation (1.6.2) changes the intrinsic geometry of matter. This new geometry is interpreted as a material manifold with defects. Until now, ϕ and Ψ are unknown. Wwe have to look for to entirely describe the motion of matter. For that purpose, variational process is given to determine governing equations of motion. That is the aim of *Chapter*-3.

3. *Chapter*-4 gives descriptions of microstructured materials as a field of applications of fiber geometry. For example, the linear microstructure may be considered as a fiber bundle $\mathscr{M} \xrightarrow{\pi} \mathscr{B}$ where $\mathscr{M}$ is isomorphic to $T\mathscr{B}$. The basic concepts of fiber bundle manifold and Ehresmann connection are first presented. The split structure of the tangent bundle over $\mathscr{M}$ derived from the Ehresmann connection recommends introducing the so-called Sasaki metric. The split structure of the metric suggests that there exists two independent mechanisms and allows us to investigate them more efficient. Soon, we can see in the next chapter that the use of such a metric is completely natural. Moreover, the components of the metric in the proper horizontal and vertical bases are entirely independent of the choice of the connection. Relations between Ehresmann connection and an affine connection are somewhat clear. The solder form is initially introduced to emphasize these relationships. Nevertheless, it may reveal some properties that enable us to investigate specific microstructures.

4. *Chapter*-5 explores how the language of fiber bundle geometry may help us overcome the limitation just obtained from the first approach (see *Chapter*-2). We use these notions Ehresmann connection, solder form, Sasaki metric to describe structural changes in real materials. In this context, a scaled material modeling is introduced, which concerns material transformations represented by fiber morphisms, an induced connection and metric are first described, then derived geometrical quantities such as curvature, torsion, and nonmetricity tensor are obtained. Alternative approaches are reviewed and compared to highlight significant features of this model. The chapter ends with a presentation of the applications of this theory.

List of publications and talks

Publications and proceedings:

1. On tangent geometry and generalized continuum with defects. Mathematics and Mechanics of Solids (published 2021).
2. Kinematics of defected material : a geometrical point of view. Conference paper - The 24th French Congress of Mechanics (CFM 2019), Brest-France.
3. Geometrical approach on kinematics of defected material. Conference paper - The 25th International Congress of Theoretical and Applied Mechanics (ICTAM 2021), Milano-Italy.

Talks at conferences and congresses:

1. The 25th International Congress of Theoretical and Applied Mechanics (ICTAM 2021), August, Milano-Italy.
2. Differential Geometry and Mechanics - GDR-GDM. July 2021, La Rochelle-France.
3. Multiscale problems and mathematical physics. June 2021, Angers-France.
4. Differential Geometry and Mechanics- GDR-GDM. November 2020, Paris-France.
5. The 24th French Congress of Mechanics - CFM. August 2019, Brest-France.
6. Differential Geometry and Mechanics - GDR-GDM. June 2019, La Rochelle-France.

Part I

Riemann-Cartan geometry applied to mechanics

Chapter 2

Geometrical approach to kinematics of defected material

It has been recognized long time ago that continuums with a distribution of defects have a close connection with RC manifolds. The equality of the torsion tensor to zero is naturally considered as a criterion for the absence of dislocations density. On the other hand, disclinations density is closely related to the curvature tensor of the material connection.

Our study consists in constructing such geometry meaning to define a metric and a connection modelling a material. To do so, we propose a new approach inspired by the microcontinuum theory where points and vectors behave independently. More precisely, the continuum is modelized by the tangent space $T\mathscr{B}$. The material transformation is then a smooth mapping Υ: $T\mathscr{B} \to T\mathbb{E}^3$ where $\mathbb{E}^3$ is the three-dimensional Euclidean space. This mapping may depend on time. In this chapter, we will show how such mapping changes the intrinsic geometry of the continuum. The resulting geometry (here, Weitzenböck manifold) is expressed on the body manifold $\mathscr{B}$, but it allows us to describe microscopic defects of the continuum. The mapping Υ may induce perturbations of the continuum that may capture the translational defects (dislocations). Hence, it permits us to highlight the role of the torsion tensor on the classification of the continuum transformations. In some senses, our model may provide a bridge between the classical geometrical theory of defects and the micromorphic theory. Additionally, the new approach could be compared with the nonholonomic principle. The advantage of the present model is that we only analyze single-valued maps rather than multivalued ones according to the nonholonomic principle. It results that the current model is the easier to handle for both numerical and theoretical analysis. The limitation of this approach is that the induced connection is metric-compatible, has torsion but has vanishing curvature. As a first step, this study provides a key idea to help

us find another geometry background that is more consistent with the microstructured medium with distributions of defects. It helps us to overcome the shortcoming that the present study captured.

Section-2.1 is devoted to describing how a material affine connection and a metric are induced by the bundle mapping Υ. In *Section*-2.2, we present a physical picture to show how micro-deformation of bodies gives rise to the extra degree of freedom necessary to characterize the microstructured continuum. Some examples are reported in *Section*-2.3. It is the occasion to exhibit the physical meaning of each geometrical quantity and then state how our model is useful to illustrate creations of defects.

2.1 Riemann-Cartan geometry and defects

A geometrical interpretation of the transformations of material is first presented in terms of RC manifold. This formalism invokes only smooth functions, but it can simulate the creation of defects. Through this, we will examine the limitation of such an approach.

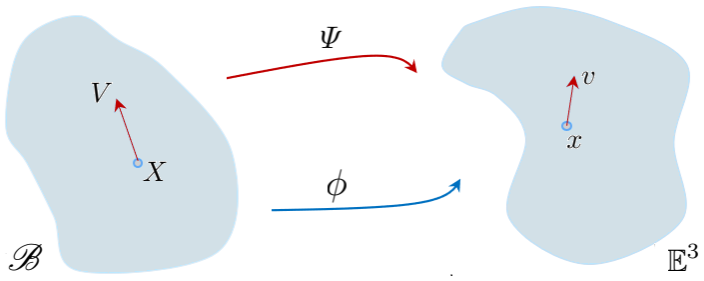

FIGURE 2.1: The bundle map Υ is defined by the transformation ϕ of the point and the tangent map Ψ at this point. The map of vector Ψ is generally not necessary the derivative of ϕ.

2.1.1 An induced geometrical structure

Let us consider a bundle mapping

$$\Upsilon \ : \ T\mathscr{B} \to T\mathbb{E}^3, \qquad (X, V) \mapsto (\phi(X), \Psi(X)V) \tag{2.1.1}$$

where Υ is smooth, has a smooth inverse and preserves orientation. In addition, one allows $\Psi \neq F$, here we remind F is the deformation gradient of ϕ. A pictorial interpretation is given in Figure 2.1. Hereafter, a standard convention is used: capital letter for the initial state and small letter are used for the current state. In particular, ∂_a (respectively ∂_A) is the natural basis defined on $\mathbb{E}^3$ (respectively $\mathscr{B}$).

The vector transformation $\Psi(X) : T_X\mathscr{B} \to T_x\mathbb{E}^3$ is linear and satisfies $\det \Psi(X) > 0$. The linear map $\Psi(X)$ can be expressed by $\Psi(X) = \Psi^a_A(X)\partial_a \otimes dX^A$. Its inverse is a map $T_x\mathbb{E}^3 \to T_X\mathscr{B}$ given by $\Psi^{-1}(x) = \Psi^A_b(x)\partial_A \otimes dx^b$ with

$$\Psi^B_b(x)\Psi^a_B(X) = \delta^a_b \qquad \text{and} \qquad \Psi^A_b(x)\Psi^b_B(X) = \delta^A_B. \tag{2.1.2}$$

The deformation gradient of ϕ is $F = D\phi$ (sometimes denoted ϕ_*). For any $X \in \mathscr{B}$, $F(X)$ is a linear map from $T_X\mathscr{B}$ into $T_x\mathbb{E}^3$. In terms of components, $F = F^a_A \partial_a \otimes dX^A$ with $F^a_A = \partial_A \phi^a$ satisfying $\det F(X) > 0$. Its inverse $\phi^*(x)$ is given by $\phi^*(x) = F^A_b(x)\partial_A \otimes dx^b$ with

$$F^A_b(x)F^a_A(X) = \delta^a_b \qquad \text{and} \qquad F^A_b(x)F^b_B(X) = \delta^A_B. \tag{2.1.3}$$

Note that the notation $x = \phi(X)$ is used with $X \in \mathscr{B}$. If there is no room for confusion, we neglect the notations x, X in some formulas.

Let us denote ∇^0 the Levi-Civita connection defined on $\mathbb{E}^3$ with coefficients $\gamma^a_{\ bc}$, the ambient metric

$$\mathsf{g}(x) = \mathsf{g}_{ab}(x)dx^a \otimes dx^b. \tag{2.1.4}$$

By definition, the connection ∇^0 is metric-compatible $\nabla^0 \mathsf{g} = 0$.
Let U, V be vector fields on $\mathscr{B}$, we define the two quantities G and ∇ given on $\mathscr{B}$ as follows:

$$\mathsf{G}(U, V) = \mathsf{g}(\Psi U, \Psi V) \qquad \text{and} \qquad \nabla_V U = \Psi^{-1}(\nabla^0_{\phi_* V}\Psi U). \tag{2.1.5}$$

In terms of components,

$$\mathsf{G}_{AB} = \Psi^a_A \mathsf{g}_{ab}\Psi^b_B \qquad \text{and} \qquad \Gamma^A_{BC} = \Psi^A_c F^b_B(\Psi^a_C \gamma^c_{\ ab} + \partial_b \Psi^c_C). \tag{2.1.6}$$

Proposition 2.1.1. *∇ is an affine connection defined on $\mathscr{B}$. Furthermore, the connection ∇ is compatible with the metric* G.

Proof. We first need to verify that ∇ is an affine connection defined on $\mathscr{B}$. Recall f is a smooth real function, V, U, W are vector fields over $\mathscr{B}$, one has

$$\begin{aligned}
\nabla_{V+U}W &= \Psi^{-1}\nabla^0_{\phi_*(V+U)}\Psi W \\
&= \Psi^{-1}(\nabla^0_{\phi_* V}\Psi W + \nabla^0_{\phi_* U}\Psi W) \\
&= \Psi^{-1}\nabla^0_{\phi_* V}\Psi W + \Psi^{-1}\nabla^0_{\phi_* U}\Psi W \\
&= \nabla_V W + \nabla_U W.
\end{aligned}
\qquad
\begin{aligned}
\nabla_V(U+W) &= \Psi^{-1}\nabla^0_{\phi_* V}\Psi(U+W) \\
&= \Psi^{-1}(\nabla^0_{\phi_* V}\Psi U + \nabla^0_{\phi_* v}\Psi W) \\
&= \Psi^{-1}\nabla^0_{\phi_* V}\Psi U + \Psi\nabla^0_{\phi_* V}\Psi W \\
&= \nabla_V U + \nabla_V W.
\end{aligned} \tag{2.1.7}$$

and

$$\begin{aligned}
\nabla_{(fV)}U &= \Psi^{-1}\nabla^0_{\phi_*(fV)}\Psi U \\
&= \Psi^{-1} f\nabla^0_{\phi_* V}\Psi U \\
&= f\Psi\nabla^0_{\phi_* V}\Psi U \\
&= f\nabla_V U.
\end{aligned}
\qquad
\begin{aligned}
\nabla_V(fU) &= \Psi^{-1}\nabla^0_{\phi_* V}\Psi(fU) \\
&= \Psi^{-1}(\phi_* V[f]\Psi U + f\nabla^0_{\phi_* V}\Psi U) \\
&= \Psi^{-1}(\phi_* V[f])\Psi U + \Psi^{-1}(f\nabla^0_{\phi_* V}\Psi U) \\
&= \phi_* V[f]U + f\nabla_V U \\
&= (\partial_A \phi^a)V^A(\partial_a f(\phi(X)))U + f\nabla_V U \\
&= (\partial_A \phi^a)V^A(\partial_B f)(\partial_a \phi^{-1B})U + f\nabla_V U \\
&= V[f]U + f\nabla_V U.
\end{aligned} \tag{2.1.8}$$

Moreover, as follow we prove that the connection ∇ is compatible with the metric G. From

$$\nabla^0_{\phi_* V}(f\circ\phi^{-1}) = \phi_* V[f\circ\phi^{-1}] = F^a_A V^A \frac{\partial(f\circ\phi)}{\partial x^a} = F^a_A V^A \frac{\partial f}{\partial X^B} F^B_a = V^A \frac{\partial f}{\partial X^A} = V[f] = \nabla_V f,$$

one gets

$$\nabla_V \mathsf{G}(W,U) = \nabla^0_{\phi_* V}\mathsf{g}(\Psi W, \Psi U).$$

Put $v = \phi_* V$, $u = \Psi U$ and $w = \Psi W$, one obtains

$$\mathsf{G}(W,\nabla_V U) + \mathsf{G}(\nabla_V W, U) = \mathsf{g}(w,\nabla^0_v u) + \mathsf{g}(\nabla^0_v w, u) = \nabla^0_v \mathsf{g}(w,u) = \nabla_V \mathsf{G}(W,U).$$

This proves that $\nabla\mathsf{G} = 0$.
To end the proof, we find out components of the induced metric G and the connection ∇: for any $U, V \in T_X\mathscr{B}$, the induced metric reads $\mathsf{G}_{AB} = \Psi^a_A \mathsf{g}_{ab}\Psi^b_B$. Remind that ∂_a (respectively ∂_A) is the natural basis defined on $\mathbb{E}^3$ (respectively $\mathscr{B}$) with respect to the chosen coordinates. One gets

$$\begin{aligned}\nabla_{\phi_*\partial_B}(\Psi\partial_A) &= \nabla^0_{F^b_B\partial_B}\Psi^a_A\partial_a \\ &= F^b_B(\Psi^a_A\nabla^0_{\partial_b}\partial_a + \partial_b\Psi^a_A\partial_a) \\ &= F^b_B(\Psi^a_A\gamma^c{}_{ab} + \partial_b\Psi^c_A)\partial_c.\end{aligned}$$

Consequently,

$$\nabla_{\partial_B}\partial_A = \Psi^{-1}(\nabla^0_{\phi_*\partial_B}\Psi\partial_A) = \Psi^C_c F^b_B(\Psi^a_A\gamma^c{}_{ab} + \partial_b\Psi^c_A)\partial_C$$

Therefore, we obtain that the connection coefficients are

$$\Gamma^C_{BA} = \Psi^C_c F^b_B(\Psi^a_A\gamma^c{}_{ab} + \partial_b\Psi^c_A). \tag{2.1.9}$$

This ends the proof. □

The antisymmetric part of the affine connection defines the torsion tensor T. When the Cartesian coordinates are used, the connection coefficients are $\gamma^c{}_{ab} = 0$, and hence the induced connection coefficients may be written as

$$\Gamma^A_{BC} = \Psi^A_a\partial_B\Psi^a_C. \tag{2.1.10}$$

and the torsion tensor becomes:

$$\mathsf{T}^A_{BC} = \Psi^A_a(\partial_B\Psi^a_C - \partial_C\Psi^a_B). \tag{2.1.11}$$

Remark 2.1.2. *The connection coefficients are exactly as the same as the so-called wryness tensor introduced by Eringen (Eringen, 1999).*

Proposition 2.1.3. *The induced torsion vanishes if and only if there exists (at least locally) a function $\psi : \mathscr{B} \to \mathbb{E}^3$ such that $\Psi = D\psi$.*

Proof. Trivially, if there exists a function $\psi : \mathscr{B} \to \mathbb{E}^3$ such that $\Psi = D\psi$ the connection induced by $\Upsilon : T\mathscr{B} \to T\mathbb{E}^3$ has zero torsion. Without losing any information, we assume that Cartesian

coordinate system on $T\mathbb{E}^3$ are used. The torsion $\mathsf{T} = 0$ yields to $\Gamma^C_{BA} = \Gamma^C_{AB}$ i.e. $\Psi^C_c \partial_B \Psi^c_A = \Psi^C_c \partial_A \Psi^c_B$. Then, one gets $\partial_B \Psi^c_A = \partial_A \Psi^c_B$. Write $\omega^c = \Psi^c_A dX^A$ (with $c = 1, 2, 3$ must be seen as labels of the one-form and not as indices). Its exterior derivative [1] is the 2-form:

$$\mathrm{d}\omega^c = (\partial_A \Psi^c_B - \partial_B \Psi^c_A) dX^A \wedge dX^B. \tag{2.1.12}$$

Hence, the torsion T vanishes if and only if $\mathrm{d}\omega^c = 0$. Remind that a r-form β is called exact if there is a $(r-1)$-form such that $\mathrm{d}\eta = \beta$. The r-form β is closed if $\mathrm{d}\beta = 0$. Note that if a 1-form is closed, there each point has a neighborhood on which it is exact (see definition in (Epstein and Segev, 2014)). Applying this result, there exists η^c (at least locally on $\mathscr{B}$) such that $\mathrm{d}\eta^c = \omega^c$ and hence $\Psi^c_A = \partial_A \eta^c$. This establishes that $\psi = (\eta^1, \eta^2, \eta^3)$. □

Proposition 2.1.4. *The connection ∇ has zero curvature.*

Proof. As the curvature tensor is a map $\mathsf{R} : T\mathscr{B} \times T\mathscr{B} \times T\mathscr{B} \to T\mathscr{B}$ defined by $\mathsf{R}(U, V)W = \nabla_U \nabla_V W - \nabla_V \nabla_U W - \nabla_{[U,V]} W$, direct computations show:

$$\begin{aligned} \mathsf{R}(U, V)W &= \nabla_U \Psi^{-1}\left(\nabla^0_{\phi_* V} \Psi W\right) - \nabla_V \Psi^{-1}\left(\nabla^0_{\phi_* U} \Psi W\right) - \Psi^{-1}\left(\nabla^0_{\phi_*[U,V]} \Psi W\right) \\ &= \Psi^{-1}\left(\nabla^0_{\phi_* U} \nabla^0_{\phi_* V} \Psi W - \nabla^0_{\phi_* V} \nabla^0_{\phi_* U} \Psi W - \nabla^0_{[\phi_* U, \phi_* V]} \Psi W\right) \\ &= \Psi^{-1} \mathsf{R}^0(\phi_* U, \phi_* V) \Psi W. \end{aligned} \tag{2.1.13}$$

Since the curvature R^0 of the Euclidean space is zero, R vanishes. □

Remark 2.1.5. *The forms of the metric and the connection looks qualitatively similar to the ones in almost all defect-theories, see Section-(1.9), (1.5.2.1). Among them, one of the powerful tools is the nonholonomic principle Kleinert, 2008; Kleinert, 2000. Roughly, Ψ plays the same roles as* **e**. *It suggests that* G *can be used to measure lengths and relative angles on $\mathscr{B}$. Nevertheless, the present approach differs on a crucial point. The motion of the material manifold $\mathscr{B}$ is presented by Υ that consists of two independent variables, ϕ and Ψ, that are both smooth and single-valued maps. This point allows wide types of mathematical analysis and numerical simulation may be more comfortably handled.*

Remark 2.1.6. *The bundle map seems to be an alternative representation of elastoplastic process with $\mathbb{F} = \Psi$, the elastic deformation part $\mathbb{F}_e = F = D\phi$, and immediately $\mathbb{F}_p = F^{-1}\Psi$. However, in such a way, the intermediate configuration is not needed. In fact, we have identified this configuration to the initial configuration.*

2.1.2 Geometrical interpretation of the induced connection

Denote $\sigma(t)$ a curve in $\mathscr{B}$, this curve generates a vector field $U = \dot{\sigma}(t)$ along σ with $t \in \mathbb{R}$. Let V be another vector field defined along σ. To determine an affine connection on the current manifold, we have to specify how the vector field V is parallel transported from one material

[1] If we denote the vector space of r-forms $\Omega^r(\mathscr{B})$, the exterior derivative d_r is a map $\Omega^r(\mathscr{B}) \to \Omega^{r+1}(\mathscr{B})$ whose action on an r-form $\omega = \frac{1}{r!}\omega_{\mu_1,..,\mu_r} dx^{\mu_1} \wedge ... \wedge dx^{\mu_r}$ is defined by $d_r\omega = \frac{1}{r!}(\partial_\nu \omega_{\mu_1,...,\mu_r} dx^{\mu_1}) \wedge ... \wedge dx^{\mu_r} \wedge dx^\nu$ Nakahara, 2003

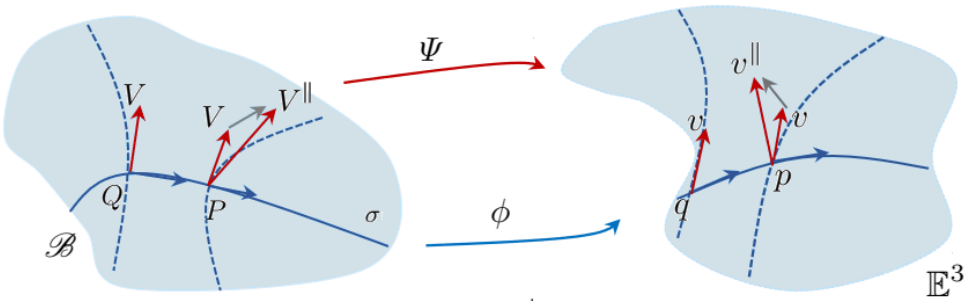

FIGURE 2.2: Pictorial representation of the induced connection: Two points P, Q belonging to $\sigma(t)$ are very close. Let $v = \Psi V$ and $v_p^{\parallel}$ be a parallel transport of v_q from q to p. The gap between $v_p^{\parallel}$ and v_p gives us a covariant variation of v along u. Hence, its pull-back is the gap between $V_P^{\parallel}$ and V_p by Ψ.

point to another along $\sigma(t)$. The following proposition establishes the link between parallel transport and a connection.

Proposition 2.1.7 (Chapter 1, Page 74, Marsden and Hughes, 1994)**.** *Let $\sigma(t)$ be a given curve in $\mathscr{B}$ generating $U := \dot{\sigma}(t)$, and V be a vector field defined along σ. Denote $\rho_{t,s} : T_{\sigma(s)}\mathscr{B} \to T_{\sigma(t)}\mathscr{B}$ is a parallel transport from $\sigma(s)$ to $\sigma(t)$. Then*

$$\nabla_{\dot{\sigma}(t)} V(\sigma(t)) = \frac{d}{ds}\Big(\rho_{t,s} V(\sigma(s))\Big)_{|s=t}.$$

Let $\ell_{t,s} : T_{\phi(\sigma(s))}\phi(\mathscr{B}) \to T_{\phi(\sigma(t))}\phi(\mathscr{B})$ denote the parallel translation from $\phi(\sigma(s))$ to $\phi(\sigma(t))$. Then, the parallel translation $\rho(t,s)$ is naturally defined by

$$\rho(t,s) = \Psi^{-1}(\sigma(t)) \circ \ell_{t,s} \circ \Psi(\sigma(s)). \tag{2.1.14}$$

Insert (2.1.7) into (2.1.14), we conclude that

$$\begin{aligned}
\nabla_{\dot{\sigma}(t)} V(\sigma(t)) &= \Psi^{-1}(\sigma(t)) \frac{d}{ds}\Big(\ell_{t,s}\Psi(\sigma(s))V(\sigma(s))\Big)_{|s=t} \\
&= \Psi^{-1}(\sigma(t))\nabla^0_{(\dot{\phi\sigma})(t)}\Psi(\sigma(t))V(\sigma(t)) \\
&= \Psi(\sigma(t))\nabla^0_{\phi^*\sigma(\dot{t})}\Psi(\sigma(t))V(\sigma(t)).
\end{aligned}$$

It verifies $\nabla_U V = \Psi^{-1}\nabla^0_{\phi_* U}\Psi V$.

2.2 Physical interpretations

Some physical illustrations are presented hereafter. It is the occasion to interrogate the physical meaning of each geometrical quantities but also the way to illustrate each phenomena.

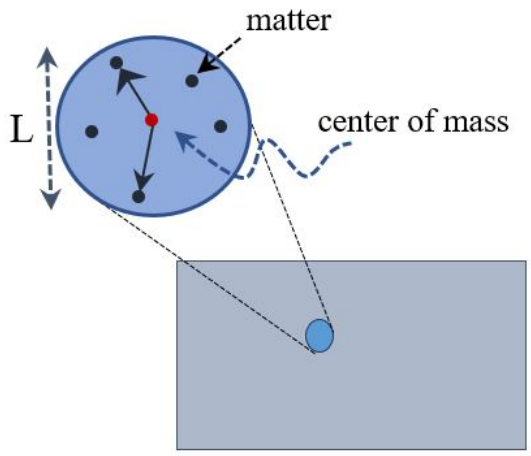

FIGURE 2.3: Micro structure of a media: a center of mass of infinitesimal element dV is assumed to be a mathematical point p belongs to $\mathscr{B}$, while an atom including the element is identified with a tangent vector to the manifold $\mathscr{B}$ at the point p.

2.2.1 Physical picture

When geometrical description is used to express mechanical processes, it is assumed that the body consists of a huge number of infinitesimal volume elements dV which are considered as mathematical points in the base manifold $\mathscr{B}$. The motion of such a point P is governed by the map ϕ. Mathematically, these points span the body continuously, whereas mechanically speaking, the volume element dV contains a finite quantity of matter (for which P is interpreted as the center of mass of dV). More interestingly, this interpretation breaks the continuous interpretation of mathematical points as matters are presented between two adjacent points P′. This remark remains without effect if the mater in dV is stretched by $D\phi$, as in the standard Riemannian description of continuum mechanics Marsden and Hughes, 1994. Relaxing this hypothesis consists in considering that each material element (*atom*) in dV supports a stretch associated with a map $\Psi \neq D\phi$.

In the reference configuration, let us denote U the local position vector of an atom relative to P, i.e. U is the two-point vector PA (with base P and head A) in dV. In a non-Riemannian case, $u = \Psi\, U$ is associated with the current position of this atom relatively to the material center of mass P. This description is closely related to the Eringen point of view in the Eringen-Mindlin theory in Suhubi and Eringen, 1964; Eringen and Suhubi, 1964; Eringen, 1999. In the following, this approach is called unique-scale modeling (*USM*).

2.2.1.1 Numerical simulation

In the present section, graphical simulations are performed in order to propose illustrations of each process. These simulations represent the current state of the material domain lying in the Euclidean space. Hence, the position of each material point P is prescribed by $x = \phi(X)$. These points are elements of a Cartesian grid in the reference configuration $\mathscr{B}$. The size of the grid is L in each direction: $X^A = n_A L$ where n_A is a natural number. Mathematically speaking, L has to be small in regard to the variation of ϕ. From the mechanical point of view, L is the typical dimension of dV. Then each atom A from a volume element dV centered around P is placed in the Euclidean space at $x + u$, where $x = \phi(X)$ and $u = \Psi(X)\, U$ (recall that $U = \vec{PA} \in T_P\mathscr{B}$). In practice, the element A of dV is chosen in a sub-Cartesian grid in $\mathscr{B}$ around P. In other words,

$U^I = (-\frac{1}{2} + n_I \frac{\mathfrak{d}}{L})L$ where n_I is an integer smaller than $L/\mathfrak{d}$. Hence, $\mathfrak{d}$ is the reference distance between two atoms, and the scale ratio $\mathfrak{d}/L$ imposes the number $L/\mathfrak{d}$ of atoms along a Cartesian direction of $\mathscr{B}$. It must be underlined that the scale ratio $\mathfrak{d}/L$ is here nothing else than a numerical and graphical choice: it does not contain any significance neither in the mechanical nor in the geometrical point of view.

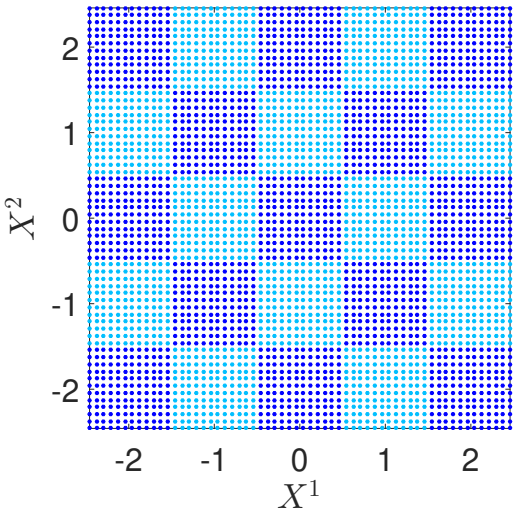

FIGURE 2.4: Graphical presentation of a reference configuration in the Euclidean space. Each color cell is macroelement. Points are atoms contained in the cells. Size of the cell $L = 1$, distance of two atoms $\mathfrak{d} = 1/12$.

2.2.2 Introducing a sub-scale

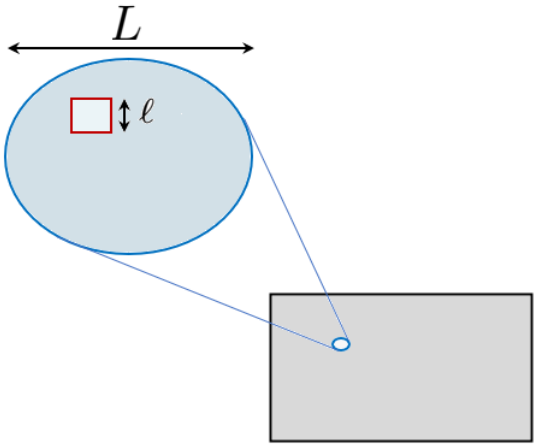

FIGURE 2.5: Various length scales of a model: microscopic and macroscopic. The scale ratio ℓ/L is defined for accounting for scaling effects.

As it has been underlined, no specific sub-scale has been introduced through preceding modeling: the new physical effect introduced by $\Psi \neq D\phi$ acts uniformly in the whole domain dV. However, from a mechanical point of view, the effect of the length scales can not be ignored. For instance, experiment tests have shown that continuum plasticity is used at macroscopic level ($\geq 300\mu m$). A macroscopic plasticity of materials involves microscopic slip ($\simeq 10^4 \mu m$). Focusing on this, the microscopic effects constitutes the basic point of view for crystalline plasticity. In between, gradient continuum models have been proposed to take into consideration mesoscopic

plasticity (Rakotomanana, 2018; Rakotomanana, 2005). A sub-scale may be introduced by considering that dV is composed of a large number of microelements δV of finite (but tiny) size. In the current state, the localization of each microelement (centered at a point Q) is prescribed by $F(X) = D\phi$ measured at P, whereas the stretch of microelement is controlled by $\Psi(X)$ still measured at P. This description is closely related to the Mindlin point of view in the Eringen-Mindlin theory Eringen and Suhubi, 1964; Suhubi and Eringen, 1964; Mindlin, 1964. Hereafter, this approach is called sub-scale modeling (*SSM*).

2.2.2.1 Numerical simulation

In a numerical point of view, let us consider a cubic microelement δV is of side ℓ. Then ℓ is the typical length for which the cut-and-glued process operates in dislocations theories (Nabarro, 1967; Acharya, Knops, and Sivaloganathan, 2019). In the reference configuration, the position of the center Q of δV relatively to P is defined by the two-point vector $U = \vec{PQ}$. For this cubic arrangement, $U^A = (-\frac{1}{2} + \frac{2n_A+1}{2}\frac{\ell}{L})L$ with n_A an integer in $[0, \frac{L}{\ell} - 1]$. The center of δV are then placed at $x + u$ in the Euclidean space, where $u = F\,U$. As F is computed at P, the center Q of microelements of dV are rearranged in a parallelipedic grid in the current configuration. An *atom* A placed in a microelement is rearranged around Q according to $v = \Psi V$ where V is the two-point vector $\vec{QA}$ in the reference state. For simulation purpose, the atoms are placed in δV according to a Cartesian grid; in other words $V^I = (-\frac{1}{2} + n_I\frac{\mathfrak{d}}{\ell})\ell$, where $n_I \in [0, \frac{\ell}{\mathfrak{d}}]$. Again $\mathfrak{d}$ is the distance between each atoms; it is introduced for graphical reasons but does not offer any physical or mathematical informations. However, the scale ratio ℓ/L (i.e. the volume-ratio $\delta V/dV$) represents the spatial gap for-which macro-stretch F and micro-stretch Ψ act uniformly. Indeed, even if $\Psi(X)$ is evaluated at P and is then homogeneous in all microelements δV of dV, the action of Ψ on all microelements of dV introduces a non-uniform pattern on dV (if $\Psi(X) \neq F(X)$). Numerically, this is obtained because Ψ and F act on position vectors relative to different origins.

Nevertheless, it must be underlined that mathematically F and Ψ act on vector belonging to $T\mathscr{B}$ and both are computed at P hence the geometrical state characterized by the metric and torsion tensor is the same in Eringen and Mindlin point of view. The sub-scale ℓ brings some interesting illustrations, but it is not unfortunately tractable in a mathematical language in the frame-work of Riemann-Cartan geometry, see examples in the next section.

2.3 Examples

We assume that the body is defect-free, and is subset in the Euclidean space. Let consider an example proposed by Acharya and Bassani, 2000 and reconsidered in Yavari and Goriely, 2012a. In this example, the material point map ϕ is identity (then $F = \mathbb{I}$) but Ψ is given as below:

$$\Psi = \mathbb{I} + \psi\,\partial_1 \otimes \partial_2 \tag{2.3.1}$$

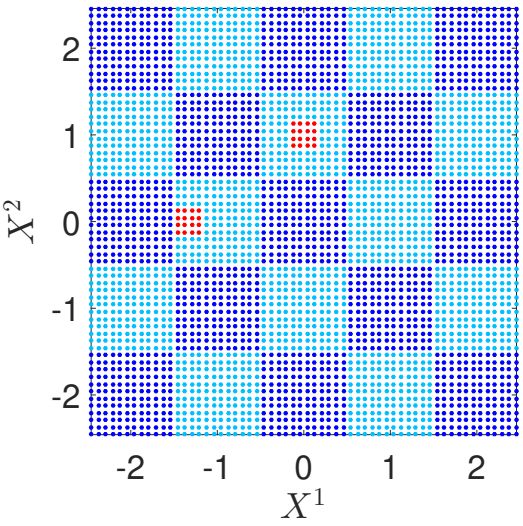

FIGURE 2.6: Graphical presentation of a reference configuration in the Euclidean space. Smaller cells are microelements dV. Each color cell is macroelement δV. Points are atoms contained in δV. Here we consider $L = 1$, and $\ell = 1/3$, and a distance of two atoms is $\mathfrak{d} = 1/12$.

where Cartesian coordinates are used both in the body and in the ambient Euclidean space (then $\mathsf{g} = \delta$ and $\gamma = 0$). Even if $\psi(X^2)$ is a function of X^2 in Yavari and Goriely, 2012a, here $\psi : \mathscr{B} \to \mathbb{R}$ is a smooth function (at least $\mathscr{C}^2$) of any (X^1, X^2, X^3).
The induced metric $\mathsf{G}_{AB} = \Psi^a_A \mathsf{g}_{ab} \Psi^b_B$ is

$$\mathsf{G} = \mathbb{I} + \psi(\partial_1 \otimes \partial_2 + \partial_2 \otimes \partial_1) + \psi^2 \partial_2 \otimes \partial_2. \tag{2.3.2}$$

In particular, $\det(\mathsf{G}) = 1$ meaning that the volume of the element dV does not change.
The connection coefficients are

$$\Gamma^1_{A2} = \partial_A \psi. \tag{2.3.3}$$

This yields to a possible non-zero torsion T with non-zero components:

$$\mathsf{T}^1_{A2} = -\mathsf{T}^1_{2A} = \partial_A \psi \qquad \text{with} \qquad A \in \{1, 3\}.$$

Specifically, if ψ depends only on X^1, $\mathsf{T}^1_{12} = \partial_1 \psi$ corresponds to a density of edge type dislocations. On the other hand, if ψ depends only on X^3, one have $\mathsf{T}^1_{32} = \partial_3 \psi$ characterizing a density of screw type dislocations. Last, suppose ψ is function of X^2, the current state is defect free even if $\Psi \neq F$.

In Figure 2.7, the illustration is provided for $A = 1$ and 2 in the *USM* framework with:

$$\psi(X^A) = \frac{1}{2L} \sin\left(\frac{X^A}{4L}\pi\right). \tag{2.3.4}$$

The magnitude of the transformation is voluntarily intensified as can be observed in the illustration. For $X^A = X^1$ (Figure 2.7-left), the presence of screw dislocations induces local transformations of the element dV that does not allow any gluing process without introducing additional elastic strain. From another point of view, the total gap of current vector field (green) along a closed material loop does not vanish as it is illustrated too. These phenomena are not observed if

$X^A = X^2$ (Figure 2.7-right), this gliding process does not introduce defects even if, as $F \neq \Psi$, two initial adjacent atoms belonging to distinct macroelements are no more neighbors after transformation.

In the end, it is in agreement with theoretical analysis since on one side (Figure 2.7-left) $\mathsf{T} \neq 0$, $\mathsf{R} = 0$ and $\nabla \mathsf{g} = 0$, and on the other side (Figure2.7-right) $\mathsf{T} = 0$, $\mathsf{R} = 0$ and $\nabla \mathsf{g} = 0$. The same

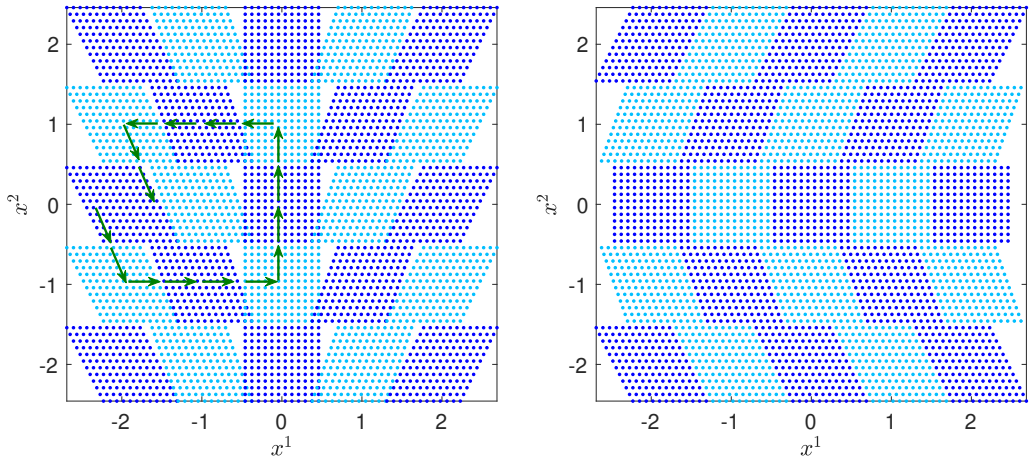

FIGURE 2.7: Current configuration in the Euclidean space for a transformation prescribed by (2.3.1) and (2.3.4) with $A = 1$ (left) and $A = 2$ (right). The *USM* point of view is used with $L = 1$ and $\mathfrak{d} = 1/12$.

transformation is observed within the *SSM* point of view in Figure 2.8. If $X^A = X^1$, the local defects look less intense but more present and distributed along the macroelement in such a way that the total amount of defect is preserved in a macroelement (Figure 2.8-left). If $X^A = X^2$, the gliding process supports a spacial dispersion too (Figure 2.8-right). Notice that if ϕ is defined by

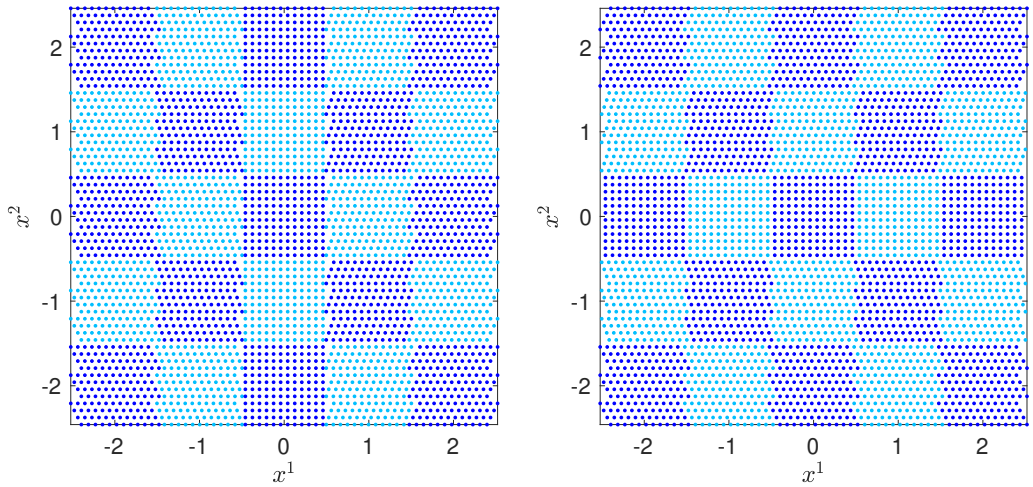

FIGURE 2.8: Same as Figure 2.7 but within the *SSM* point of view with $L = 1$, $\mathfrak{d} = 1/12$ and $\ell = 1/3$.

$$x^1 = X^1 - \frac{2}{\pi}\cos\left(\frac{X^A}{4L}\pi\right) \qquad \text{and} \qquad x^2 = X^2, \tag{2.3.5}$$

then $F = \Psi$ if $X^A = X^2$. In that case, the resulting transformation is the same whatever the choice of either *USM* or *SSM* computation (see Figure 2.9).

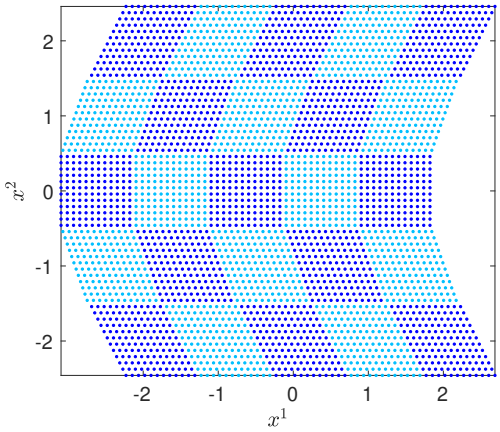

FIGURE 2.9: Current configuration for a compatible transformation prescribed by (2.3.1) and (2.3.4) with $A = 2$ and $\phi : (X^1, X^2) \to (X^1 - \frac{2}{\pi}\cos(\frac{X^A}{4L}\pi),\ X^2)$. Computation is performed within the *SSM* point of view with $L = 1$, $\mathfrak{d} = 1/12$ and $\ell = 1/3$. Same result is obtained if *USM* is chosen.

It is the occasion to underline a risk of confusion introduced through *SSM* simulations. Here, the lowest pattern is a dot with a typical size $\mathfrak{d}$. If ℓ is similar or smaller than $\mathfrak{d}$, no transformation is observed: *atoms* are along the Cartesian grid in the current state. Nonetheless, in a mathematical point of view, the torsion is unchanged. As already underlined $\mathfrak{d}$ does not have physical or mathematical significance, this observation is just a numerical artifact. This motivates to impose $\ell > \mathfrak{d}$ in the same spirit than the Nyquist criteria in signal processing.

2.4 Conclusion

A simple geometric theory of defects inspired by the micromorphic models has been introduced. It shows how the new transformation changes the intrinsic geometry of matter, from which dislocations may be created. The interesting thing is that we have proved that even if the map yields perturbation of the body at the micro scale, it may not create defects. The example has shown how this situation may be captured. Even though the models do not incorporate all classes of defects in the topological point of view, it motivates the development of geometrical modelling that fullfils this gap. A further generalization of the present theory is mentioned in the following tasks.

Another important thing is that starting with the transformation, Eringen defined some strain and the wryness tensor is one of them (Eringen, 1999). Nevertheless, we have proved in our theory that the wryness tensor is a connection, then it is not a tensor in the geometrical sense. Hence, the wryness tensor can not be defined as a strain. Additionally, one of the incompatibility conditions, being a measurement of the disclinations, is precisely equal to the curvature tensor of our connection. Hence, the incompatibility law is always satisfied. To sum up, the present theory modify this misfit.

Chapter 3

Field equations

In the preceding chapter, we see how the material transformation Υ changes the intrinsic geometry of matter. This new geometry is interpreted as a material manifold with defects. Up to present, ϕ and Ψ are unknown that we have to look for in order to describe the motion of matter entirely.

We begin with some strain measurements in *Section*-3.1. *Section*-3.2 gives a formula of internal energy and the stress tensors. *Section*-3.3 is devoted to the concepts of mass, microinertia, and kinetic energy; these points play central roles in the dynamical equations of microcontinuum. In continuum mechanics, it is possible to derive all the balance equations by using Hamilton's principle; this point is displayed in *Section*-3.4. Linear constitutive equations for isotropic material are collected in *Section*-3.5.

3.1 Strain measures

Recall the bundle map (2.1.1), for simplicity, the manifold $\mathscr{B}$ is assumed to be a subset evolving within Euclidean space; the Cartesian coordinate is used on $\mathbb{E}^3$. To keep things simple, we suppose that the reference configuration and the manifold $\mathscr{B}$ are merged together. The Kronecker metric δ_{AB} and the Levi-Civita connection γ are employed on the reference configuration. The current state is described by the metric G and the connection Γ that are derived from the material transformation (see (2.1.6)).

3.1.1 Green-Lagrange measure

The change of the distance and angle between the material point and its neighbourhood during the motion is measured by the classical (Green-Lagrange) strain E (Marsden and Hughes, 1994;

Gonzalez and Stuart, 2008). This is defined by the change of the material matrices

$$\mathsf{E} = \frac{1}{2}(\mathsf{G} - \delta). \tag{3.1.1}$$

3.1.2 Relative strain

The measurement of the difference between the micro and macro-deformation is obtained by the relative strain, and it is formalized by

$$\mathcal{E} = \Psi^{-1}F - \mathbb{I}, \tag{3.1.2}$$

where $\mathbb{I} = \delta^A_B \partial_A \otimes dX^B$ is the identity tensor. This strain was introduced by Eringen (Eringen, 1999).
Alternatively, one can define another relative strain as

$$\underset{\sim}{\mathcal{E}} = F^{-1}\Psi - \mathbb{I}.$$

3.1.3 Change of torsion

The changes in the intrinsic material manifold can be considered as strains measurement. By the construction, the new defects may be created by the material transformation. It is crucial to exhibit a dedicated tool measuring such creation of dislocations. This tool is in agreement with the torsion tensor T.

3.2 Internal energy density and stress tensors

Let us denote Ξ internal or free energy density. Throughout the remainder of our developments, we assume that Ξ is in the form:

$$\Xi = \Xi(\mathsf{E}, \mathcal{E}, \mathsf{T}) \tag{3.2.1}$$

All the arguments of Ξ are components of tensors. They are invariant under the action of the diffeomorphism (in the sense that they transform covariantly according to usual tensor transformations depending on their type). Therefore, the Lagrangian function is covariant. Now, we can define the set of stress tensors as follows:

$$\mathsf{S} = \frac{\partial \Xi}{\partial \mathsf{E}}, \quad \mathscr{D} = \frac{\partial \Xi}{\partial \mathcal{E}}, \quad \mathscr{T} = \frac{\partial \Xi}{\partial \mathsf{T}}. \tag{3.2.2}$$

3.3 Mass, inertia and kinetic energy

The results appearing here are similar to Eringen, 1999. However, to make the section self-contained and easy for the readers, we would like to reformulate these results ourselves.

The concepts of mass and inertia require a finite volume of the material body. Before we take an asymptotic analysis of each material point: indeed one considers a particle "P" having volume

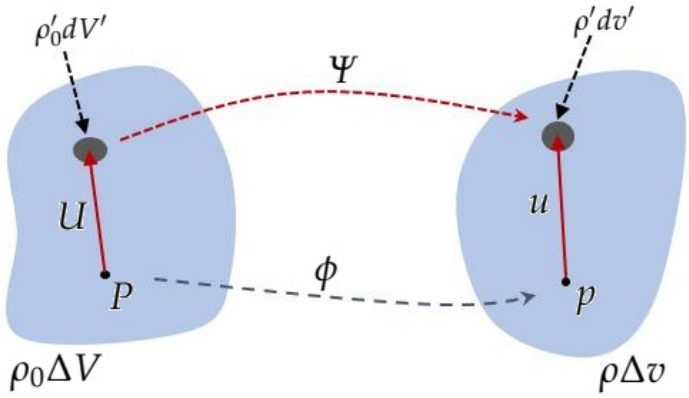

FIGURE 3.1: Micro-volume element.

ΔV, in the reference state and its image "p" within a volume Δv, in the current configuration at time t. The total mass of these particles is the sum of the masses of microelements i.e.

$$\rho_0 \Delta \mathrm{V} = \int_{\Delta V} \rho'_0 d\mathrm{V}' \qquad\qquad \rho \Delta \mathrm{v} = \int_{\Delta v} \rho' d\mathrm{v}', \tag{3.3.1}$$

where primed quantities refer to microelements contained in "P" and "p", respectively. A pictorial interpretation is given in Figure 3.1. We assume that the mass of the microelements is conserved during the motion

$$\rho'_0 d\mathrm{V}' = \rho' d\mathrm{v}'. \tag{3.3.2}$$

This implies that, in the limit as $\Delta \mathrm{V} \to 0$ and $\Delta \mathrm{v} \to 0$, one gets

$$\rho_0 d\mathrm{V} = \rho d\mathrm{v} \tag{3.3.3}$$

The relative position vectors U and u of the elements are taken with respect to center mass "P" and "p", so that.

$$\int_{\Delta \mathrm{V}} \rho'_0 U \, d\mathrm{V}' = 0 \qquad\qquad \int_{\Delta \mathrm{v}} \rho' u \, d\mathrm{v}' = 0. \tag{3.3.4}$$

Consequently,

$$\frac{\mathrm{d}}{\mathrm{d}t} \int_{\Delta \mathrm{v}} \rho' u \, d\mathrm{v}' = \frac{\mathrm{d}}{\mathrm{d}t} \int_{\Delta \mathrm{V}} \rho'_0 \Psi U \, d\mathrm{V}' = \int_{\Delta \mathrm{V}} \rho'_0 \dot{\Psi} U \, d\mathrm{V}' = \int_{\Delta \mathrm{v}} \rho' \dot{u} \, d\mathrm{V}' = 0. \tag{3.3.5}$$

Now, let us denote $\mathcal{K}$ a kinetic energy density per unit mass:

$$\mathcal{K} = \frac{1}{2\rho d\mathrm{v}} \int_{\Delta v} \rho' (\dot{x} + \dot{u}) \cdot (\dot{x} + \dot{u}) \, d\mathrm{v}'. \tag{3.3.6}$$

Here, the "cdot" product is defined by: for arbitrary vectors $v, u \in T_x \mathbb{E}^3$, $u \cdot v = u^a \mathrm{g}_{ab} v^b$. Applying (3.3.4) and (3.3.5), we conclude

$$\mathcal{K} = \frac{1}{2} V \cdot V + \frac{1}{2} \frac{1}{\rho d\mathrm{v}} \int_{\Delta \mathrm{v}} \rho' \dot{u}^a \mathrm{g}_{ab} \dot{u}^b \, d\mathrm{v}' \tag{3.3.7}$$

where V is a material velocity

$$V^a(X,t) = \frac{\partial \phi^a(X,t)}{\partial t}. \tag{3.3.8}$$

The first part is analogous to the macroscopic kinetic energy, while the second term is associated with the kinetic energy of microelements.

Next, since $\dot{u}^a = \dot{\Psi}^a_A U^A = \dot{\Psi}^a_A \Psi^A_c u^c = \nu^a{}_c u^c$. It is time to define a so-called microgyration variable (Eringen, 1999).

$$\nu^a{}_c = \dot{\Psi}^a_A \Psi^A_c. \tag{3.3.9}$$

Applying this notion, one gets $\dot{u}^a = \nu^a{}_c u^c$ and hence the microscopic kinetic energy can be rewritten as

$$\frac{1}{2}\frac{1}{\rho dv}\int_{\Delta v} \rho' \dot{u}^a \mathsf{g}_{ab} \dot{u}^b \, dv' = \frac{1}{2}\nu^a{}_s \mathsf{g}_{ab} \nu^b{}_h \frac{1}{\rho dv}\int_{\Delta v} \rho' u^s u^h \, dv' = \frac{1}{2}\nu^a{}_s \mathsf{g}_{ab} \nu^b{}_h \mathsf{i}^{sh}, \tag{3.3.10}$$

where a microinertia tensor i is given by (Eringen, 1999)

$$\mathsf{i}^{sh} = \frac{1}{\rho dv}\int_{\Delta v} \rho' u^s u^h dv'. \tag{3.3.11}$$

Insert (3.3.10) into (3.3.7), one gets

$$\mathcal{K} = \frac{1}{2} V \cdot V + \frac{1}{2}\mathsf{i} : \nu \mathsf{g} \nu. \tag{3.3.12}$$

It is called the spatial formula of the kinetic energy. Its material form will be constructed as follows: first of all, similar to (3.3.11) a material microinertia tensor I is defined by (Eringen, 1999)

$$\mathsf{I}^{SH} = \frac{1}{\rho_0 dV}\int_{\Delta V} \rho_0' U^S U^H \, dV'. \tag{3.3.13}$$

After that, upon using the law of conversation of mass (3.3.3), we conclude a law of conservation of microinertia (Eringen, 1999)

$$\mathsf{i}^{sh} = \Psi^s_S \Psi^h_H \frac{1}{\rho dv}\int_{\Delta V} \rho_0' U^S U^H \, dV' = \Psi^s_S \mathsf{I}^{SH} \Psi^h_H. \tag{3.3.14}$$

Thanks to this relation and (3.3.9), we obtain

$$\begin{aligned} \mathsf{i} : \nu \mathsf{g} \nu = \nu^a{}_s \mathsf{g}_{ab} \nu^b{}_h \mathsf{i}^{sh} &= \dot{\Psi}^a_A \Psi^A_s \mathsf{g}_{ab} \dot{\Psi}^b_B \Psi^B_h \Psi^s_S \mathsf{I}^{SH} \Psi^h_H \\ &= \mathsf{I}^{SH} \, \dot{\Psi}^a_A \mathsf{g}_{ab} \dot{\Psi}^b_B \, (\Psi^A_s \Psi^s_S) \, (\Psi^B_h \Psi^h_H) = \mathsf{I}^{SH} \, \dot{\Psi}^a_S \mathsf{g}_{ab} \dot{\Psi}^b_H = \mathsf{I} : \dot{\Psi} \mathsf{g} \dot{\Psi}. \end{aligned} \tag{3.3.15}$$

Finally, inserting (3.3.15) into (3.3.12), the kinetic energy can be rewritten as

$$\mathcal{K} = \frac{1}{2} V \cdot V + \frac{1}{2}\mathsf{I} : \dot{\Psi} \mathsf{g} \dot{\Psi}. \tag{3.3.16}$$

3.4 Variational equations

In continuum mechanics, it is possible to derive all the balance equations by using a Hamilton's principle. The principle states that the dynamics of a physical system are determined by a variational problem for a functional based on a single function, the Lagrangian, which may contain all physical information concerning the system and the forces acting on it. Now, we first consider the infinitesimal variations of the coordinates

$$x \to \tilde{x} = x + \delta u \qquad\qquad \Psi \to \tilde{\Psi} = \Psi + \delta\Psi \tag{3.4.1}$$

Variation δu is called external variation, whereas variation of fields $\delta\Psi$ are called internal (Capozziello and De Laurentis, 2011; Rakotomanana, 2018). We write Hamilton's principle for independent variations δu and $\delta\Psi$ between fixed limits of u and Ψ at times t_0 and t_1:

$$\int_{t_0}^{t_1} \delta\mathcal{K}\, dt + \int_{t_0}^{t_1} \delta\mathcal{W}_e\, dt = \int_{t_0}^{t_1} \delta\mathcal{W}\, dt, \tag{3.4.2}$$

where $\mathcal{K}$ and $\mathcal{W}_e$ are the total kinetic energy and the work done by external forces, respectively. $\mathcal{W}$ designates the work of the internal forces.

3.4.1 Work of the internal forces

The virtual work of the internal forces will be stored in the material

$$\delta\mathcal{W} = \int_{\mathscr{B}} \delta\Xi\, dV \qquad \text{with} \qquad \delta\Xi = \mathsf{S} : \delta\mathsf{E} + \mathscr{D} : \delta\mathcal{E} + \mathscr{T} : \delta\mathsf{T}. \tag{3.4.3}$$

Firstly, as $\mathsf{E}_{AB} = \dfrac{1}{2}(\Psi^a_A \mathsf{g}_{ab} \Psi^b_B - \delta_{AB})$, one obtains

$$\begin{aligned} \mathsf{S} : \delta\mathsf{E} = \ \mathsf{S}^{AB}\delta\mathsf{E}_{AB} = \ & \frac{1}{2}\mathsf{S}^{AB}\Big(\mathsf{g}_{ab}\Psi^a_A\delta\Psi^b_B + \mathsf{g}_{ab}\Psi^b_B\delta\Psi^a_A\Big) \\ = \ & \Big(\Psi^a_A\mathsf{S}^{AB}\mathsf{g}_{ab}\Big)\delta\Psi^b_B = \ \mathsf{P} : \delta\Psi, \qquad \text{with} \quad \mathsf{P}_b{}^B = \mathsf{g}_{ba}\Psi^a_A\mathsf{S}^{AB}. \end{aligned} \tag{3.4.4}$$

Second, as $\delta(\Psi^a_C\Psi^C_b) = 0$, one obtains $\delta\Psi^a_C\Psi^C_b + \Psi^a_C\delta\Psi^C_b = 0$ and then

$$\delta\Psi^B_b = \ \Psi^B_a\Psi^a_C\delta\Psi^C_b = \ -\Psi^B_a\delta\Psi^a_C\Psi^C_b. \tag{3.4.5}$$

Applying the above relation, one obtains

$$\begin{aligned} \mathscr{D} : \delta\Psi^{-1}F = \ & \mathscr{D}_B{}^A\delta\Psi^B_b F^b_A = \ \mathscr{D}_B{}^A F^b_A\delta\Psi^B_b \\ = \ & -\Big(\mathscr{D}_B{}^A F^b_A\Psi^B_a\Psi^C_b\Big)\delta\Psi^a_C := \ -\widetilde{\mathscr{D}} : \delta\Psi, \qquad \text{with} \quad \widetilde{\mathscr{D}}_a{}^C := \ \Psi^B_a\mathscr{D}_B{}^A F^b_A\Psi^C_b. \end{aligned} \tag{3.4.6}$$

Then, we can write

$$\mathscr{D} : \delta\mathcal{E} = \mathscr{D} : \delta\Psi^{-1}F + \mathscr{D} : \Psi^{-1}\delta F = -\widetilde{\mathscr{D}} : \delta\Psi + \overline{\mathscr{D}} : \delta F, \qquad \text{with} \quad \overline{\mathscr{D}}_b{}^A := \Psi^B_b\mathscr{D}_B{}^A. \tag{3.4.7}$$

Next, as $\Gamma^C_{AB} = \Psi^C_b \partial_A \Psi^b_B$, variation of the connection reads

$$\delta\Gamma^C_{AB} = \delta\Psi^C_b \partial_A \Psi^b_B + \Psi^C_b \partial_A \delta\Psi^b_B = -\Psi^C_a \delta\Psi^a_D \Psi^D_b \partial_A \Psi^b_B + \Psi^C_b \partial_A \delta\Psi^b_B. \tag{3.4.8}$$

We deduce that

$$\begin{aligned}
\mathscr{T} : \delta\mathsf{T} = \mathscr{T}^{AB}_C \delta\mathsf{T}^C_{AB} &= \left(\mathscr{T}^{AB}_C \Psi^C_a \Psi^D_b \partial_B \Psi^b_A - \mathscr{T}^{AB}_C \Psi^C_a \Psi^D_b \partial_A \Psi^b_B\right)\delta\Psi^a_D \\
&\quad + \left(\mathscr{T}^{AB}_C \Psi^C_b\right)\partial_A \delta\Psi^b_B - \left(\mathscr{T}^{AB}_C \Psi^C_b\right)\partial_B \delta\Psi^b_A \\
&= 2\left(\mathscr{T}^{AB}_C \Psi^C_a \Psi^D_b \partial_B \Psi^b_A\right)\delta\Psi^a_D + 2\left(\mathscr{T}^{AB}_C \Psi^C_b\right)\partial_A \delta\Psi^b_B \\
&= \widetilde{\mathscr{T}} : \delta\Psi + \overline{\mathscr{T}} : \nabla\delta\Psi.
\end{aligned} \tag{3.4.9}$$

Here, we have used the fact that $\mathscr{T}^{AB}_C = -\mathscr{T}^{BA}_C$, and have defined

$$\widetilde{\mathscr{T}}^D_a := 2\left(\mathscr{T}^{AB}_C \Psi^C_a \Psi^D_b \partial_B \Psi^b_A\right) \qquad \text{and} \qquad \overline{\mathscr{T}}^{AB}_b := 2\left(\mathscr{T}^{AB}_C \Psi^C_b\right) \tag{3.4.10}$$

Insert (3.4.4), (3.4.7), and (3.4.9) into (3.4.3), the virtual work of the internal forces reads

$$\delta\mathcal{W} = \int_{\mathscr{B}} \overline{\mathscr{D}} : \delta F + (\mathsf{P} - \widetilde{\mathscr{D}} + \widetilde{\mathscr{T}}) : \delta\Psi + \overline{\mathscr{T}} : \nabla\delta\Psi \, dV. \tag{3.4.11}$$

Notice that the first term can be expressed by

$$\overline{\mathscr{D}}_a{}^A \delta F^a_A = \partial_A(\overline{\mathscr{D}}_a{}^A \delta u^a) - \partial_A(\overline{\mathscr{D}}_a{}^A)\delta u^a, \tag{3.4.12}$$

and the third one is reformulated by

$$\overline{\mathscr{T}}^{AB}_b \partial_A \delta\Psi^b_B = \partial_A(\overline{\mathscr{T}}^{AB}_b \delta\Psi^b_B) - \partial_A(\overline{\mathscr{T}}^{AB}_b)\delta\Psi^b_B. \tag{3.4.13}$$

Denote "N" a unit normal vector to $\partial\mathscr{B}$, employing the Divergence Theorem (Marsden and Hughes, 1994; Gonzalez and Stuart, 2008), it yields that

$$\begin{aligned}
\delta\mathcal{W} = \int_{\mathscr{B}} &-\mathrm{Div}\overline{\mathscr{D}} \cdot \delta u + (\mathsf{P} - \widetilde{\mathscr{D}} + \widetilde{\mathscr{T}} - \mathrm{Div}\overline{\mathscr{T}}) : \delta\Psi \, dV \\
&+ \int_{\partial\mathscr{B}} \overline{\mathscr{D}} \cdot N \cdot \delta u + \overline{\mathscr{T}} \cdot N : \delta\Psi \, dS.
\end{aligned} \tag{3.4.14}$$

3.4.2 Work of the external forces

The form of (3.4.14) is the motivation for the variation of work done by external forces:

$$\delta\mathcal{W}_e = \int_{\mathscr{B}} \mathfrak{b} \cdot \delta u + \mathfrak{Z} : \delta\Psi \, dV + \int_{\partial\mathscr{B}} \mathfrak{s} \cdot \delta u + \mathfrak{D} : \delta\Psi \, dS, \tag{3.4.15}$$

where $\mathfrak{b}$ is the body force per unit volume, $\mathfrak{s}$ is the surface force per unit area (stress-vector or traction), and $\mathfrak{Z}$ is interpreted as a double force per unit volume and $\mathfrak{D}$ is a double force per unit area.

3.4.3 Work of the kinetic energy

The kinetic work is known as

$$\int_{t_0}^{t_1} \delta\mathcal{K} dt = \int_{t_0}^{t_1} \int_{\mathscr{B}} \rho_0 \, \delta\left(\frac{1}{2} V \cdot V + \frac{1}{2} \mathsf{I} : \dot{\Psi} \mathsf{g} \dot{\Psi}\right) dV dt. \tag{3.4.16}$$

Firstly, we noticed that $\delta\left(V^a \mathsf{g}_{ab} V^b\right) = 2V^a \mathsf{g}_{ab} \delta V^b$ and $\delta V^a(X,t) = \partial \delta u^a(X,t)/\partial t$, in the usual way (see Love, 1944, p.166) we find

$$\begin{aligned} \int_{t_0}^{t_1} \int_{\mathscr{B}} \frac{1}{2} \rho_0 \, \delta\left(V^a \mathsf{g}_{ab} V^b\right) dV dt &= \int_{t_0}^{t_1} \int_{\mathscr{B}} V^a \mathsf{g}_{ab} \delta V^b \, dV dt \\ &= -\int_{t_0}^{t_1} \int_{\mathscr{B}} \rho_0 \, A \cdot \delta u \, dV dt \end{aligned}$$

where the material acceleration A is given by $A(X,t) = \dfrac{\partial V(X,t)}{\partial t}$.
Secondly, it can be verify that

$$\frac{1}{2} \mathsf{I} : \delta(\dot{\Psi} \mathsf{g} \dot{\Psi}) = \mathsf{I}^{AB} \dot{\Psi}^a_A \mathsf{g}_{ab} \delta \dot{\Psi}^b_B. \tag{3.4.17}$$

Consequently, one gets

$$\int_{t_0}^{t_1} \int_{\mathscr{B}} \frac{1}{2} \rho_0 \mathsf{I} : \delta(\dot{\Psi} \mathsf{g} \dot{\Psi}) \, dV dt = -\int_{t_0}^{t_1} \int_{\mathscr{B}} \rho_0 \Lambda : \delta\Psi \, dV dt, \tag{3.4.18}$$

where the micro acceleration *or* spin inertia Λ is defined by

$$\Lambda^B_b = \mathsf{g}_{ab} \ddot{\Psi}^a_A \mathsf{I}^{AB}. \tag{3.4.19}$$

Furthermore, if we apply $\delta\Psi = \dot{\Psi}$ to (3.4.18), one gets

$$\Lambda : \dot{\Psi} = \frac{1}{2} \frac{\mathrm{d}}{\mathrm{d}t} \left(\mathsf{I} : \dot{\Psi} \mathsf{g} \dot{\Psi}\right). \tag{3.4.20}$$

Finally, insert (3.4.17) and (3.4.18) into (3.4.16), we conclude that

$$\int_{t_0}^{t_1} \delta\mathcal{K} dt = -\int_{t_0}^{t_1} \int_{\mathscr{B}} \rho_0 \left(A \cdot \delta u + \Lambda : \delta\Psi\right) dV dt. \tag{3.4.21}$$

3.4.4 Local equations of motion

Substituting (3.4.14) - (3.4.15) - (3.4.21) into (3.4.2) (drop the integration with respect to time), one obtains

$$\begin{aligned} \int_{\mathscr{B}} (\mathfrak{b} - \rho_0 \, A + \operatorname{Div} \overline{\mathscr{D}}) \cdot \delta u + (\mathfrak{Z} - \rho_0 \Lambda + \widetilde{\mathscr{D}} - \mathsf{P} - \widetilde{\mathscr{T}} + \operatorname{Div} \overline{\mathscr{T}}) : \delta\Psi \, dV \\ + \int_{\partial\mathscr{B}} (\mathfrak{s} - \overline{\mathscr{D}} \cdot N) \cdot \delta u + (\mathfrak{D} - \overline{\mathscr{T}} \cdot N) : \delta\Psi \, dS = 0. \end{aligned} \tag{3.4.22}$$

The necessary and sufficient conditions to ensure the above equation to be satisfied for arbitrary variation δu and $\delta\Psi$

$$\begin{cases} \mathfrak{b} + \mathrm{Div}\,\overline{\mathscr{D}} & = \rho_0 A \\ \mathfrak{Z} + \widetilde{\mathscr{D}} - \mathsf{P} - \widetilde{\mathscr{T}} + \mathrm{Div}\,\overline{\mathscr{T}} & = \rho_0 \Lambda \end{cases} \tag{3.4.23}$$

together with its boundary conditions:

$$\mathfrak{s} = \overline{\mathscr{D}} \cdot N \qquad \text{and} \qquad \mathfrak{D} = \overline{\mathscr{T}} \cdot N. \tag{3.4.24}$$

These are local equations of motion, of which the first equations are the local balance of momentum while the second is balance of moment of momentum.

3.5 Linear equations

This section concerns the linear theory of the equations of motion. In what follows we use, for instance, we write $u^a_{,A}$ instead of $\partial_A u^a$.

3.5.1 General equations

Due to the aim of the section, we employ linear approximations

$$F^a_A \simeq (\delta^a_b + u^a_{,b})\delta^b_A \qquad \begin{aligned} \Psi^a_A &\simeq (\delta^a_b + m^a_b)\delta^b_A \\ \Psi^A_a &\simeq \delta^A_b(\delta^b_a - m^b_a). \end{aligned} \tag{3.5.1}$$

where u is small displacement vector field. With these, in the first approximation, one gets

$$\begin{aligned} \Gamma^A_{BC} &\simeq m^a_{c,b}\delta^A_a\delta^c_C\delta^b_B & \mathsf{E}_{AB} &\simeq \frac{1}{2}(\delta_{cb}m^c_a + \delta_{ac}m^c_b)\delta^a_A\delta^b_B \\ \mathsf{T}^A_{BC} &\simeq (m^a_{c,b} - m^a_{b,c})\delta^A_a\delta^b_B\delta^c_C & \mathcal{E}^A_B &\simeq (u^a_{,b} - m^a_b)\delta^A_a\delta^b_B. \end{aligned} \tag{3.5.2}$$

This is the occasion to define:

$$\mathfrak{t}_{abc} = \delta_{ae}(m^e_{c,b} - m^e_{b,c}) \tag{3.5.3}$$

$$\mathfrak{d}_{ab} = \delta_{ae}(u^e_{,b} - m^e_b) \tag{3.5.4}$$

$$\epsilon_{ab} = \frac{1}{2}(\delta_{cb}m^c_a + \delta_{ac}m^c_b). \tag{3.5.5}$$

The linear approximation for the stress, and the stress fields require a quadratic approximation for the stored energy Ξ, in its variables. In this work, we suppose that

$$\begin{aligned}\Xi = \frac{1}{2}c\ \epsilon_{aa}\epsilon_{bb} + d\ \epsilon_{ab}\epsilon_{ab} + \frac{1}{2}\varrho\ \mathfrak{d}_{aa}\mathfrak{d}_{bb} + \frac{1}{2}\eta\ \mathfrak{d}_{ab}\mathfrak{d}_{ba} + \frac{1}{2}(\eta+\varepsilon)\ \mathfrak{d}_{ab}\mathfrak{d}_{ab}\\ g\ \mathfrak{d}_{aa}\epsilon_{bb} + h\ (\mathfrak{d}_{ab}+\mathfrak{d}_{ba})\epsilon_{ba} - \frac{1}{4}\alpha\ \mathfrak{t}_{bba}\mathfrak{t}_{cac}\\ + \frac{1}{8}\beta\ \mathfrak{t}_{bca}\mathfrak{t}_{bca} + \frac{1}{4}\gamma\ \mathfrak{t}_{bca}\mathfrak{t}_{cab}.\end{aligned} \tag{3.5.6}$$

In which,"$-\frac{1}{4}\alpha\ \mathfrak{t}_{bba}\mathfrak{t}_{cac} + \frac{1}{8}\beta\ \mathfrak{t}_{bca}\mathfrak{t}_{bca} + \frac{1}{4}\gamma\ \mathfrak{t}_{bca}\mathfrak{t}_{cab}$" is coming from a distribution of dislocations. It is similar to one in (Katanaev, 2005).

For the homogeneous isotropic material, the linear constitutive equations for stresses read

$$\sigma^{ab} \simeq \frac{\partial \Xi}{\partial \epsilon_{ab}} = c\ \delta_{ab}\epsilon_{ii} + 2d\ \epsilon_{ab} + g\ \delta_{ab}\mathfrak{d}_{ii} + h\ (\mathfrak{d}_{ab}+\mathfrak{d}_{ba}) \tag{3.5.7}$$

$$\tau^{ab} \simeq \frac{\partial \Xi}{\partial \mathfrak{d}_{ab}} = \varrho\ \delta_{ab}\mathfrak{d}_{ii} + (\varepsilon+\eta)\ \mathfrak{d}_{ab} + \eta\ \mathfrak{d}_{ba} + g\ \delta_{ab}\ \epsilon_{ii} + 2h\ \epsilon_{ab}. \tag{3.5.8}$$

The last ones $\mu^{qrp} \simeq \dfrac{\partial \Xi}{\partial \mathfrak{t}_{qrp}}$ are explicitly expressed by

$$2\mu^{aab} = \alpha \mathfrak{t}_{qqb} + (\beta-\gamma)\mathfrak{t}_{aab} = -2\mu^{aba}, \qquad a \neq b \tag{3.5.9}$$

$$2\mu^{abc} = \beta \mathfrak{t}_{abc} + \gamma(\mathfrak{t}_{cab} + \mathfrak{t}_{bca}),\ a \neq b \neq c. \tag{3.5.10}$$

By the way, the components μ^{aab} are associated with edge dislocations, while the other ones are related to screw dislocation.

For the homogeneous, isotropic material the micro acceleration (3.4.19) reads

$$\Lambda^B_b = \mathsf{I}^{AB}\ddot{\Psi}^a_A \mathsf{g}_{ab} \qquad \Rightarrow \qquad \Lambda^B_b = \mathsf{I}^{AB}\ddot{m}^a_c \delta^c_A \delta_{ab} = \ddot{m}_{bc}\delta^c_B \mathsf{I}^{BB} \tag{3.5.11}$$

with I^{BB} are constants.

Next, from (3.5.2), (3.5.3), (3.5.7), and (3.5.9), one gets

$$\mathsf{S}^{AB} = \frac{\partial \Xi}{\partial \mathsf{E}_{AB}} \simeq \delta^A_a \sigma^{ab}\delta^B_b \tag{3.5.12}$$

$$\mathscr{D}_A{}^B = \frac{\partial \Xi}{\partial \mathcal{E}^A_{\ B}} \simeq \delta^a_A \delta_{ae}\tau^{eb}\delta^B_b \tag{3.5.13}$$

$$\mathscr{T}_A{}^{BC} = \frac{\partial \Xi}{\partial \mathsf{T}^A_{\ BC}} \simeq \delta^a_A \delta_{ae}\mu^{ebc}\delta^B_b\delta^C_c. \tag{3.5.14}$$

Consequently,

$$\mathsf{P}_b^{\ B} = \mathsf{g}_{ba}\Psi_A^a\mathsf{S}^{AB} \simeq \delta_{bc}\sigma^{cd}\delta_d^B \tag{3.5.15}$$
$$\widetilde{\mathscr{D}}_a^{\ C} = \Psi_a^B\mathscr{D}_B^{\ A}F_A^b\Psi_b^C \simeq \delta_{ae}\tau^{ed}\delta_d^C \tag{3.5.16}$$
$$\overline{\mathscr{D}}_b^{\ A} = \Psi_b^B\mathscr{D}_B^{\ A} \simeq \delta_{be}\tau^{ed}\delta_d^A \tag{3.5.17}$$
$$\widetilde{\mathscr{T}}_a^D = 2(\mathscr{T}_C^{AB}\Psi_a^C\Psi_b^D\partial_B\Psi_A^b) \simeq 0 \tag{3.5.18}$$
$$\overline{\mathscr{T}}_b^{AB} = 2(\mathscr{T}_C^{AB}\Psi_b^C) \simeq 2\delta_{be}\mu^{edc}\delta_d^A\delta_c^B. \tag{3.5.19}$$

Finally, insert these into (3.4.23), the linearization of the local equations of motion on m and u are given by (as the infinitesimal transformation, there is no distinction between the upper and lower indices, all the equations as below will be written with indices down with the small letter (x^a))

$$\begin{cases} \mathfrak{b}_a + \tau_{ab,b} &= \rho_0\ddot{u}_a \\ \\ \mathfrak{Z}_{ab} + \tau_{ab} - \sigma_{ab} + 2\mu_{acb,c} &= \rho_0\mathsf{I}_{bb}\ddot{m}_{ab}. \end{cases} \tag{3.5.20}$$

It looks quantitatively the same as the linear equations of the micromorphic continuum (Eringen, 1999). The linear equations of a Cauchy continuum (Marsden and Hughes, 1994) are obtained by setting: $c = g$, $d = h$, $F = \Psi$, $\mathsf{I}_{bb} = 0$, and $\varrho = \varepsilon = \eta = \alpha = \beta = \gamma = 0$.

3.5.2 One dimensional dynamics

We investigate here a simplified solution for which all kinematic variable are just dependent on time and x^3. We focus on self-sustained waves (or vibrations), then $\mathfrak{b} = 0$ and $\mathfrak{Z} = 0$.
The first equation of (3.5.20) is $\tau_{a3,3} = \rho_0\ddot{u}_a$. It gives explicitly:

$$\begin{aligned} &\varrho\ \delta_{a3}u_{3,33} + (\varepsilon+\eta)\ u_{a,33} + \eta\ u_{3,a3} \\ &+(g-\varrho)\ \delta_{a3}\ m_{ii,3} + (h-\varepsilon-\eta)\ m_{a3,3} + (h-\eta)\ m_{3a,3} = \rho_0\ddot{u}_a. \end{aligned} \tag{3.5.21}$$

The second equation of (3.5.20) is $\tau_{ab} - \sigma_{ab} + 2\mu_{a3b,3} = \rho_0\mathsf{I}_{bb}\ddot{m}_{ab}$. In which, (3.5.7) gives

$$\begin{aligned} \tau_{ab} - \sigma_{ab} = &\ (\varrho-g)\ \delta_{ab}u_{3,3} + (\varepsilon+\eta-h)\ u_{a,b} + (\eta-h)\ u_{b,a} \\ &+ (2g-\varrho-c)\ \delta_{ab}m_{ii} + (2h-\varepsilon-\eta-d)\ m_{ab} + (2h-\eta-d)\ m_{ba}. \end{aligned} \tag{3.5.22}$$

Using the constitutive laws (3.5.9), we obtain:

$$2\mu_{113} = -(\alpha+\beta-\gamma)m_{11,3} - \alpha m_{22,3} \tag{3.5.23}$$
$$2\mu_{123} = -\beta m_{12,3} + \gamma m_{21,3}. \tag{3.5.24}$$
$$2m_{213} = -\beta m_{21,3} + \gamma m_{12,3} \tag{3.5.25}$$
$$2m_{223} = -\alpha m_{11,3} - (\alpha+\beta-\gamma)m_{22,3}. \tag{3.5.26}$$
$$2m_{313} = -(\alpha+\beta-\gamma)m_{31,3} \tag{3.5.27}$$
$$2m_{323} = -(\alpha+\beta-\gamma)m_{32,3}. \tag{3.5.28}$$

The other components are zero. Therefore, the second equation of (3.5.20) gives explicitly

$$\begin{aligned}
(\varrho - g)\, u_{3,3} + (2g - \varrho - c)\, m_{ii} + (4h - \varepsilon - 2\eta - 2d)\, m_{11} & \\
+(\alpha + \beta - \gamma)\, m_{11,33} + \alpha\, m_{22,33} &= \rho_0 \mathsf{I}_{11} \ddot{m}_{11} \\
(2h - \varepsilon - \eta - d)\, m_{12} + (2h - \eta - d)\, m_{21} + \beta\, m_{12,33} - \gamma\, m_{21,33} &= \rho_0 \mathsf{I}_{22} \ddot{m}_{12} \\
(\varepsilon + \eta - h)\, u_{1,3} + (2h - \varepsilon - \eta - d)\, m_{13} + (2h - \eta - d)\, m_{31} &= \rho_0 \mathsf{I}_{33} \ddot{m}_{13}
\end{aligned} \tag{3.5.29}$$

$$\begin{aligned}
(2h - \varepsilon - \eta - d)\, m_{21} + (2h - \eta - d)\, m_{12} + \beta\, m_{21,33} - \gamma\, m_{12,33} &= \rho_0 \mathsf{I}_{11} \ddot{m}_{21} \\
(\varrho - g)\, u_{3,3} + (2g - \varrho - c)\, m_{ii} + (4h - \varepsilon - 2\eta - 2d)\, m_{22} & \\
+\alpha\, m_{11,33} + (\alpha + \beta - \gamma)\, m_{22,33} &= \rho_0 \mathsf{I}_{22} \ddot{m}_{22} \\
(\varepsilon + \eta - h)\, u_{2,3} + (2h - \varepsilon - \eta - d)\, m_{23} + (2h - \eta - d)\, m_{32} &= \rho_0 \mathsf{I}_{33} \ddot{m}_{23}
\end{aligned} \tag{3.5.30}$$

$$\begin{aligned}
(\eta - h)\, u_{1,3} + (2h - \varepsilon - \eta - d)\, m_{31} + (2h - \eta - d)\, m_{13} & \\
+(\alpha + \beta - \gamma)\, m_{31,33} &= \rho_0 \mathsf{I}_{11} \ddot{m}_{31} \\
(\eta - h)\, u_{2,3} + (2h - \varepsilon - \eta - d)\, m_{32} + (2h - \eta - d)\, m_{23} & \\
+(\alpha + \beta - \gamma)\, m_{32,33} &= \rho_0 \mathsf{I}_{22} \ddot{m}_{32} \\
(\varrho - g + \varepsilon + 2\eta - 2h)\, u_{3,3} + (2g - \varrho - c)\, m_{ii} + (4h - \varepsilon - 2\eta - 2d)\, m_{33} &= \rho_0 \mathsf{I}_{33} \ddot{m}_{33}.
\end{aligned} \tag{3.5.31}$$

The systems (3.5.21) and (3.5.29)-(3.5.30)-(3.5.31) form a linear differential system of 12 unknowns. Even if this system is strongly coupled, some simplified solutions are exhibited hereafter in the case where the micro-inertia phenomena are isotropic : $\mathsf{I}_{11} = \mathsf{I}_{22} = \mathsf{I}_{33} := \mathsf{I}$.

By means of linear combinations, the systems (3.5.21) and (3.5.29)-(3.5.30)-(3.5.31) can be decomposed into three independent systems of equations:

Micro-rotation:

$$\begin{aligned}
(2h - \varepsilon - \eta - d)\, m_{12} + (2h - \eta - d)\, m_{21} + \beta\, m_{12,33} - \gamma\, m_{21,33} &= \rho_0 \mathsf{I} \ddot{m}_{12} \\
(2h - \varepsilon - \eta - d)\, m_{21} + (2h - \eta - d)\, m_{12} + \beta\, m_{21,33} - \gamma\, m_{12,33} &= \rho_0 \mathsf{I} \ddot{m}_{21}.
\end{aligned} \tag{3.5.32}$$

Let us consider a micro-rotation such that $m_{12} = -m_{21}$. In this case, the above systems reduce to

$$-\varepsilon\, m_{12} + (\beta + \gamma)\, m_{12,33} = \rho_0 \mathsf{I} \ddot{m}_{12}. \tag{3.5.33}$$

Transversal waves:

$$\begin{aligned}
(\varepsilon + \eta)\, u_{1,33} + (h - \varepsilon - \eta)\, m_{13,3} + (h - \eta)\, m_{31,3} &= \rho_0 \ddot{u}_1 \\
(\varepsilon + \eta - h)\, u_{1,3} + (2h - \varepsilon - \eta - d)\, m_{13} + (2h - \eta - d)\, m_{31} &= \rho_0 \mathsf{I} \ddot{m}_{13} \\
(\eta - h)\, u_{1,3} + (2h - \eta - d)\, m_{13} + (2h - \varepsilon - \eta - d)\, m_{31} + (\alpha + \beta - \gamma) m_{31,33} &= \rho_0 \mathsf{I} \ddot{m}_{31}.
\end{aligned} \tag{3.5.34}$$

The other transversal systems are the same as before except u_1, m_{13} and m_{31} are replaced with u_2, m_{23} and m_{32}, respectively.

Longitudinal waves:

$$\begin{aligned} \lambda_1\, u_{3,33} + \alpha_1\, m_{11,3} + \alpha_1\, m_{22,3} + \lambda_2\, m_{33,3} &= \rho_0 \ddot{u}_3 \\ \alpha_2\, u_{3,3} + \lambda_3\, m_{11} + \zeta_2\, m_{22} + \zeta_2\, m_{33} + \lambda_4 m_{11,33} + \alpha m_{22,33} &= \rho_0 \mathsf{I} \ddot{m}_{11} \\ \alpha_2\, u_{3,3} + \zeta_2\, m_{11} + \lambda_3\, m_{22} + \zeta_2\, m_{33} + \alpha m_{11,33} + \lambda_4 m_{22,33} &= \rho_0 \mathsf{I} \ddot{m}_{22} \\ \zeta_1\, u_{3,3} + \zeta_2\, m_{11} + \zeta_2\, m_{22} + \lambda_3\, m_{33} &= \rho_0 \mathsf{I} \ddot{m}_{33}, \end{aligned} \tag{3.5.35}$$

where

$$\begin{aligned} \lambda_1 &= \varrho + 2\eta + \varepsilon & \alpha_1 &= g - \varrho \\ \lambda_2 &= 2h - \varepsilon - 2\eta + g - \varrho & \alpha_2 &= \varrho - g \\ \lambda_3 &= 4h - \varepsilon - 2\eta - 2d + 2g - \varrho - c & \zeta_1 &= \varrho - g + \varepsilon + 2\eta - 2h \\ \lambda_4 &= \alpha + \beta - \gamma & \zeta_2 &= 2g - \varrho - c. \end{aligned}$$

We try to find harmonic solutions of the form:

$$u_a(X_3, t) = U_a i e^{i(kX_3 - \omega t))}, \qquad m_{ab}(X_3, t) = M_{ab} e^{i(kX_3 - \omega t))}, \tag{3.5.36}$$

where ω is the frequency and k is the wavenumber. Three dispersion relations (the relations between ω and k) result:

Micro-rotation:

$$\omega^2 = \frac{\varepsilon + (\beta + \gamma)k^2}{\rho_0 \mathsf{I}}. \tag{3.5.37}$$

Transversal waves: ω^2 are the eigenvalues of $\mathcal{A}$ with

$$\mathcal{A} = \frac{1}{\rho_0 \mathsf{I}} \begin{pmatrix} (\varepsilon + \eta)\mathsf{I}k^2 & -(h - \varepsilon - \eta)\mathsf{I}k & -(h - \eta)\mathsf{I}k \\ (\varepsilon + \eta - h)k & -(2h - \varepsilon - \eta - d) & -(2h - \eta - d) \\ (\eta - h)k & -(2h - \eta - d) & (\alpha + \beta - \gamma)k^2 - (2h - \varepsilon - \eta - d) \end{pmatrix}. \tag{3.5.38}$$

Longitudinal waves: ω^2 are the eigenvalues of $\mathcal{A}$ with

$$\mathcal{A} = \frac{1}{\rho_0 \mathsf{I}} \begin{pmatrix} \lambda_1 \mathsf{I}k^2 & -\alpha_1 \mathsf{I}k & -\alpha_1 \mathsf{I}k & -\lambda_2 \mathsf{I}k \\ \alpha_2 k & \lambda_4 k^2 - \lambda_3 & \alpha k^2 - \zeta_2 & -\zeta_2 \\ \alpha_2 k & \alpha k^2 - \zeta_2 & \lambda_4 k^2 - \lambda_3 & -\zeta_2 \\ \zeta_1 k & -\zeta_2 & -\zeta_2 & -\lambda_3 \end{pmatrix}. \tag{3.5.39}$$

Only one eigenvector may be computed analytically, it corresponds to $(0, 1, -1, 0)$ and is associated with the eigenfrequency

$$\omega^2 = -\frac{4h - \varepsilon - 2\eta - 2d + (\gamma - \beta)k^2}{\rho_0 \mathsf{I}}. \tag{3.5.40}$$

3.6 Conclusion

In this chapter, we have presented kinematics of a defected medium in terms of Riemann-Cartan geometry, supposing the inconsistent transformation (i.e. the internal state vector is associated with the micro-deformation of material with the internal structure. The map of vectors is not consistent with the transformation of the material point). The theory is very close to the micromorphic theories. Nevertheless, the present model seems to clarify the interaction of a defected continuum with the microcontinuum. Variational equations and their linearizations are derived from this perspective. The number of material parameters has been reduced in comparison with the classical micromorphic theories (Mindlin, 1964; Eringen, 1999 for example). The theory is applied to wave propagation in a fixed direction. The physical meaning of the material parameters as well as the relation between the present model and the second-order gradient continuum (Polizzotto, 2013 an example) is still missing and would be a perspective of future works.

Part II

Tangent geometry and applications to mechanics

Chapter 4

Fiber bundle manifolds: a geometry of a microstructured material

As mentioned several times, the evolution of the internal state is the cause of defects in the body. We want to look for a mathematical framework that could help us to examine effectively this physical intuition. I recently became conscious that such a framework exists based on the notions of the fiber bundle manifold and Ehresmann connection.

The fiber bundle manifold is an "extra" structure generalized to the product of the base (material) manifold and the space of internal state. The total space can be equipped with a connection- namely Ehresmann connection N and metric tensor G of Sasaki form. In general, these geometric objects and derived quantities (torsion, curvature) may not only depend on the position but also on the internal state (Wang, 1967/68). The fiber bundle equipped with the connection and the metric is known as a fiber geometry (Epstein, 2010; Epstein, 2014; Nakahara, 2003). This extends the Riemannian geometry for which (relative) position of material points control all geometrical objects as underlined by Weyl, 1918. It encompasses various geometries among Euclidean, Riemannian, Weitzenböck, Weyl manifolds. The satisfactory framework could be adapted in a natural way for several phenomena in physics. As examples, its application concerns mainly general relativity theory - the theory of gravity, but other applications are already investigated by Iliev, 2001; Romano, 2007.

As a field of applications, the microcontinuum can be modeled as a fiber bundle because it suffices to mention that each point on the base manifold can be endowed with additional degrees of freedom or internal states. As a consequence, a motion of the microcontinuum is formally a fiber morphism (Epstein and Elżanowski, 2007), see also the next chapter. As such approach encompasses the macroscopic and microscopic universes as a whole, all the physical quantities may be considered as single-valued and smooth (outside macroscopic inhomogeneities). Accordingly,

both theoretical and numerical analysis may be handled without additional difficulties. Furthermore, the complete description of the microcontinuum is derived from introducing an additional field - namely a solder form. At the same time, the solder form enriches the fiber geometry somehow.

This chapter is organized as follows: *Section*-4.1 gives a short review about general fiber bundles, Ehresmann connection on a fiber bundle. These concepts are essential ingredients in this thesis. This connection is a generalization of the affine connection. All concepts explained throughout this chapter can be found in detail in (Epstein, 2010; Epstein, 2014; Nakahara, 2003). *Section*-4.2 gives a presentation of a microstructured material in terms of fiber geometry.

4.1 Fiber bundle manifolds

To get some intuition for the bundle concept, let us start with a definition of a product bundle. Let $\mathscr{B}$ and $\mathcal{F}$ be smooth manifolds, equipped with the coordinates (x^a), and (y^i) respectively. Consider the Cartesian product $\mathscr{B} \times \mathcal{F}$ - a so-called product bundle. It is endowed with two natural projection maps, namely:

$$\begin{array}{rccc} pr_1 & : & \mathscr{B}\times\mathcal{F} & \longrightarrow & \mathscr{B} \\ & & (x^a, y^i) & \longmapsto & x^a \end{array} \quad \text{and} \quad \begin{array}{rccc} pr_2 & : & \mathscr{B}\times\mathcal{F} & \longrightarrow & \mathcal{F} \\ & & (x^a, y^i) & \longmapsto & y^i \end{array} .$$

The concept of fiber bundle is a generalization of the product bundle. Essentially, what we want to achieve is the loss of the second projection pr_2, while preserving the first pr_1.

4.1.1 Smooth fiber bundle manifold

In order to define the notion carefully, we first review some basic properties of group actions:

Definition 4.1.1 (Topological group Epstein, 2010)**.** *Recall that a group is a set $\mathscr{G}$ endowed with a binary associative internal operation, called group multiplication or group product, which is usually indicated by simple apposition, namely: if $g, h \in \mathscr{G}$ then the product is $gh \in \mathscr{G}$. Associativity means that $(gh)k = g(hk)$, for all $g, h, k \in \mathscr{G}$. Moreover, it is assumed that there exists an identity element $e \in \mathscr{G}$ such that $eg = ge = g$ for all $g \in \mathscr{G}$. Finally, for each $g \in \mathscr{G}$, there exists an inverse $g^{-1} \in \mathscr{G}$ such that $gg^{-1} = g^{-1}g = e$. The identity can be shown to be unique, and so is also the inverse of each element of the group.*
A topological group is a topological space (or, in particular, a topological manifold) $\mathscr{G}$ with a group structure that is compatible with the topological structure, namely, such that the multiplication $\mathscr{G} \times \mathscr{G} \to \mathscr{G}$ and the inversion $\mathscr{G} \to \mathscr{G}$ are continuous maps.

Definition 4.1.2 (Left action Epstein, 2010)**.** *If $\mathscr{G}$ is a group and $\mathscr{M}$ is a set, we say that $\mathscr{G}$ acts on the left on $\mathscr{M}$, if for each $g \in \mathscr{G}$, there is a map L_g: $\mathscr{M} \to \mathscr{M}$ such that: (i) $L_e(m) = m$ for all $m \in \mathscr{M}$, where e is the group identity; (ii) $L_g \circ L_h = L_{gh}$ for all $g, h \in \mathscr{G}$. When there is no room for confusion, we also use the notation gm for $L_g m$.*
The action of $\mathscr{G}$ on $\mathscr{M}$ is said to be effective if $L_g(m) = m$ for every $m \in \mathscr{M}$ implies $g = e$.

Definition 4.1.3 (Epstein, 2010). *Let $\mathscr{G}$ be a topological group acting on a topological manifold $\mathscr{M}$. The topological group $\mathscr{G}$ is said to act on the left on a manifold $\mathscr{M}$ if: (i) Every element $g \in \mathscr{G}$ induces a homeomorphism $L_g : \mathscr{M} \to \mathscr{M}$. (ii) $L_g \circ L_h = L_{gh}$, namely, $(gh)(x) = g(h(x))$ for all $g, h \in \mathscr{G}$ and $m \in \mathscr{M}$. (iii) The left action $L : \mathscr{G} \to \mathscr{M}$ is a continuous map. In other words, $L(g, m) = L_g(m)$ is continuous in both variables (g and m).*

The object $\mathscr{M} \xrightarrow{\pi} \mathscr{B}$ (obviously, $(\mathscr{M}, \pi, \mathscr{B}, \mathcal{F}, \mathscr{G})$) is called *a fiber bundle manifold*, consisting of smooth manifolds $\mathscr{M}$, called the total space, $\mathscr{B}$ as the base manifold, typical fiber $\mathcal{F}$ and structure group $\mathscr{G}$ (acting effectively on the left on $\mathcal{F}$) and a continuous surjective bundle-projection map $\pi : \mathscr{M} \to \mathscr{B}$ such that there exists an open covering of $\mathscr{B}$, with open sets $\mathcal{U}_\omega$, and respective homeomorphisms (called local trivializations)

$$\varsigma_\omega : \pi^{-1}(\mathcal{U}_\omega) \to \mathcal{U}_\omega \times \mathcal{F}, \tag{4.1.1}$$

with the property $\pi = pr_1 \circ \varsigma_\omega$. This property means that for every point x in $\mathcal{U}_\omega$ the fiber $\pi^{-1}(x)$ is entirely mapped onto the fiber $pr_1^{-1}(x)$ of the product $\mathcal{U}_\omega \times \mathcal{F}$. More precisely, a local trivialization ς_ω consists of the identity map of $\mathcal{U}_\omega$ and a continuous family of fiber-wise homeomorphisms $\tilde{\varsigma}_{\omega,x} : \pi^{-1}(x) \to pr_1^{-1}(x)$.

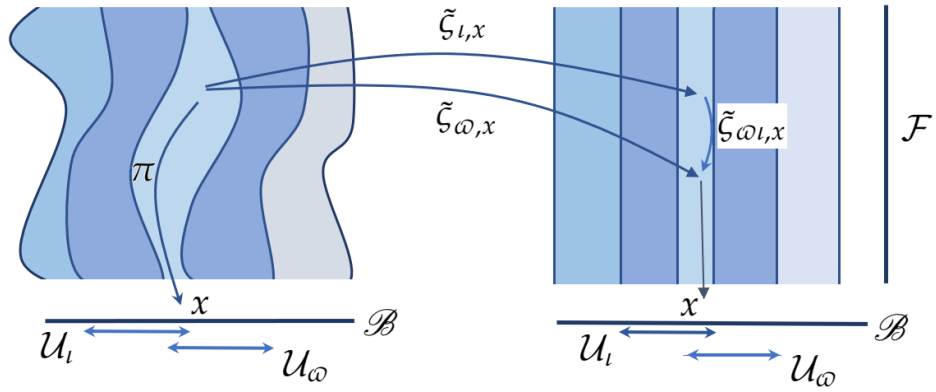

FIGURE 4.1: Pictorial representation of local trivializations and transition functions

Consider two trivializations, ς_ω and ς_ι, such that their respective open sets have a non-empty intersection $\mathcal{U}_\omega \cap \mathcal{U}_\iota$. At each point $x \in \mathcal{U}_\omega \cap \mathcal{U}_\iota$, we obtain two different homeomorphisms $\tilde{\varsigma}_{\omega,x}$ and $\tilde{\varsigma}_{\iota,x}$. We call the composition

$$\tilde{\varsigma}_{\omega\iota,x} = \tilde{\varsigma}_{\iota,x} \circ \tilde{\varsigma}_{\omega,x}^{-1} : \mathcal{F} \to \mathcal{F}, \tag{4.1.2}$$

the transition map at x between the first and the second trivializations. We demand to each transition map to be a transformation of $\mathcal{F}$ induced by some elements $g(x)$ of the structure group $\mathscr{G}$. The dependence on x must be continuous.

Definition 4.1.4. *A fiber-bundle morphism between $\mathscr{M} \xrightarrow{\pi} \mathscr{B}$ and $\mathscr{M}' \xrightarrow{\pi'} \mathscr{B}'$ as a pair of (smooth) maps, K: $\mathscr{M} \to \mathscr{M}'$ and k: $\mathscr{B} \to \mathscr{B}'$ such that*

$$\pi' \circ K = k \circ \pi. \tag{4.1.3}$$

4.1.1.1 The tangent bundle manifold

The tangent bundle of a manifold is a special fiber bundle which is naturally constructed for every smooth n-dimensional manifold $\mathscr{B}$. It is denoted by $T\mathscr{B}$, obtained by attaching to each point b on $\mathscr{B}$ its tangent space $T_b\mathscr{B}$. Explicitly,

$$T\mathscr{B} = \bigcup_{b\in\mathscr{B}} T_b\mathscr{B}. \tag{4.1.4}$$

More precisely, an element in $T\mathscr{B}$ is a pair (b, v) where $b \in \mathscr{B}$ and v is a tangent vector to $\mathscr{B}$ at the point b. The canonical projection is given by the assignation:

$$\begin{array}{rccc} \pi & : & T\mathscr{B} & \longrightarrow & \mathscr{B} \\ & & (b, v) & \longmapsto & b. \end{array}$$

$T\mathscr{B}$ is also a smooth manifold with dimension $2n$. Indeed, let $(\mathcal{U}, (x^a)_{a=1,..,n})$ be a local chart in $\mathscr{B}$ around b. This yields a natural basis $\partial/\partial x^a$ at $T_b\mathscr{B}$ with $b \in \mathscr{B}$. For any tangent vector $v \in T_b\mathscr{B}$, we can identify it with its components v^a. Hence, we assign to each point $(b, v) \in T\mathscr{B}$ the $2n$ numbers $(x^1, .., x^n, v^1, .., v^n)$, namely, a point in $\mathbb{R}^{2n}$. Thus, the coordinate chart in $\pi^{-1}(\mathcal{U})$ is obtained. The fiber at the point $b \in \mathscr{B}$ is $\pi^{-1}(b) = T_b\mathscr{B}$. Since each fiber is an n-dimensional vector space, we say that the typical fiber of $T\mathscr{B}$ is $\mathbb{R}^n$. To construct its group action $\mathcal{G}$, let us denote $(\tilde{x}^a)$ an other coordinate chart at b. The components $\tilde{v}^a$ of v in the new natural basis $\partial/\partial\tilde{x}^a$ are related to the old ones

$$\tilde{v}^a = \frac{\partial\tilde{x}^b}{\partial x^a} v^a. \tag{4.1.5}$$

Last, for (x^a) and $(\tilde{x}^a)$ to be good coordinate systems, the matrix $A^b_a = \partial\tilde{x}^b/\partial x^a$ must be non-singular. Consequently, the structure group of the tangent bundle is indeed the general linear group $GL(n, \mathbb{R})$.

4.1.2 Vertical tangent spaces

Recall $x^a (a = 1, ..., n = \dim(\mathscr{B}))$ and $y^i (i = 1, ..., m = \dim(\mathcal{F}))$ are the coordinate charts in $\mathscr{B}$ and $\mathcal{F}$, respectively. Their Cartesian product constitutes a local coordinate chart x^a, y^i for the fiber bundle $\mathscr{M}$. A given tangent vector field w over $\mathscr{M}$ evaluated at $c \in \mathscr{M}$ can be expressed as

$$w = w^a(c)\frac{\partial}{\partial x^a} + w^i(c)\frac{\partial}{\partial y^i}. \tag{4.1.6}$$

By the definition of the projection π, it induces a tangent mapping π_*: $T\mathscr{M} \to T\mathscr{B}$ which acts in the following way

$$\pi_* : T_c\mathscr{M} \to T_{\pi(c)}\mathscr{B}, \quad w \mapsto w^a \frac{\partial}{\partial x^a}. \tag{4.1.7}$$

The kernel $\ker(\pi_*)$ is exactly that part of the tangent space $T\mathscr{M}$ spanned by the induced basis elements $\frac{\partial}{\partial y^i}$ which comes from the fiber $\mathcal{F}$, while the image of π_* is a vector tangent to the base space at $\pi(c)$ expressed in the coordinate basis from the base space. Hence, at each point $c \in \mathscr{M}$

the tangent space $T_c\mathscr{M}$ has a *canonically vertical subspace* $V_c\mathscr{M}$, explicitly defined by

$$V_c\mathscr{M} = \ker(\pi_*) = \text{span}(\frac{\partial}{\partial y^i}). \tag{4.1.8}$$

4.1.3 Ehresmann connection

Given a fiber $\mathscr{M}_p$ at p and a fiber $\mathscr{M}_q$ at q, we want to connect them from a given point belonging to the fiber $\mathscr{M}_p$. To do so, we have to build a "bridge". If p and q are infinitesimally close, it can be identified with a tangent vector v to $\mathscr{B}$ at p. At this stage, the bridge is a lift of v to the bundle $\mathscr{M}$. We require this assignment to be smooth and unique. For instance, let m be the starting point belonging to the fiber $\mathscr{M}_p$, the collection of all the possible bridges is called the horizontal space, see Figure 4.2. This task is performed by Ehresmann connections and formulated by the following definition:

Formally, Ehresmann connection consists of a smooth assignment to each point $m \in \mathscr{M}$ of an n-dimensional subspace $H_m\mathscr{M} \subset T_m\mathscr{M}$ the tangent bundle of $\mathscr{M}$, called the horizontal subspace at c, such that

$$T_m\mathscr{M} = H_m\mathscr{M} \oplus V_m\mathscr{M}. \tag{4.1.9}$$

In this equation, $\oplus$ denotes the direct sum of vector spaces. In the other words, each tangent vector $w \in T_m\mathscr{M}$ is uniquely decomposable as the sum of a horizontal part $\text{hor}(w) \in H_m\mathscr{M}$ and a vertical part $\text{ver}(w) \in V_m\mathscr{M}$.

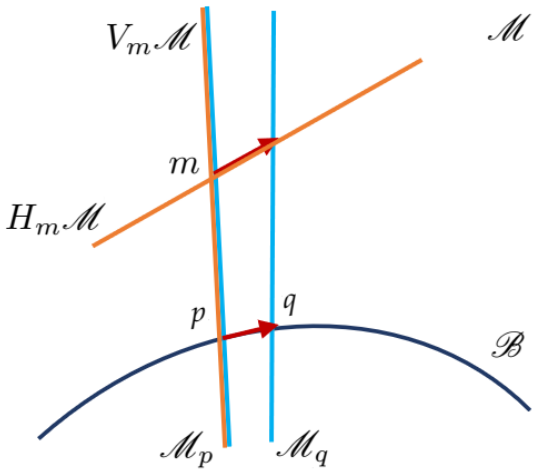

FIGURE 4.2: An Ehresmann connection

Equivalently, Ehresmann connection can be formalized by a lift operator defined as follows.

Definition 4.1.5. *An Ehresmann connection on $\mathscr{M}$ is a morphism $N : T\mathscr{B} \underset{\mathscr{B}}{\times} \mathscr{M} \to T\mathscr{M}$ such that $d\pi \circ N(v, m) = v$. In local coordinates,*

$$N = \left(\frac{\partial}{\partial x^a} - N_a^i(m)\frac{\partial}{\partial y^i}\right) \otimes dx^a.$$

We can lift the natural local basis $\partial/\partial x^a$ of $T_p\mathscr{B}$ to respective bases of the horizontal spaces at any point $c \in \mathscr{M}_p$:

$$H_c\mathscr{M} = \text{span}\,(\frac{\delta}{\delta x^a} := \frac{\partial}{\partial x^a} - N^i_a(c)\frac{\partial}{\partial y^i}) \qquad \text{and} \qquad V_c\mathscr{M} = \text{span}(\frac{\partial}{\partial y^i}). \tag{4.1.10}$$

The dual of the horizontal and vertical tangent spaces are given by

$$H^*_c\mathscr{M} = \text{span}(dx^a) \qquad \text{and} \qquad V^*_c\mathscr{M} = \text{span}(\delta y^i := dy^i + N^i_a(c)dx^a). \tag{4.1.11}$$

4.1.4 Parallel transport

A smooth curve in a fiber bundle $\mathscr{M}$ always projects, by composition, onto a unique smooth curve in the base manifold $\mathscr{B}$. The converse is, of course, not true since a curve σ in the base manifold can be obtained as the projection of any of an infinite number of curves in the fiber. However, if the fiber bundle is endowed with an Ehresmann connection N, it is possible to lift the curve σ to a unique horizontal curve $\sigma^\uparrow$ in the fiber through a given point $c \in \mathscr{M}$. Such curve is defined as the following:

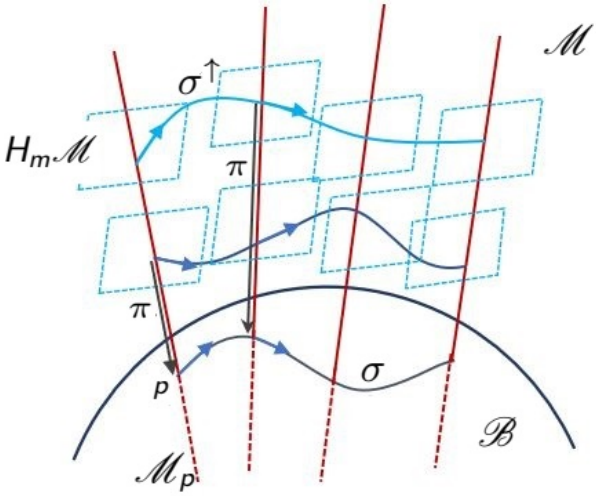

FIGURE 4.3: Parallel transport along a curve

Consider a curve σ: $[0,1] \to \mathscr{B}$, with $\sigma(0) = a$, $\sigma(1) = b$, $a, b \in \mathscr{B}$, and a point $c \in \mathscr{M}$. The unique horizontal lift $\sigma^\uparrow$ satisfies the following properties: for all $t \in (0,1)$

$$\pi \circ \sigma^\uparrow = \sigma. \tag{4.1.12a}$$

$$\text{ver}(\dot{\sigma^\uparrow}(t)) = 0. \tag{4.1.12b}$$

$$\pi_*(\dot{\sigma^\uparrow}) = \dot{\sigma}(t). \tag{4.1.12c}$$

This horizontal lift of a base curve σ through any point $c \in \mathscr{M}$ exists locally and is unique Epstein, 2010; Epstein, 2014; Nakahara, 2003. As this horizontal curve cuts through the various fibers hovering over the original curve σ, the point c is said to undergo a parallel transport with respect to the given connection and the given curve., see Figure 4.3.

We end this section with the auto-parallel equations:

Definition 4.1.6 (Auto-parallels of an Ehresmann connection). *With the smooth curve σ on $\mathscr{B}$, its natural lift to the tangent bundle is $\hat{\sigma} = (\sigma, \dot{\sigma}) \in \mathscr{M}$. The curve σ is said to be an auto-parallel of an Ehresmann connection N if and only if its natural lift is a horizontal curve. In coordinates, this yields to the auto-parallel equations (Miron, 1994)*

$$\ddot{\sigma}^{\alpha} + N^{\alpha}_{a}(\sigma, \dot{\sigma})\dot{\sigma}^{a} = 0. \tag{4.1.13}$$

4.1.5 Ehresmann curvature

The split of the tangent spaces of $\mathscr{M}$ into the horizontal and vertical subspaces gives rise to the question whether these subspaces belong to integral manifolds which are sub manifolds of $\mathscr{M}$. The answer to this question is given by the definition of the curvature of a connection with the help of the Fröbenius theorem which we cite here without proof (the proof is reported in Epstein, 2010; Epstein, 2014).

Theorem 4.1.7. Fröbenius Theorem
A k-dimensional distribution $\mathcal{D}$ in a smooth m-dimensional $\mathscr{M}$ (with $k < n$) is a smooth assignment of a k-dimensional subspace $\mathcal{D}_p \subset T_p\mathscr{M}$ to each point $p \in \mathscr{M}$. A distribution with the property that the Lie bracket of any two vector fields belonging to the distribution also belongs to the distribution is said to be involutive. Theorem of Fröbenious states that a distribution is an integration if and only if it is involutive.

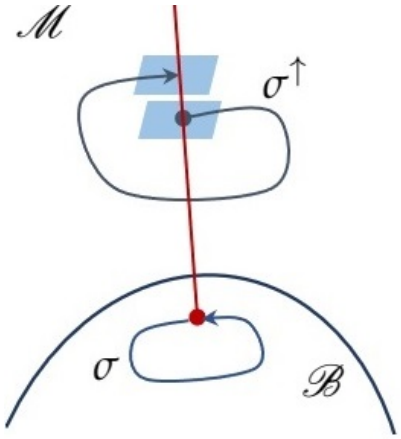

FIGURE 4.4: Lack of vertical closure of the horizontal lift of a loop.

Applying Fröbenius theorem, we conclude that there exists a submanifold of $\mathscr{M}$ for which $V_c\mathscr{M}$ is the tangent space; this submanifold is the fiber $\mathscr{M}_c$. Since for arbitrary basis $\partial/\partial y^i$ and $\partial/\partial y^j$, one has $[\partial/\partial y^i, \partial/\partial y^j] = 0$.

For the horizontal tangent spaces the situation is more complicated. To analyse whatever this distribution is integrable we calculate the Lie bracket of the basis vector fields. This failure of integrability leads to the definition of the curvature coefficients of the connection as

$$\mathfrak{R}^{i}{}_{ab} = \left\langle \delta y^{i}, [\frac{\delta}{\delta x^{a}}, \frac{\delta}{\delta x^{b}}] \right\rangle,$$

in the coordinates expression,

$$\mathfrak{R}^i{}_{ab} = \frac{\partial N^i_a}{\partial x^b} - N^j_b \frac{\partial N^i_a}{\partial y^j} + N^j_a \frac{\partial N^i_b}{\partial y^j} - \frac{\partial N^i_b}{\partial x^a}. \tag{4.1.14}$$

The geometrical interpretation of the curvature is the following: let σ be a loop in the base manifold. For zero curvature case, its horizontal lift will be closed. Otherwise, it may not be closed, see Figure 4.5.

4.2 Geometry of a microstructured material

A microstructured material is modeled by a fiber bundle $\mathscr{M} \xrightarrow{\pi} \mathscr{B}$ with extra data described in this section. The three-dimensional differentiable manifold $\mathscr{B}$ is compact (in general with boundaries, even if this point is not addressed in this manuscript) and orientable. It is the geometrical support of the material, hereafter called the *body*. Fiber of the bundle $\mathscr{M}$ at $p \in \mathscr{B}$ is denoted by $\mathscr{M}_p$. It is considered as the microelement present in the material at the point p.

After the general definitions, each subsection will end by the application of the definition in a special case where $\mathscr{M} = T\mathscr{B}$ meaning that microelements are interpreted as a first order infinitesimal neighborhoods of points. Such interpretation coincides with standard analysis with defective crystals or grained material. This equality means that the same mathematical object, namely $T\mathscr{B}$, is used to model different mechanical objects: the space of "velocities" of geometrical point $p : T_p\mathscr{B}$ on the one hand and the microelement at $p : \mathscr{M}_p$ on the other hand.

This general formalism, supposing possibly that $\mathscr{M} \neq T\mathscr{B}$, also has the advantage to extend the present theoretical background to other physical materials (porous media, phase transformation, soft mater, etc.; see for example Epstein, 2012; Bradlyn and Read, 2015; Lychev et al., 2020).

4.2.1 The solder form

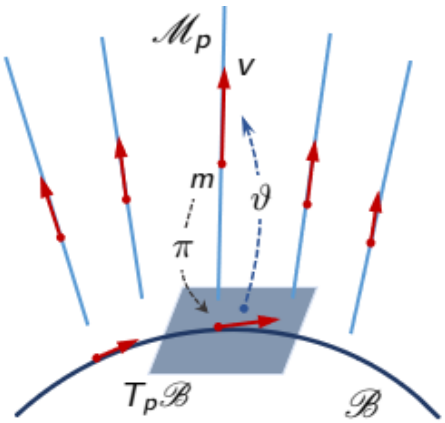

FIGURE 4.5: A vertical vector v is a tangent to $\mathscr{M}_p$. The solder form is used to glue the tangent to the fiber to the tangent to the body manifold $\mathscr{B}$.

Let us denote by $V(\mathscr{M})$ the vertical tangent bundle of $\mathscr{M} \xrightarrow{\pi} \mathscr{B}$, i.e. the subbundle $\ker d\pi \subset T\mathscr{M}$. The fiber of $V(\mathscr{M})$ at $p \in \mathscr{B}$ is the tangent bundle to the microelement $\mathscr{M}_p$, namely $T(\mathscr{M}_p)$. One supposes that the tangent at the microelement at $m \in \mathscr{M}_p$, namely $T_m(\mathscr{M}_p) \equiv V_m\mathscr{M}$, should be $T_p\mathscr{B}$, meaning that microelements are tangent to the body $\mathscr{B}$. It is formalized in the following definition:

Definition 4.2.1. *A solder form on $\mathscr{M}$ is an isomorphism $T\mathscr{B} \underset{\mathscr{B}}{\times} \mathscr{M}$[1] $\xrightarrow{\vartheta} V(\mathscr{M})$.*

The definition (4.2.1) implies that the dimension of a microelement is equal to the dimension of $\mathscr{B}$. Hereafter, we consider the case where $\dim \mathscr{B} = \dim \mathscr{M}_p$. An alternative definition of the solder form can be found in (Hélein, 2009). Note however this latter reference is only related to vector bundles and is then less general. On the other hand, the definition of a solder form (4.2.1) does not correspond to the original definition by Ehresmann for general fiber bundles e.g (Kobayaschi, 1957).

Let (x^a) be coordinates on $\mathscr{B}$. Let us complete the definition of the solder form in a coordinate system (x^a, y^i) on $\mathscr{M}$. A solder form can be written accordingly:

$$\vartheta = \vartheta^i_a(m) \frac{\partial}{\partial y^i} \otimes dx^a.$$

If $\widetilde{x}^a(x^b)$ and $\widetilde{y}^i(x^b, y^j)$ define another coordinate systems on the bundle $\mathscr{M}$ then we have:

$$\vartheta = \widetilde{\vartheta}^i_a(m) \frac{\partial}{\partial \widetilde{y}^i} \otimes d\widetilde{x}^a = \left(\widetilde{\vartheta}^i_a(m) \frac{\partial y^j}{\partial \widetilde{y}^i} \frac{\partial \widetilde{x}^a}{\partial x^b} \right) \frac{\partial}{\partial y^j} \otimes dx^b.$$

When $\mathscr{M}$ is a vector bundle[2] on $\mathscr{B}$, then one obtains $V(\mathscr{M}) \cong \mathscr{M} \underset{\mathscr{B}}{\times} \mathscr{M}$[3]. A particular type of solder form can be defined by a bundle map over $\mathscr{M}$, $T\mathscr{B} \underset{\mathscr{B}}{\times} \mathscr{M} \xrightarrow{\vartheta} \mathscr{M} \underset{\mathscr{B}}{\times} \mathscr{M}$, induced by an isomorphism $T\mathscr{B} \to \mathscr{M}$. This is a strong interpretation of the tangency condition of $V(\mathscr{M})$ with $\mathscr{B}$ modeled by the solder form.

One should keep in mind that the bundle $T\mathscr{B}$ is used to model two different objects: the tangent spaces $T\mathscr{B}$ on the one hand, and the microelements $\mathscr{M}$ on the other hand.
For the special case $\mathscr{M} = T\mathscr{B}$, the canonical solder form is reduced to the isomorphism associated with the identity $T\mathscr{B} = \mathscr{M}$. This isomorphism $T\mathscr{B} \underset{\mathscr{B}}{\times} \mathscr{M} \xrightarrow{\vartheta_{can}} V(\mathscr{M})$ is given by the following construction. A coordinate system (x^a) on $\mathscr{B}$ induces coordinates (x^a, y^i) on $T\mathscr{B}$ such that for $v \in T\mathscr{B}$, $v = \delta^a_i y^i(v) \frac{\partial}{\partial x^a}$. Expressed in these coordinates, the canonical solder form is:

$$\vartheta_{can} = \delta^j_b \frac{\partial}{\partial y^j} \otimes dx^b.$$

[1] $T\mathscr{B} \underset{\mathscr{B}}{\times} \mathscr{M} = \{(v, u) \in T\mathscr{B} \times \mathscr{M} \mid \pi_{T\mathscr{B}}(v) = \pi(u)\}$.

[2] A vector bundle $\mathscr{E} \xrightarrow{\pi} \mathscr{N}$ is a fiber bundle whose fiber is a vector space. The tangent bundle $T\mathscr{E}$ over an m-dimensional manifold $\mathscr{N}$ is a vector bundle whose typical fiber is $\mathbb{R}^m$ with $m = \dim \mathscr{N}$.

[3] Indeed, for any $m, n \in \mathscr{M}_p$ with $p \in \mathscr{B}$, $(1-t)m + tn \in \mathscr{M}_p$ since $\mathscr{M}_p$ is a vector space. Therefore, $\frac{d((1-t)m+tn)}{dt} \in V_m\mathscr{M}$. It establishes a isomorphism between $\mathscr{M} \underset{\mathscr{B}}{\times} \mathscr{M}$ and $V(\mathscr{M})$.

4.2.2 Connections

For infinitesimally close points p and q in $\mathscr{B}$, the identification of the microelements $\mathscr{M}_p$ and $\mathscr{M}_q$ is a matter of choice that takes part in the overall model. This identification is performed by using a field of tangent vector to $\mathscr{M}$ along $\mathscr{M}_p$ whose projection on $\mathscr{B}$ is the constant vector $\vec{pq}$. This should be done along any fiber $\mathscr{M}_p$ and this assignment should be smooth and unique. This task is performed by Ehresmann connections. Let N be the connection, in local coordinates (x^a, y^i),

$$N = \left(\frac{\partial}{\partial x^a} - N_a^i(m) \frac{\partial}{\partial y^i} \right) \otimes dx^a.$$

This formula can be read as follow: the microelement $\mathscr{M}_p$ at p (with coordinates (x^a)) is identified with its neighbor $\mathscr{M}_q$ at q (with coordinates $(x^a + dx^a)$) using the infinitesimal transformation $\left(-N_a^i(m)dx^a\right) \frac{\partial}{\partial y^i}$ where $m \in \mathscr{M}_p$. If the points p and q are connected by a finite path σ, then $\mathscr{M}_q$ is identified with $\mathscr{M}_p$ by solving $(dy^i + N_a^i(m)dx^a)|_\sigma = 0$ *with* $m = (x, y)$. This last ordinary differential equation (ODE) may not have solution defined on the whole path σ and then the finite identification may not exist. A large class of connections ensuring the existence of finite identification is given by principal connections. Among them, the linear and affine connections are described below.

Definition 4.2.2. *Given a connection N and a solder form ϑ, another connection $N - \vartheta$ is defined by expression in local coordinate is:*

$$N - \vartheta = \left(\frac{\partial}{\partial x^a} - (N_a^i(m) + \vartheta_a^i(m)) \frac{\partial}{\partial y^i} \right) \otimes dx^a.$$

If $\mathscr{M} = T\mathscr{B}$, one may be especially interested in the particular case of linear connection meaning that $N_a^i(x, y) = \Gamma^i_{aj}(x)y^j$. In that case, the connection $N - \vartheta_{can}$ is will be called the associated linear connection. For a change of the coordinate system on $\mathscr{B}$: $\widetilde{x}^a = \widetilde{x}^a(x^b)$ leading to $\widetilde{y}^i = (\partial \widetilde{x}^i / \partial x^j) y^j$ on $T\mathscr{B}$, the connection coefficient satisfies the specific transformation rule:

$$\frac{\partial \widetilde{x}^b}{\partial x^a} \widetilde{N}_b^k = \frac{\partial \widetilde{x}^k}{\partial x^b} N_a^b - \frac{\partial^2 \widetilde{x}^k}{\partial x^a \partial x^b} y^b. \tag{4.2.1}$$

For linear connections, this implies that Γ satisfies the transformation law (1.2.3) (properties of the covariant derivative are given in (1.2)). It means that from any linear connection N on $\mathscr{M} = T\mathscr{B}$ one gets a covariant derivative ∇ on $\mathfrak{X}(\mathscr{B})$ with Christoffel symbols Γ and vice-versa (see Kolev and Desmorat, 2021 for discussion on covariant derivatives). Remark that all along the thesis the terminology *Christoffel symbols* will refer to coefficient of a covariant derivative or connection (see (1.2)) and they are not necessarily related to Riemannian metric.

4.2.3 Parallel and rolling transport

Let $\sigma : [0, 1] \to \mathscr{B}; t \mapsto \sigma(t) = (x^a(t))$ be a curve on $\mathscr{B}$. If $\mathscr{B}$ is an open subset of $\mathbb{E}^3$ this curve may be defined by the prescription of its origin $p = \sigma(0)$ and its tangent (velocity) field $\dot{\sigma}(t) = \dot{x}^a(t)\partial/\partial x^a$. For more general (non-euclidean) manifold $\mathscr{B}$, special attention should be paid to

such integration. Indeed, parallel and rolling without slipping transports along σ are usually defined for the Levi-Civita connection on a Riemannian manifold. In our context, "parallel" refers to the connection N and "rolling"[4] to the connection $N - \vartheta$. The definitions are as follows.

1. Its parallel lift is defined by

$$\dot{x}^a(\partial/\partial x^a - N^i_a(\sigma(t), y)\partial/\partial y^i).$$

   Hence the parallel lift of σ is obtained by solving

$$\dot{y}^i = -N^i_a(\sigma(t), y)\dot{x}^a.$$

2. Its rolling lift is defined by

$$\dot{x}^a(\partial/\partial x^a - \left(N^i_a(\sigma(t), y) + \vartheta^i_a(\sigma(t), y)\right)\partial/\partial y^i).$$

   Accordingly, the rolling lift of σ is obtained by solving

$$\dot{y}^i = -(N^i_a(\sigma(t), y) + \vartheta^i_a(\sigma(t), y))\dot{x}^a.$$

These lifts of the curve through any point $m \in \mathscr{M}$ exists locally and is unique, but it may not have solutions defined on the whole path σ (Epstein, 2010; Epstein, 2014; Nakahara, 2003). The above equations can be understood as they transport a point $(y^i(0)) \in \mathscr{M}_{\sigma(0)}$ along a curve σ into a point $(y^i(t)) \in \mathscr{M}_{\sigma(t)}$. Particularly, $\mathscr{M} = T\mathscr{B}$ so that $y^i(t)$ are components of vector $y(t) = y^i(t)\partial/\partial x^i \in T_{\sigma(t)}\mathscr{B}$. Hence, it can be interpreted as a transport of vectors.

Let us consider the particular case where $\mathscr{M} = T\mathscr{B}$, the connection is linear ($N^i_a(x, y) = \Gamma^i_{aj}(x)y^j$) and the solder form is the canonical one. The coordinate system (x^a) defines a basis $e_i = \delta^a_i \frac{\partial}{\partial x^a}$ in each tangent space. Writing $\mathcal{O}^i_j = \Gamma^i_{aj}(x)dx^a$ and $\mathsf{J}^i = \delta^i_a dx^a$, the above systems can be read as follows:

1. The parallel transport by the connection N of a vector $(y^i(0)) \in T_p\mathscr{B}$ along a curve σ on $\mathscr{B}$ with $\sigma(0) = p$ is obtained by solving the equations

$$\mathrm{d}Y = -\mathcal{O}Y \qquad \text{with} \qquad Y(t) = (y^i(t)). \tag{4.2.2}$$

2. The rolling transport by the connection $N - \vartheta$ of a point $p + y^i(0)e_i \in \mathscr{M}_p$ along σ is $\sigma(t) + y^i(t)e_i \in \mathscr{M}_{\sigma(t)}$ where $Y(t) = y^i(t)e_i \in T_{\sigma(t)}\mathscr{B}$ solves the equations

$$\mathrm{d}Y = -\mathcal{O}Y - \mathsf{J}\,. \tag{4.2.3}$$

[4]The name "rolling" transport is motivated by Cartan who generalized the notion of an affine connection. It may also be regarded as a specialization of the general concept of a principal connection, in which the geometry of the principal bundle is tied to the geometry of the base manifold using a solder form. Consider a smooth surface S in 3D $\mathbb{E}^3$. Every smooth surface S has a unique affine plane tangent to it at each point. A tangent plane can be "rolled" along S, and as it does so the point of contact traces out a curve on S. Conversely, given a curve on S, the tangent plane can be rolled along that curve. This provides a way to identify the tangent planes at different points along the curve.

4.2.4 Curvature and torsion

The total curvature $\mathcal{R}$ of our material (i.e. the bundle $\mathscr{M}$) measures the compatibility of $N - \vartheta$ with Lie brackets of vector fields. For two vector fields V and W on the base manifold $\mathscr{B}$, the curvature,

$$\mathcal{R}(V,W) = (N-\vartheta)\,[V,W] - \big[(N-\vartheta)V, (N-\vartheta)W\big]$$

is a vertical vector field on $\mathscr{M}$. This formula can be divided into two terms

$$\begin{aligned}\mathcal{R}(V,W) =& \Big(N[V,W] - [NV,NW] \Big) \\ &+ \Big(-[\vartheta V, \vartheta W] + [NV, \vartheta W] + [\vartheta V, NW] - \vartheta[V,W] \Big).\end{aligned}$$

At this step two contributions have to be highlighted:

Definition 4.2.3. *The first term is the Ehresmann curvature, namely $\mathfrak{R}(V,W)$, also called the* curvature of the connection. *The second term is the weak torsion, namely $\mathfrak{T}(V,W)$. We can write, $\mathfrak{R} = \mathfrak{R}^i{}_{ab}\dfrac{\partial}{\partial y^i} \otimes dx^a \otimes dx^b$ and $\mathfrak{T} = \mathfrak{T}^i{}_{ab}\dfrac{\partial}{\partial y^i} \otimes dx^a \otimes dx^b$ where their components are respectively given by:*

$$\mathfrak{R}^i{}_{ab} = \frac{\partial N^i_b}{\partial x^a} - \frac{\partial N^i_a}{\partial x^b} - N^j_a \frac{\partial N^i_b}{\partial y^j} + N^j_b \frac{\partial N^i_a}{\partial y^j}, \tag{4.2.4}$$

$$\mathfrak{T}^i{}_{ab} = -\vartheta^j_a \frac{\partial \vartheta^i_b}{\partial y^j} + \vartheta^j_b \frac{\partial \vartheta^i_a}{\partial y^j} + \frac{\partial \vartheta^i_b}{\partial x^a} - N^j_a \frac{\partial \vartheta^i_b}{\partial y^j} + \vartheta^j_b \frac{\partial N^i_a}{\partial y^j} - \vartheta^j_a \frac{\partial N^i_b}{\partial y^j} - \frac{\partial \vartheta^i_a}{\partial x^b} + N^j_b \frac{\partial \vartheta^i_a}{\partial y^j}. \tag{4.2.5}$$

The geometrical interpretation of the curvature is as follows.

Lemma 4.2.4. *If the curvature of a connection vanishes, then the lift of any loop σ on base manifold $\mathscr{B}$, when defined, is closed Epstein, 2010; Epstein, 2014.*

One gets two connections from one, adding or not the solder form. In general, the vanishing of $\mathcal{R}$ and the vanishing of $\mathfrak{R}$ are independent. When the connection have a special structure, it can happen that $\mathcal{R}$ controls $\mathfrak{R}$ as it is the case in the linear situation below where $\mathcal{R} = 0$ implies $\mathfrak{R} = 0$ and $\mathfrak{T} = 0$.

Lemma 4.2.5. *Let us consider the case where $\mathscr{M} = T\mathscr{B}$ and N linear, meaning that $N^i_a(x,y) = \Gamma^i{}_{aj}(x)y^j$, and $\vartheta = \vartheta_{can}$. It follows by direct computation :*

$$\mathfrak{R}^i{}_{ab} = \left(\frac{\partial \Gamma^i{}_{bj}}{\partial x^a} - \frac{\partial \Gamma^i{}_{aj}}{\partial x^b} + \Gamma^k{}_{bj}\Gamma^i{}_{ak} - \Gamma^k{}_{aj}\Gamma^i{}_{bk} \right) y^j = \mathsf{R}^i{}_{jab} y^j, \tag{4.2.6}$$

$$\mathfrak{T}^i{}_{ab} = \vartheta^j_b \Gamma^i{}_{aj} - \vartheta^j_a \Gamma^i{}_{bj} = \mathsf{T}^i{}_{ab}. \tag{4.2.7}$$

Here R and T are respectively the associated curvature and torsion tensor of the covariant derivative ∇ associated with Christoffel symbols Γ. In this sense, the derived tensors $\mathfrak{R}$ and $\mathfrak{T}$ of the connection N on $\mathscr{M}$ are a geometrical reformulation of the ones of ∇ on $\mathfrak{X}(\mathscr{B})$.

The curvature and torsion can be interpreted as an obstruction: let us remind that the rolling transport of $Y = (y^i) \in \mathscr{M}_p$ along the path σ is obtained by solving the equations (4.2.3): $\mathrm{d}Y =$

$-\mathcal{O}Y - \mathsf{J}$. Solutions may depend on the chosen path. It is not always possible to solve this system. In practice, this is possible if and only if $\mathrm{d}\mathrm{d}Y = 0$, otherwise the multivaluedness is measured by the non vanishing of

$$\mathrm{d}\mathrm{d}Y = -(\mathrm{d}\mathcal{O} + \mathcal{O} \wedge \mathcal{O})Y - (\mathrm{d}\mathsf{J} + \mathcal{O} \wedge \mathsf{J}). \tag{4.2.8}$$

The first component $\mathrm{d}\mathcal{O} + \mathcal{O} \wedge \mathcal{O}$ is the usual curvature matrix valued two-form R. The second term $\mathrm{d}\mathsf{J} + \mathcal{O} \wedge \mathsf{J}$ is the torsion vector valued two-form of T. Both are tensors over $\mathscr{B}$. By the way, the total curvature vanishes if and only if both the usual curvature and the usual torsion vanish.

4.2.5 Sasaki metric

At this stage, no metric tensor g has to be prescribed on $\mathscr{M}$. This latter is then, at this stage, a free parameter that could complete the characterization of the material manifold. In the following, particular metrics would appear naturally. These are Sasaki metrics (Bao, Chern, and Shen, 2000; Bucataru and Miron, 2007a; Pfeifer, 2013) defined in the coordinates (x^a, y^i) by:

$$\mathfrak{g}(m) = \mathsf{g}^h{}_{ab}(m) dx^a \otimes dx^b + \mathsf{g}^v{}_{ij}(m) \delta y^i \otimes \delta y^j. \tag{4.2.9}$$

The first term is called the horizontal metric and the other one is the vertical metric.

The benefit of this type of metric is that the split structure of the metric is preserved under any change of coordinates. This effect is ensured by the proper bases of such metric tensor that preserves the split structure of the tangent space $T\mathscr{M}$ involved by using the Ehresmann connection N. Indeed, it was stressed in (4.1.10) and (4.1.11) that for a given Ehresmann connection, the nonholonomic bases (δ_a, ∂_i) and $(dx^a, \delta y^i)$ are convenient local basis on $T\mathscr{M}$ and $T^*\mathscr{M}$, respectively. In practice, this illustrates that the notion of angle and length are meaningful only if such quantities are related to neighbouring points belonging to the same micro- or macro-universe. More precisely the horizontal metric is related to the macroscopic observations on the material, whereas the vertical part is related to points belonging to a given microelement.

4.3 Conclusion

A new description of a generalized microcontinuum in considering a vector bundle of fiber geometry character has been introduced. Even if no material transformation and no equation are mentioned at the moment, we believe that it demonstrates the power of geometric methods applied towards the framework of mechanics of the microstructured continuum. The geometrical construction encompasses many kinds of geometry. In this sense, it may capture a wide physical phenomenon. The application of our approach to model material with a distribution of defects is presented in the following research.

Chapter 5

On tangent geometry and generalized continuum with defects

The concepts of the geometrical structure of a microstructured continuum in terms of fiber character such as a solder form, an Ehresmann connection and a Sasaki metric are discussed just before. This chapter introduces tools on fiber geometry towards the framework of mechanics of microstructured continuum. The material is modeled by an appropriate bundle for which the associated connection and metric are induced from the Euclidean space by a smooth transformation represented by a fiber morphism from the bundle to the Euclidean space. Furthermore, the general kinematic structure of the theory includes macroscopic and microscopic fields in a multiscaled approach, including large transformation. Defects appear in this geometrical point of view by an induced curvature, torsion and non-metricity tensor in the induced geometry. Special attention is given to transport along a finite path in order to extend the standard infinitesimal analysis of torsion and curvature to a macroscopic point of view. Both theoretical and numerical analysis may be handled without additional difficulties. Accordingly, several examples of transformation involving the distribution of material defects are exhibited and analysed.

This chapter is organized as follows: *Section*-5.2 uses the notions in the previous chapter to material transformations. The primary intention is to describe structural changes in real materials; special attention is paid to kinematical interpretation. In this context, a scaled material modelling is introduced, which concerns material transformations represented by fiber morphisms. An induced connection and metric are first described, then derived geometrical quantities such as curvature, torsion, and non-metricity tensor are obtained. In *Section*-5.4, alternative approaches are reviewed and compared, significant features of this model are also exhibited. The applications of this theory are presented in *Section*-5.5. Special attention is paid to the simulation

of each process (transformation, parallel transport) in a dedicated space (tangent space, body, etc.) At the same time, several examples of material transformation with distributed defects are proposed and discussed. Conclusions follow in *Section*-5.6.

5.1 Toward transformation of microstructured media

On the one side, a continuum with microstructure is assumed to be a tangent bundle over a three-dimensional differentiable manifold $\mathscr{B}$. On the other side, $\mathbb{E}^3$ is the three-dimensional Euclidean space. For instance a fiber morphism or so-called bundle map $\mathscr{M} \to T\mathbb{E}^3$ presents the evolution of the microstructured material manifold $\mathscr{M}$ in the Euclidean space (Epstein, 2010; Epstein, 2014). It may possibly depend on time. By a language shortcut, such bundle map is sometimes called transformation hereafter.

The configuration of the body is described by the geometrical structure induced by pulling-back from $T\mathbb{E}^3$ onto $\mathscr{M}$. This current-induced geometry must be able to reveal if material defects are present or created by a material transformation. The main objective of this chapter is to specify how such defective configuration is obtained via such type of bundle mapping or generalization of this latter.

In particular, the complete characterization of the current configuration have to specify how measures and variations are performed around an infinitesimal neighbourhood of an element of $\mathscr{M}$. Such information is encoded on the covariant derivative ∇ and the metric tensor. These latter are acting on elements on $T\mathscr{M}$. In other words, the full configuration is controlled by the bundle map $T\mathscr{M} \to TT\mathbb{E}^3$. The following section is dedicated to this crucial point.

5.2 Scaled material model

Briefly, the model in *Chapter*-2 is not sufficient to describe all topological defects: even if dislocation densities are simulated, it looks impossible to introduce curvature that is the geometrical quantities measuring disclination densities. Additionally, some artifacts observed in the simulations seems to be not quantified by the geometrical properties of the manifold.

However, the language of fiber bundle geometry presented in *Section*-4.1 may help to overcome this drawback. For this purpose, the way how the pull-back operation of a fiber-mapping is used to construct an induced geometry of the transformed material body is presented and studied.

5.2.1 Preliminary

Here a special model is presented. It is restricted to the particular case where $\mathscr{M}$ is isomorphic to $T\mathscr{B}$ and where the solder form is canonical (in the following $\vartheta = \vartheta_{can}$).

Let us first remind some standard conventions: denote (X^A, Y^I) (respectively (x^a, y^i)) a chart on $\mathscr{M}$ (respectively $T\mathbb{E}^3$). The Euclidean space $\mathbb{E}^3$ has a canonical affine connection, namely the Levi-Civita connection γ of the Euclidean metric g (of course, if Cartesian chart is used on the Euclidean space, the connection coefficients vanish). Its tangent bundle, as any tangent bundle,

has a canonical solder form denoted by $\underline{\delta}$ as its component (δ^i_a) in any frame of $\mathbb{E}^3$ is the identity. Last the tangent bundle of the Euclidean space may be equipped with a trivial Ehresmann connection, with the following expression in a local coordinate system

$$n^i_a(x,y) = \gamma^i{}_{aj}(x)y^j, \tag{5.2.1}$$

and a metric tensor $\mathfrak{g}$ having a Sasaki form:

$$\mathfrak{g} = \mathrm{g}_{ab}(x)dx^a \otimes dx^b + \mathrm{g}_{ij}(x)\delta y^i \otimes \delta y^j. \tag{5.2.2}$$

Define $(E^K) = (dX^A, dY^I)$ with K running from 1 to 6, the first three basis elements are dX^A, the others are dY^I (A and I run from 1 to 3). Similarly, $(e_k) = (\partial_a, \partial_i)$ with k running from 1 to 6. The first three basis elements denote the ∂_a basis, the others coincide with ∂_i.

A geometrical transformation $\phi : \mathscr{B} \to \mathbb{E}^3$ is inducing an "idealized" material transformation

$$\mathscr{M} \to T\mathbb{E}^3$$

using the derivative and the canonical solder form : $(X,Y) \mapsto (\phi(X), \underline{\delta}F(X)\vartheta(Y))$ with $F = \phi_*$. In local coordinates the latter can be written $\delta^i_a F^a_A \vartheta^A_I Y^I$. From now on, the formula will be in shorter form: $F^i_I Y^I$. In that way, we define

$$F^i_I = \delta^i_a F^a_A \vartheta^A_I \qquad \text{and} \qquad F^a_I = F^a_A \vartheta^A_I \tag{5.2.3}$$

5.2.2 Overall approach

In most of standard works on the geometrical analysis of defective media, the tangent transformation $T\mathscr{M} \to TT\mathbb{E}^3$ is induced by the derivative of $\mathscr{M} \to T\mathbb{E}^3$ but this choice is not a strict constraint and could be relaxed. For this purpose, an Ehresmann connection has to be created. In the present chapter, the solder form defined on $T\mathscr{B}$ is always assumed to be the canonical form. The Ehresmann connection may be linear or not. However, in the following, special attention is given to the linear case for which Ehresmann curvature and weak torsion will coincide with the ones defined through covariant derivatives.

Mathematically, it is assumed that the continuum consists of a huge number of infinitesimal volume elements dV, located at point p in the base manifold $\mathscr{B}$ (p may be interpreted as the center of mass of dV, see Figure 2.5). The motion of p is governed by the map ϕ. Deformation of dV is controlled by $F = \phi_*$. In addition, the volume elements dV are composed of a large number of sub-domains/microelements δV of finite (but tiny) size. As δV contains a finite quantity of matter, its stretch may be considered. In this context, the continuum is deformed by two independent maps: F defines the stretch at a macroscopic scale whereas Θ defines the stretch at a microscopical scale.

If the material transformation is described by the bundle mapping $\mathscr{M} \to T\mathbb{E}^3$, $(X,Y) \mapsto (\phi(X), \Theta(X)Y)$ the scaling effect is not easily tractable as F and Θ are acting on vector belonging to $T_p\mathscr{B}$ and $\mathscr{M}_p$, respectively, that are equivalent manifolds (as $\mathscr{M} = T\mathscr{B}$ then $\mathscr{M}_p = T_p\mathscr{B}$), see also *Section*-2.

This difficulty can be circumvented in the following way: let us consider that the local change of a vector Y associated with the microstructure and belonging to $\mathscr{M}$, is measured by an element Z^v of $V(\mathscr{M})$. Hence, the material transformation is represented by a smooth map

$$\Upsilon^v : V(\mathscr{M}) \to VT\mathbb{E}^3, \quad (X, Y, Z^v) \mapsto (\phi(X), \underline{\delta}F(X)\vartheta Y, \Theta(X)Z^v)\,, \tag{5.2.4}$$

where $\Theta(X)$ is smooth, invertible and orientation preserving. Accordingly, such sub-scale modeling is no longer redundant since the maps related to each scale are separated.

To construct an induced Ehresmann connection the first idea is to extend Υ^v to the whole space i.e. find a bundle map Υ: $T\mathscr{M} \to TT\mathbb{E}^3$ of the form

$$(X, Y, Z) \mapsto (\phi(X), \underline{\delta}F(X)\vartheta Y, \Omega(X, Y)Z), \tag{5.2.5}$$

with $X \in \mathscr{B}$, $Y \in \mathscr{M}_X$, $Z \in T_{(X,Y)}\mathscr{M}$. At this stage the attention is now focused on $\Omega = \Omega^k_K e_k \otimes E^K$ or, in detail:

$$\Omega = \Omega^a_A \partial_a \otimes dX^A + \Omega^a_I \partial_a \otimes dY^I + \Omega^i_A \partial_i \otimes dX^A + \Omega^i_I \partial_i \otimes dY^I,$$

for which one has a great freedom of choice. The image of (X, Y) is already partially prescribed. Indeed, as the restriction of Υ for any element of $V(\mathscr{M})$ is imposed by (5.2.4):

$$\Omega^i_I(X, Y) = \Theta^i_I(X). \tag{5.2.6}$$

In order to avoid too complex interpretations, a second idea is proposed by considering that if $\Theta = F$ the scaling effect must not be observed. Then, if $\Theta = F$, the material transformation has to coincide with the simpler one $\mathcal{H} : \mathscr{M} \to T\mathbb{E}^3$, $(X, Y) \mapsto (\phi(X), \underline{\delta}F(X)\vartheta Y)$ for which Ω is nothing else than the total gradient $\mathcal{H}_*$. Accordingly, one gets:

$$\Omega^a_A(X, Y) = F^a_A(X) \qquad \text{and} \qquad \Omega^a_I = 0. \tag{5.2.7}$$

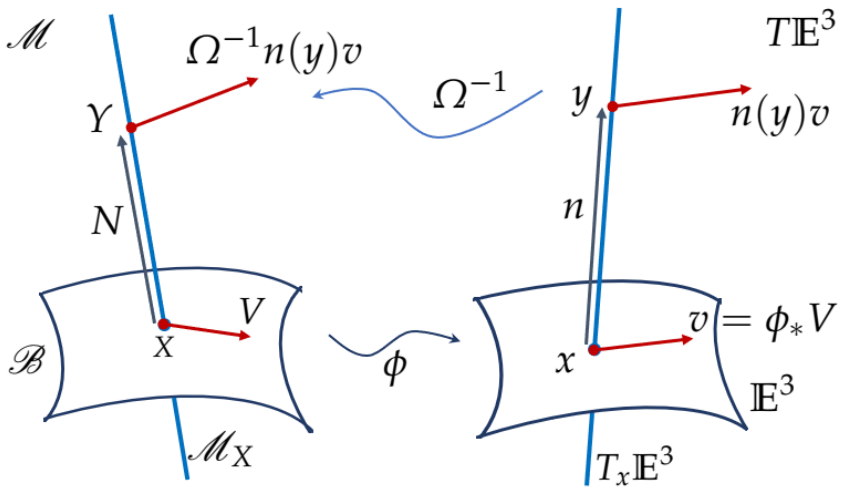

FIGURE 5.1: Pictorial representation of an induced Ehresmann connection.

5.3 Induced structure

At this stage Ω takes the following form:

$$\Omega = F^a_A \partial_a \otimes dX^A + \Omega^i_A \partial_i \otimes dX^A + \Theta^i_I \partial_i \otimes dY^I, \tag{5.3.1}$$

where the choice of $\Omega^i_A(X,Y)$ is still free. The inverse of Ω is given by $\Omega^{-1} = \Omega^K_k E_K \otimes e^k$ with $\Omega^K_k \Omega^\ell_K = \delta^\ell_k$ and $\Omega^K_k \Omega^k_L = \delta^K_L$. This later is of the form:

$$\Omega^{-1} = F^A_a \partial_A \otimes dx^a + \Omega^I_a \partial_I \otimes dx^a + \Theta^I_i \partial_I \otimes dy^i, \tag{5.3.2}$$

where $\Theta^I_i \Theta^j_I = \delta^j_i$ and $F^A_a F^b_A = \delta^b_a$.

Let V be an arbitrary tangent vector to $\mathscr{B}$ at a point $X \in \mathscr{B}$, the induced Ehresmann connection is naturally defined by considering its horizontal lift given by (a pictorial interpretation is given in Figure 5.1)

$$\begin{aligned} N(X,Y)V &= \Omega^{-1}\Big(n(\phi(X), \underline{\delta}F(X)\vartheta Y)(\phi_* V)\Big) \\ \text{with coefficients} \qquad N^I_A &= \Theta^I_i \Omega^i_A + \Theta^I_i n^i_a F^a_A. \end{aligned} \tag{5.3.3}$$

Here, we remind that n is the ambient Ehresmann connection. The connection coefficients $n^i_a(x,y) = \gamma^i{}_{aj}(x) y^j$, and γ the Levi-Civita connection given on $\mathbb{E}^3$ (see the beginning of *Section*-5.2). Note that the definition of the induced connection is independent of the chosen chart.

Proof. Firstly, let us define $v := \phi_* V = (F^a_A V^A)\partial_a$ a tangent vector to $\mathscr{B}$ at the point $x = \phi(X)$. Secondly, applying the ambient Ehresmann connection n, there is a unique horizontal lift $v^\uparrow = n(y)v = v^a \partial_a - n^i_a v^a \partial_i$ as a tangent vector to $T\mathscr{B}$ at $(x = \phi(X), y = \underline{\delta}F(X)\vartheta Y)$. Finally, the natural lift of V is obtained by solving the equation (5.3.3). Straightforward computations, using $\Omega^J_a = 0$, give

$$\begin{aligned} V^\uparrow &= \Omega^B_a v^{\uparrow a} \partial_B + \Omega^B_i v^{\uparrow i} \partial_B + \Omega^J_a v^{\uparrow a} \partial_J + \Omega^J_i v^{\uparrow i} \partial_J \\ &= \Omega^B_a F^a_A V^A \partial_B + \Omega^J_a F^a_A V^A \partial_J - \Omega^J_i n^i_a F^a_A V^A \partial_J \\ &= F^B_a F^a_A V^A \partial_B + \Omega^J_a F^a_A V^A \partial_J - \Omega^J_i n^i_a F^a_A V^A \partial_J \\ &= V^A \partial_A - \Big(\Omega^J_i n^i_a F^a_A - \Omega^J_a F^a_A\Big) V^A \partial_J. \end{aligned}$$

It claims that the connection coefficients are

$$N^J_A = \Omega^J_i n^i_a F^a_A - \Omega^J_a F^a_A.$$

Finally, because $\Omega^i_Z \Omega^Z_a = \Omega^i_B \Omega^B_a + \Omega^i_J \Omega^J_a = 0$, one has $\Omega^i_J N^J_A = -\Omega^i_J \Omega^J_a F^a_A + \Omega^i_J \Omega^J_j n^j_a F^a_A = \Omega^i_B \Omega^B_a F^a_A + n^i_a F^a_A = \Omega^i_A + n^i_a F^a_A$. Once again, writing $\Omega^z_J \Omega^I_z = \Omega^a_J \Omega^I_a + \Omega^i_J \Omega^I_i = \Omega^i_J \Omega^I_i = \delta^I_J$, the connection can be rewritten in the form

$$N^I_A = \Omega^I_i \Omega^i_J N^J_A = \Omega^I_i \Omega^i_A + \Omega^I_i n^i_a F^a_A.$$

Using the notation $\Omega_i^I(X,Y) = \Theta_i^I(X)$ introduced in the section 5.2, the formula (5.3.3) is verified. □

Proposition 5.3.1. *If the manifold $\mathscr{M}$ is endowed with the connection N given in (5.3.3), one obtains*

$$\Omega = F_A^a \frac{\delta}{\delta x^a} \otimes dX^A + \Theta_I^i \frac{\partial}{\partial y^i} \otimes \delta Y^I. \tag{5.3.4}$$

Hence Ω may be seen as the collection of two maps: $H_m(\mathscr{M}) \to H_{(x,y)}T\mathbb{E}^3$ and $V_m(\mathscr{M}) \to V_{(x,y)}T\mathbb{E}^3$. Roughly speaking, this states the existence of two independent mechanisms, the first one is the ordinary dragging of vectors by means of the deformation gradient $F = \phi_*$ of the macrostructure; the second mechanism is associated with the transformation Θ of the microstructure.

Proof. Without loss of generality Cartesian coordinate system is used on $T\mathbb{E}^3$ and accordingly $\delta/\delta x^a = \partial_a$. Combining with a fact that $\Omega_I^i \Omega_j^I = \Theta_I^i \Omega_j^I = \delta_j^i$, one obtains

$$\Omega = F_A^a \frac{\delta}{\delta x^a} \otimes dX^A + \Theta_I^i \frac{\partial}{\partial y^i} \otimes (\Omega_j^I \Omega^j{}_A dX^A + dY^I).$$

The proof of the proposition ends because $N_A^I = \Omega_i^I \Omega^i{}_A$ and $\delta Y^I = N_A^I dX^A + dY^I$. □

The induced metric is given by $\mathcal{G} = \Omega^* \mathfrak{g}$ or explicitly $\mathcal{G}(V,U) = \mathfrak{g}(\Omega V, \Omega U)$ for all $V, U \in T\mathscr{M}$. According to the connection N given in (5.3.3), this metric tensor has a Sasaki structure:

$$\begin{aligned} \mathcal{G}(X,Y) &= \mathsf{G}^h{}_{AB}(X) dX^A \otimes dX^B + \mathsf{G}^v{}_{IJ}(X) \delta Y^I \otimes \delta Y^J \\ \text{with} \qquad & \mathsf{G}^h{}_{AB} = F_A^a \mathsf{g}_{ab} F_B^b \qquad \mathsf{G}^v{}_{IJ} = \Theta_I^i \mathsf{g}_{ij} \Theta_J^j. \end{aligned} \tag{5.3.5}$$

Their components are just functions of the base coordinates X: the metric is uniquely defined at the point p of $\mathscr{B}$. Besides, it can be seen that the vertical metric component is always given by $\mathsf{G}^v{}_{IJ} = \mathcal{G}(\partial_I, \partial_J) = \Theta_I^i \mathsf{g}_{ij} \Theta_J^j$ what is explicitly independent of the definition of the Ehresmann connection N (even if the latter is a key ingredient of the definition of proper bases for the horizontal and vertical sub-spaces, see (4.1.10) and (4.1.11)). More precisely, the components of $\mathcal{G}$ in the proper horizontal and vertical bases are completely specified by Υ^v and they are independent of the choice of the (possibly non-linear) connection $N(X,Y)$.

From (5.3.4) and (5.3.5) it is observed that microscopic and macroscopic processes are naturally separated. More specifically, for microscopic process, the solder form is an important tool that relates the microscopic quantities (belonging to $V(\mathscr{M})$) to macroscopic quantities (belonging to $T\mathscr{B}$). By way of illustration, let us consider a vector field $V = V^A \partial/\partial X^A$ on $\mathscr{B}$. Its canonical vertical lift is $\vartheta V = \delta_A^I V^A \partial/\partial Y^I$ at any point along the fiber $\mathscr{M}_X$. The vertical metric G^v induces a metric G on $\mathscr{B}$ defined by $\mathsf{G}(X)(V,W) = \mathsf{G}^v(X)(\vartheta V, \vartheta W)$ for every $V, W \in T_X\mathscr{B}$. In a coordinates system:

$$\mathsf{G}_{AB} = \vartheta_A^I \Theta_I^i \mathsf{g}_{ij} \Theta_J^j \vartheta_B^J \qquad \left(\text{in short} \quad \mathsf{G}_{AB} = \Theta_A^a \mathsf{g}_{ab} \Theta_B^b \right). \tag{5.3.6}$$

This metric G may be chosen as a measure on $\mathscr{B}$ of the current configuration of the microsctructure. The construction of the connection N from this split-structure allows us to interpret macroscopically a change of microscopic quantities, this is evident through the mix-indices of the connection N^I_A.

5.3.1 Linear induced connection

Remind that the Euclidean space $\mathbb{E}^3$ has a canonical connection: the Levi-Civita connection γ of the Euclidean metric g. More precisely, the trivial Ehresmann connection n has the form $n^i_a(x,y) = \gamma^i{}_{aj}y^j$.

Lemma 5.3.2. *The connection is linear i.e.* $N^I_A(X,Y) = \Gamma^I{}_{AJ}(X)Y^J$ *if and only if* $\Omega^i{}_A(X,Y)$ *is linear i.e.* $\Omega^i{}_A(X,Y) = \Omega^i{}_{AJ}(X)Y^J$. *In that case, one obtains*

$$\Gamma^I{}_{AJ} = \Theta^I_i\Omega^i{}_{AJ} + \Theta^I_i\gamma^i{}_{aj}F^j_JF^a_A, \tag{5.3.7}$$

and if Cartesian coordinates are applied on $T\mathbb{E}^3$, $\Gamma^I{}_{AJ} = \Theta^I_i\Omega^i{}_{AJ}$.

Proof. It is direct thanks to (5.3.3) as Θ is independent of Y. Keep in mind that $n^i_a = \gamma^i{}_{aj}(x)y^j$ with $x = \phi(X)$ and $y = \underline{\delta}F\vartheta Y$, then straightforward computations gives $N^I_A(X,Y) = \Theta^I_i\Omega^i{}_A - \Theta^I_in^i_aF^a_A = \Theta^I_i\Omega^i{}_{AJ}Y^J - \Theta^I_i\gamma^i{}_{aj}y^jF^a_A = \Theta^I_i\Omega^i{}_{AJ}Y^J - \Theta^I_i\gamma^i{}_{aj}F^j_JY^JF^a_A$ which verifies (5.3.7). □

One considers hereafter $\Omega^i{}_A(X,Y) = \Omega^i{}_{AI}(X)Y^I$ where $\Omega^i{}_{AI}$ is free up to now. In order to remove this indeterminacy $\Omega^i{}_{AI}$ is constructed by a linear balance between the stretching variations at each scale (Figure 2.5):

$$\boxed{\Omega^i{}_{AI} = (1-\zeta)\partial_AF^i_I + \zeta\partial_A\Theta^i_I\,,} \tag{5.3.8}$$

where $0 < \zeta \leq 1$ is a free parameter controlling the scaling effect. For example and without any loss of generality, it can be defined as $\zeta = \ell/L$ where L and ℓ are the macroscopic and microscopic characteristic scales, respectively. The parameter ζ is called *scaling factor* hereafter.

The map Ω coincides with the total gradient of a linear bundle map $\mathscr{M} \to T\mathbb{E}^3$, $(X,Y) \mapsto (\phi(X), \underline{\delta}F(X)\vartheta Y)$ if $\Theta^i_I = F^i_I$. On the other hand, if $\zeta = 1$, the transformation coincides formally with the total gradient of $\mathscr{M} \to T\mathbb{E}^3$, $(X,Y) \mapsto (\phi(X), \Psi(X)Y)$ with $\Psi^i_I = \Theta^i_I$ (note that Ψ and Θ are not exactly the same tensor as they act on different spaces: $\mathscr{M}_p$ and $V_m(\mathscr{M})$ respectively).

Corollary 5.3.2.1. *If* $\Omega^i{}_A$ *satisfies* (5.3.8), *then one gets*

$$\Gamma^I{}_{AJ} = \Theta^I_i\Big((1-\zeta)\partial_AF^i_I + \zeta\partial_A\Theta^i_I\Big) + \Theta^I_i\gamma^i{}_{aj}F^j_JF^a_A\,, \tag{5.3.9}$$

and if Cartesian chart applied on $T\mathbb{E}^3$ *is used,* $\gamma^i{}_{aj} = 0$ *gives*

$$\boxed{\Gamma^I{}_{AJ} = \Theta^I_i\Big((1-\zeta)\partial_AF^i_J + \zeta\partial_A\Theta^i_J\Big)\,.} \tag{5.3.10}$$

5.3.2 Induced torsion, curvature and non-metricity tensor

As the induced Ehresmann connection N (5.3.10) is linear and the solder form defined on the tangent bundle is the canonical form, the affine connection Γ and the connection N contain the same information. Hence, following results are presented with Γ instead of N. From these connection and metric, it is easy to obtain the derived geometrical quantities such as curvature, torsion and non-metricity tensors.

The torsion of the connection is given by

$$\begin{aligned}
\mathsf{T}^I{}_{AB} &= \vartheta^J_B \Gamma^I_{AJ} - \vartheta^J_A \Gamma^I_{BJ}\,, \\
&= (1-\zeta)\Theta^I_i \left(\delta^J_B \partial_A F^i_J - \delta^J_A \partial_B F^i_J\right) + \zeta \Theta^I_i \left(\delta^J_B \partial_A \Theta^i_J - \delta^J_A \partial_B \Theta^i_J\right)\,, \\
&= (1-\zeta)\Theta^I_i \delta^i_c \left(\partial_A F^c_B - \partial_B F^c_A\right) + \zeta \Theta^I_i \left(\delta^J_B \partial_A \Theta^i_J - \delta^J_A \partial_B \Theta^i_J\right)\,, \\
&= \zeta \Theta^I_i \left(\delta^J_B \partial_A \Theta^i_J - \delta^J_A \partial_B \Theta^i_J\right)\,.
\end{aligned} \tag{5.3.11}$$

Here, we have used the fact that since $F = \phi_*$ then $\partial_A F^c_B = \partial_B F^c_A$. The torsion is proportional to the scaling factor ζ.

Second, the induced curvature of the connection is directly obtained from (4.2.6):

$$\mathsf{R}^I{}_{JAB} = \Omega^i_{BJ}\partial_A \Theta^I_i - \Omega^i_{AJ}\partial_B \Theta^I_i + \Theta^I_i \Theta^K_j \left(\Omega^i_{BJ}\Omega^j_{AK} - \Omega^i_{AJ}\Omega^j_{BK}\right). \tag{5.3.12}$$

According to (5.3.8) the curvature contains both linear and quadratic dependency on the scaling factor.

Finally, the connection may be not compatible with the vertical metric. It is measured by the non metricity tensor $\mathsf{Q} = \nabla \mathsf{G}$ for which components are $\mathsf{Q}_{IJA} = \nabla_A \mathsf{G}_{IJ}$. Let us compute the general form of the non metricity tensor by computing separately each contribution of $\partial_A \mathsf{G}_{IJ} - \Gamma^K_{AI}\mathsf{G}_{KJ} - \Gamma^K_{AJ}\mathsf{G}_{IK}$.

$$\begin{aligned}
\partial_A \mathsf{G}_{IJ} &= \partial_A \left(\Theta^i_I \mathsf{g}_{ij} \Theta^j_J\right) \\
&= \left(\partial_A \Theta^i_I\right)\mathsf{g}_{ij}\Theta^j_J + \Theta^i_I \mathsf{g}_{ij}\left(\partial_A \Theta^j_J\right) + \Theta^i_I \partial_A \mathsf{g}_{ij} \Theta^j_J.
\end{aligned}$$

Keep in mind that on the Euclidean space the connection is metric compatible

$$\begin{aligned}
\partial_A \mathsf{g}_{ij} &= \delta^a_i \delta^b_j \partial_A \mathsf{g}_{ab} = \delta^a_i \delta^b_j \partial_c \mathsf{g}_{ab} F^c_A = \delta^a_i \delta^b_j \left(\gamma^d{}_{ca}\mathsf{g}_{db} + \gamma^d{}_{cb}\mathsf{g}_{da}\right) F^c_A \\
&= \left(\gamma^k{}_{ai}\mathsf{g}_{kj} + \gamma^k{}_{aj}\mathsf{g}_{ki}\right) F^a_A.
\end{aligned}$$

Hence, one gets

$$\begin{aligned}
\partial_A \mathsf{G}_{IJ} &= \partial_A \left(\Theta^i_I \mathsf{g}_{ij} \Theta^j_J\right) \\
&= \left(\partial_A \Theta^i_I\right)\mathsf{g}_{ij}\Theta^j_J + \Theta^i_I \mathsf{g}_{ij}\left(\partial_A \Theta^j_J\right) + \Theta^i_I \left(\gamma^k{}_{ai}\mathsf{g}_{kj} + \gamma^k{}_{aj}\mathsf{g}_{ki}\right) F^a_A \Theta^j_J.
\end{aligned}$$

$$\begin{aligned}\Gamma^K_{AI}\mathsf{G}_{KJ} &= \Theta^K_i((1-\zeta)\partial_A F^i_I + \zeta\partial_A\Theta^i_I)\Theta^k_K \mathsf{g}_{kj}\Theta^j_J + \Theta^K_k\gamma^k_{ai}F^i_I F^a_A(\Theta^l_K \mathsf{g}_{lj}\Theta^j_J) \qquad \Theta^K_i\Theta^k_K = \delta^k_i\\ &= \delta^k_i((1-\zeta)\partial_A F^i_I + \zeta\partial_A\Theta^i_I)\mathsf{g}_{kj}\Theta^j_J + \gamma^k_{ai}F^i_I F^a_A\mathsf{g}_{kj}\Theta^j_J\\ &= ((1-\zeta)\partial_A F^i_I + \zeta\partial_A\Theta^i_I)\mathsf{g}_{ij}\Theta^j_J + \gamma^k_{ai}F^i_I F^a_A\mathsf{g}_{kj}\Theta^j_J.\end{aligned}$$

$$\begin{aligned}\Gamma^K_{AJ}\mathsf{G}_{IK} &= \Gamma^K_{AJ}\mathsf{G}_{KI} \qquad \mathsf{G}_{IK} = \mathsf{G}_{KI}\\ &= ((1-\zeta)\partial_A F^i_J + \zeta\partial_A\Theta^i_J)\mathsf{g}_{ij}\Theta^j_I + \gamma^k_{ai}F^i_J F^a_A\mathsf{g}_{kj}\Theta^j_I \qquad i\leftrightarrow j\\ &= \Theta^i_I\mathsf{g}_{ij}((1-\zeta)\partial_A F^j_J + \zeta\partial_A\Theta^j_J) + \gamma^k_{aj}F^j_J F^a_A\mathsf{g}_{ki}\Theta^i_I.\end{aligned}$$

$$\begin{aligned}\mathsf{Q}_{IJA} &= \Big(\partial_A\Theta^i_I\Big)\mathsf{g}_{ij}\Theta^j_J + \Theta^i_I\mathsf{g}_{ij}\Big(\partial_A\Theta^j_J\Big) - ((1-\zeta)\partial_A F^i_I + \zeta\partial_A\Theta^i_I)\mathsf{g}_{ij}\Theta^j_J\\ &\quad - \Theta^i_I\mathsf{g}_{ij}((1-\zeta)\partial_A F^j_J + \zeta\partial_A\Theta^j_J)\\ &\quad + \left(\Theta^i_I\Big(\gamma^k_{ai}\mathsf{g}_{kj} + \gamma^k_{aj}\mathsf{g}_{ki}\Big)F^a_A\Theta^j_J - \gamma^k_{ai}F^i_I F^a_A\mathsf{g}_{kj}\Theta^j_J - \gamma^k_{aj}F^j_J F^a_A\mathsf{g}_{ki}\Theta^i_I\right)\\ &= (1-\zeta)\left(\Big(\partial_A\Theta^i_I\Big)\mathsf{g}_{ij}\Theta^j_J + \Theta^i_I\mathsf{g}_{ij}\Big(\partial_A\Theta^j_J\Big)\right) - (1-\zeta)\left(\partial_A F^i_I\mathsf{g}_{ij}\Theta^j_J + \Theta^i_I\mathsf{g}_{ij}\partial_A F^j_J\right)\\ &\quad + \left(\gamma^k_{ai}\mathsf{g}_{kj}F^a_A\Theta^j_J(\Theta^i_I - F^i_I) + \gamma^k_{aj}\mathsf{g}_{ki}F^a_A\Theta^i_I(\Theta^j_J - F^j_J)\right)\\ &= (1-\zeta)\mathsf{g}_{ij}\left(\Theta^j_J\partial_A\Big(\Theta^i_I - F^i_I\Big) + \Theta^i_I\partial_A\Big(\Theta^j_J - F^j_J\Big)\right)\\ &\qquad + \gamma^k_{ai}\mathsf{g}_{kj}F^a_A\Big(\Theta^j_J(\Theta^i_I - F^i_I) + \Theta^j_I(\Theta^i_J - F^i_J)\Big).\end{aligned}$$

For Cartesian coordinates on the Euclidean space, $\mathsf{g}_{ij} = \delta_{ij}$ and the Christoffel symbols are $\gamma^k_{ij} = 0$, in such a case the formulas are simpler:

$$\begin{aligned}\mathsf{Q}_{IJA} &= \partial_A\mathsf{G}_{IJ} - \Gamma^K_{AI}\mathsf{G}_{KJ} - \Gamma^K_{AJ}\mathsf{G}_{IK},\\ &= (1-\zeta)\left(\Theta^i_J\partial_A\Big(\Theta^i_I - F^i_I\Big) + \Theta^i_I\partial_A\Big(\Theta^i_J - F^i_J\Big)\right).\end{aligned} \tag{5.3.13}$$

The metric is compatible with the connection, i.e. $\mathsf{Q} = 0$ if $\zeta = 1$ (no scaling effect) or if $\Theta = F$ (Euclidean manifold). Metricity of a transformation written in Cartesian coordinates on $\mathbb{E}^3$ is equivalent to the equation

$$\Theta^i_J\partial_A\Big(\Theta^i_I - F^i_I\Big) = -\Theta^i_I\partial_A\Big(\Theta^i_J - F^i_J\Big), \qquad \forall I, J, A\,, \tag{5.3.14}$$

meaning that, for any A, the tensor $\Theta^i_I\partial_A\Big(\Theta^i_J - F^i_J\Big)\partial_I\otimes\partial_J$ must be skew symmetric.

5.3.3 Summary

The manifold $(\mathscr{M}, \mathcal{G}, \Gamma)$ provides a complete description of the current configuration of the microstructured material. If (5.3.8) is assumed, it is governed by three independent quantities ϕ, Θ and ζ. The split structure of the transformation and metrics, underlined at the end of the section 5.3, allows us to describe the current state as the superposition of a microscopic and macroscopic

processes. These latters are coupled as they are driven by the same kinematic quantities ϕ and Θ. The scalar ζ governs such coupling, this has motivated the *scaling factor* name. This structure is able to describe the current configuration on $\mathscr{B}$ by defining a micro-manifold $(\mathscr{B}, \mathsf{G}, \Gamma)$ with $\mathsf{G} \equiv \mathsf{G}^v$ (see (5.3.6)) and a macro-manifold $(\mathscr{B}, \mathsf{G}^h, \mathsf{L})$ with

$$\mathsf{L}^C{}_{AB} = \frac{1}{2}\mathsf{G}^{hCD}\left(\partial_A \mathsf{G}^h{}_{BD} + \partial_B \mathsf{G}^h{}_{AD} - \partial_D \mathsf{G}^h{}_{AB}\right), \tag{5.3.15}$$

being the Christoffel symbols of the horizontal metric. This connection has no torsion and no curvature and is metric-compatible. The properties of $(\mathscr{B}, \Gamma, \mathsf{G})$ is richer:

Proposition 5.3.3. *If Ω^i_A satisfies lemma-5.3.2, with Ω^i_{AJ} satisfying (5.3.8), the manifold $(\mathscr{B}, \mathsf{G}, \Gamma)$ has the following properties:*

- *If $\Theta = F$, then macro and microelements behave in the same way. It yields that $\mathsf{T} = 0$; $\mathsf{R} = 0$ and $\nabla \mathsf{G} = 0$. The manifold behaves as an Euclidean space.*
- *If $\zeta = 1$, then the scaling effect is no longer considered. In that case the manifold behaves as a Weitzenböck manifold with $\mathsf{T} \neq 0$, $\mathsf{R} = 0$ and $\nabla \mathsf{G} = 0$.*
- *If $\zeta \to 0$, then the size of the microsctructure tends to be negligible. Even if $\mathsf{T} \to 0$, one may observe $\mathsf{R} \neq 0$ and $\nabla \mathsf{G} \neq 0$. In particular, if $\nabla \mathsf{G} = 0$ the manifold tends to behaves as Riemann-Cartan manifold.*
- *If $\Theta \neq F$ and $0 < \zeta < 1$, then $\mathsf{T} \neq 0$, $\mathsf{R} \neq 0$ and $\nabla \mathsf{G} \neq 0$. The manifold behaves as a Weyl manifold.*

5.4 Alternative approaches

5.4.1 Non-scale material modeling

In the previous section, the material transformation has been enriched by introducing a map Θ specifying how vector belonging to $V(\mathscr{M})$ is transformed independently on ϕ. An alternative method consists in prescribing an enrichment on the tangent-map acting on $\mathscr{M}_p = T_p\mathscr{B}$. In such a case, the transformation is specified by the bundle map:

$$\mathcal{H} \,:\, \mathscr{M} \to T\mathbb{E}^3 \quad (X, Y) \mapsto (\phi(X), \Psi(X, Y)), \tag{5.4.1}$$

where $\Psi(X, Y)$ is supposed to be smooth, with a smooth inverse and satisfies the condition that $\Psi(X, Y) = 0$ if and only if $Y = 0$. Accordingly, the total gradient $\mathcal{H}_* = D\mathcal{H}$ of the bundle mapping is given by

$$\begin{aligned} \mathcal{H}_* &= \mathcal{H}^k_K \, e_k \otimes E^K = \partial_K \mathcal{H}^k \, e_k \otimes E^K \,, \\ &= \partial_A \phi^a \, \partial_a \otimes dX^A + \partial_A \Psi^i \, \partial_i \otimes dX^A + \partial_I \Psi^i \, \partial_i \otimes dY^I. \end{aligned} \tag{5.4.2}$$

Its inverse is given by $\mathcal{H}^* = \mathcal{H}^K_k E_K \otimes e^k$ with $\mathcal{H}^K_k \mathcal{H}^\ell_K = \delta^\ell_k$ and $\mathcal{H}^K_k \mathcal{H}^k_L = \delta^K_L$. It givens explicitly:

$$\mathcal{H}^* = F^A_a \partial_A \otimes dx^a + \partial_a \Psi^I \partial_I \otimes dx^a + \partial_i \Psi^I \partial_I \otimes dy^i. \tag{5.4.3}$$

With the same spirit as (5.3.3), an induced Ehresmann connection is obtained by

$$\begin{aligned} N(Y)V &= \mathcal{H}^* n\Big(\phi(X), \Psi(X,Y)\Big)\phi_* V \\ \text{with coefficients} \qquad N_A^I &= \partial_j \Psi^I n_a^j F_A^a + \partial_i \Psi^I \partial_A \Psi^i. \end{aligned} \tag{5.4.4}$$

The induced connection is not necessarily linear as soon as it is not the case for $\Psi(X,Y)$.

Proof. Define $V^\uparrow = N(Y)V = \mathcal{H}^* n(y)v$ where $v^\uparrow = n(y)v = v^a\partial_a - n_a^i v^a \partial_i$ with $v = \phi_* V = F_A^a V^A \partial_A$. Using (5.4.3), straightforward computations give

$$\begin{aligned} V^\uparrow &= \mathcal{H}_a^B v^{\uparrow a}\partial_B + \mathcal{H}_i^B v^{\uparrow i}\partial_B + \mathcal{H}_a^J v^{\uparrow a}\partial_J + \mathcal{H}_i^J v^{\uparrow i}\partial_J \\ &= F_a^B v^a \partial_B + \mathcal{H}_a^J v^a \partial_J + \mathcal{H}_i^J v^{\uparrow i}\partial_J \\ &= F_a^B F_A^a V^A \partial_B + \mathcal{H}_a^J F_A^a V^A \partial_J - \mathcal{H}_i^J n_a^i F_A^a V^A \partial_J \\ &= \delta_A^B V^A \partial_B - (\mathcal{H}_i^J n_a^i F_A^a - \mathcal{H}_a^J F_A^a) V^A \partial_J \\ &= V^A \partial_A - (\mathcal{H}_i^J n_a^i F_A^a - \mathcal{H}_a^J F_A^a) V^A \partial_J. \end{aligned}$$

Hence, the connection coefficients are

$$N_A^J = \mathcal{H}_i^J n_a^i F_A^a - \mathcal{H}_a^J F_A^a.$$

Next, using a fact that $\mathcal{H}_Z^i \mathcal{H}_a^Z = \partial_B \Psi^i F_a^B + \partial_I \Psi^i \partial_a \Psi^I = 0$, one gets

$$\begin{aligned} \partial_I \Psi^i N_A^I &= \partial_I \Psi^i \Big(\partial_j \Psi^I n_a^j F_A^a - \partial_a \Psi^I F_A^a\Big) \\ &= \partial_I \Psi^i \partial_j \Psi^I n_a^j F_A^a + \partial_B \Psi^i F_a^B F_A^a \\ &= \partial_I \Psi^i \partial_j \Psi^I n_a^j F_A^a + \partial_A \Psi^i. \end{aligned}$$

Once again, writing $\mathcal{H}_I^z \mathcal{H}_z^J = \mathcal{H}_I^a \mathcal{H}_a^J + \mathcal{H}_I^i \mathcal{H}_i^J = \mathcal{H}_I^i \mathcal{H}_i^J = \partial_I \Psi^i \mathcal{H}_i^J = \delta_I^J$, one obtains

$$\begin{aligned} N_A^J &= \mathcal{H}_i^J \partial_I \Psi^i N_A^I = \mathcal{H}_i^J \partial_I \Psi^i \partial_j \Psi^I n_a^j F_A^a + \mathcal{H}_i^J \partial_A \Psi^i \\ &= \partial_j \Psi^J n_a^j F_A^a + \partial_i \Psi^J \partial_A \Psi^i. \end{aligned}$$

This is the end of the proof. □

Lemma 5.4.1. *The associated Ehresmann curvature $\mathfrak{R}$ always vanishes.*

Proof. From definition 4.2.3, for arbitrary vectors field V and U on $\mathscr{B}$, one has

$$\begin{aligned} \mathfrak{R}(U,V) = &\; N\left[V,U\right] - \left[NV, NU\right] \\ = &\; \mathcal{H}^*\Big(n\left(\phi_*\left[V,U\right]\right)\Big) - \Big[\mathcal{H}^*(n\left(\phi_* V\right)), \mathcal{H}^*(n\left(\phi_* U\right))\Big] \\ = &\; \mathcal{H}^*\Big(n\Big(\left[\phi_* V, \phi_* U\right]\Big)\Big) - \mathcal{H}^*\Big[n\left(\phi_* V\right), n\left(\phi_* U\right)\Big]. \end{aligned} \tag{5.4.5}$$

Since the curvature of the connection n vanishes, $n([\phi_* V, \phi_* U]) = [n(\phi_* V), n(\phi_* U)]$. This proves that $\mathfrak{R}(U,V) = 0$ yielding that the Ehresmann curvature $\mathfrak{R}$ vanishes [1]. □

To go further the pull-back operator has not to be defined by the total gradient $\mathcal{H}_*$. This is exactly what has been done in the *scaled material model*, see *Section*-5.2.

Proposition 5.4.2. *If the manifold $\mathscr{M}$ is endowed with the connection N, the total gradient $\mathcal{H}_*$ becomes*

$$\mathcal{H}_* = F^a_A \frac{\delta}{\delta x^a} \otimes dX^A + \partial_I \Psi^i \frac{\partial}{\partial y^i} \otimes \delta Y^I. \tag{5.4.6}$$

Next, an induced metric is defined by $\mathcal{G} = \mathcal{H}^* \mathfrak{g}$ i.e. $\mathcal{G}(V,U) = \mathfrak{g}(\mathcal{H}_* V, \mathcal{H}_* U)$ with $V, U \in T\mathscr{M}$. With respect to the connection N, this tensor splits like Sasaki metric:

$$\begin{aligned} \mathcal{G}(X,Y) &= \mathsf{G}^h{}_{AB}(X) dX^A \otimes dX^B + \mathsf{G}^v{}_{IJ}(X,Y) \delta Y^I \otimes \delta Y^J, \\ \text{with} \qquad & \mathsf{G}^h_{AB} = F^a_A \mathsf{g}_{ab} F^b_B, \qquad \mathsf{G}^v_{IJ} = \partial_I \Psi^i \mathsf{g}_{ij} \partial_J \Psi^j. \end{aligned} \tag{5.4.7}$$

Similarly, it can be seen that the vertical metric components are always given by $\mathsf{G}^v{}_{IJ} = \mathcal{G}(\partial_I, \partial_J) = \partial_I \Psi^i \mathsf{g}_{ij} \partial_J \Psi^j$, then the vertical metric is independent of the induced connection N.

Keeping in mind that our objective was to construct a linear Ehresmann connection with torsion and curvature, the present bundle maps fail for the following reasons: (1) the vertical metric $\mathsf{G}^v(X,Y)$ is generally dependent on fiber coordinates; (2) the connection is not linear; (3) the curvature of the connection is always zero.
However, in the linear situation for which $\Psi^i(X,Y) = \Psi^i_I(X) Y^I$, the non-scale material modeling may be seen as a subset of the scaled material model. Indeed, the micro-manifold on $\mathscr{B}$ (specified in *Section*-5.3.3) shares the same properties as the manifold induced by (5.4.1) if $\Theta = \Psi$ and/or $\zeta = 1$. More precisely, one gets

Theorem 5.4.3. *If* (5.4.1) *is linear, one gets*

- $N^I_A(X,Y) = \Gamma^I{}_{AJ}(X) Y^J$; *with* $\Gamma^C_{AB} = \Psi^C_c \partial_A \Psi^c_B$ *if Cartesian coordinates are used on* $T\mathbb{E}^3$.
- *The metric* G^v *induces a metric on* $\mathscr{B}$ *by* $\mathsf{G} = \vartheta^* \mathsf{G}^v$, *locally* $\mathsf{G}_{AB} = \Psi^a_A \mathsf{g}_{ab} \Psi^b_B$.

This elements construct a Weitzenböck manifold $(\mathscr{B}, \Gamma, \mathsf{G})$ with metric-compatible connection and torsion while vanishing curvature. Obviously, if $\Psi = F$, no defect appears meaning that the torsion and curvature of the connection vanish.

Remark 5.4.4. *Our approach may be interesting to those who are familiar with (pseudo-)Finsler geometry and its applications. For Finsler space, the connection and its derived geometric quantities (curvature, etc.) are generated by a metric tensor that is driven by a fundamental scalar function $L(X,Y)$ exists at every point (except for $Y = 0$), homogeneous of degree one in Y (Bao, Chern, and Shen, 2000). Our geometric construction resembles a so-called pseudo-Finsler space (Bejancu, 1990) where the fundamental scalar function with requisite properties Bao, Chern, and Shen, 2000, from which the components of the metric are obtained by differentiation, does not exist. Consequently, the connection and metric are*

[1] In the above proof, we have used the fact that let $\mathfrak{M}$ and $\mathfrak{N}$ be arbitrary differential manifolds, for any vector u, v on $\mathfrak{M}$ and differential map h: $\mathfrak{M} \to \mathfrak{N}$, then $h_*[u,v] = [h_* u, h_* v]$ see Chapter 5.3.2 in Nakahara, 2003

completely independent. The geometrical construction affords great generality for describing several phenomena in physics. Application of (pseudo-)Finsler geometry in continuum mechanics and physics have been suggested earlier by Kondo, 1963, later by Saczuk, 1997; Fu, Saczuk, and Stumpf, 1998; Stumpf and Saczuk, 2000, and nowadays by Pfeifer, 2013; Clayton, 2015; Clayton, 2017a; Clayton, 2017b; Yajima and Nagahama, 2020. Non-conservative mechanical systems may be explored through a non-linear connection in the Riemannian and Finslerian framework Bucataru and Miron, 2007b. Such non-linear connections are mainly used to express the non-linear relation between fields having different natures Yajima and Nagahama, 2007. An example of an application for a Rikitake system may be found in Yajima and Nagahama, 2007.

5.4.2 On comparison with the *nonholonomic principle*

The forms of the metric and the connection presented in *Theorem*-5.4.3 look qualitatively similar to the ones in numerous other defect-theories Bilby, Bullough, and Smith, 1955; Noll, 1967/68; Kröner, 1981; Le and Stumpf, 1996a; Yavari and Goriely, 2012a. Among them, one of the powerful tools is the *nonholonomic principle* Kleinert, 2000; Katanaev, 2005; Kleinert, 2008. In this context, the continuum is modeled by a differential manifold $\mathscr{B}$ supporting a non-standard material transformation: a map from $\mathscr{B}$ into $\mathbb{E}^3$) $X \mapsto x$ which is not smooth in general and may be multivalued (to simplify problem we assume (x^a) is Cartesian). However, it is possible to map the points surrounding X defined by the tangent vector dX to dx via an infinitesimal transformation thanks to triads $\mathbf{e}^a_A$ such that

$$dx^a = \mathbf{e}^a_A dX^A. \tag{5.4.8}$$

Their reciprocal triads are introduced by $\mathbf{e}^a_A \mathbf{e}^A_b = \delta^a_b$ and $\mathbf{e}^a_A \mathbf{e}^B_a = \delta^B_A$. It is therefore usual to define metric-components, as extension of the usual definitions

$$\widehat{\mathsf{G}}_{AB} = \mathsf{g}(\mathbf{e}^a_A e_a, \mathbf{e}^b_B e_b) = \mathbf{e}^a_A \mathsf{g}_{ab} \mathbf{e}^b_B, \tag{5.4.9}$$

where g is the metric tensor of the Euclidean space $\mathbb{E}^3$.

On the other hand, one can differentiate the vector base, and implicitly define an affine connection coefficients

$$\widehat{\nabla}_B e_C = \frac{\partial e_C}{\partial X^B} = \frac{\partial \mathbf{e}^c_C}{\partial X^B} e_c = \left(\mathbf{e}^A_c \frac{\partial \mathbf{e}^c_C}{\partial X^B} \right) e_A := \widehat{\Gamma}^A_{BC} e_A. \tag{5.4.10}$$

The connection may have both torsion and curvature. Furthermore, the connection is metric-compatible.

By construction, several cases may occur, it permits us to highlight the role of torsion and curvature tensors on the classification of continuum transformation:

Holonomic transformation: If the mapping $X \mapsto x$ is smooth and single-valued, the triads are usually the deformation gradient of the map with $\mathbf{e}^a_A = \partial x^a / \partial X^A$. Then it is straightforward to check that the torsion and curvature are equal to zero during the holonomic transformation. The same result is obtained if $F = \Psi$ in *Theorem*-(5.4.3), or if $F = \Theta$ in *Proposition*-(5.3.3).

Nonholonomic transformation and torsion: If **e** are single-valued but they are not the deformation gradient in the case of the mapping $X \mapsto x$ is smooth and/or not single-valued. the induced manifold is a Weitzenböck manifold like in *Theorem*-5.4.3. In that sense, Ψ plays the same role than the triads e. However, the presented approach differs on a crucial point: in the present model the material manifold is a fiber bundle and the material transformation is a fiber morphism. Such a map is smooth and single-valued and is sufficient to define the induced metric and connection thanks to the concepts of Ehresmann connection. This point allows wide type of mathematical analysis and numerical simulation is more comfortably handled.

Nonholonomic transformation and curvature: let us focus on some modeling for which triads are multivalued. As a consequence, the connection has both torsion and curvature. This connection is metric compatible. However, the connection and metric are, generally, also multivalued. This could cause difficulties in performing consistent length measuring and parallel transport. On the contrary, to achieve this goal the *scaled material model* in *Section*-5.2 is still driven by smooth fields (without additional degree-of-freedom if (5.3.8) is used). Furthermore, the large class of manifold have been observed, see *Proposition*-(5.3.3).

5.4.3 Spin connection

Remind that connection having both torsion and curvature cannot be obtained with single-valued triads. Another method consists in introducing an additional field to give a connection (Obukhov, Ponomariev, and Zhytnikov, 1989) (see discussion Rakotomanana, 2018; Katanaev, 2005):

$$\widetilde{\Gamma}^{A}_{BC} = \mathbf{e}^{A}_{c}\partial_{B}\mathbf{e}^{c}_{C} + \mathbf{e}^{A}_{c}\omega^{c}{}_{Ba}\mathbf{e}^{a}_{C}, \tag{5.4.11}$$

where the first term reduces to the Weitzenböck connection with non-zero torsion but zero curvature. The second term has a role of spin connection, with possibly non-zero torsion and/or non-zero curvature. Such a connection is metric compatible, see *Section*-1.5.2.3.

The similarity with (5.3.10) has to be underlined even if the overall approach is different. One can write

$$\Gamma^{A}_{BC} = \zeta\Theta^{A}_{a}\partial_{A}\Theta^{a}_{C} + (1-\zeta)\Theta^{A}_{a}\partial_{B}F^{a}_{C}, \tag{5.4.12}$$

in which the first term is the Weitzenböck connection, whereas the other $\Theta^{A}_{a}\partial_{B}F^{a}_{C}$ plays the role of spin connection. Here, the sum of the two distributions is controlled by the factor ζ in the linear way.

5.4.4 On comparison with Kröner-Lee-decomposition

Lee and his coworker Le and Stumpf, 1996a; Le and Stumpf, 1996c starting with the ideas from Noll, 1967/68; Wang, 1967/68 and the multiplicative decomposition $\mathbb{F} = \mathbb{F}_{e}\mathbb{F}_{p}$ generally used for elastoplastic transformation of material, see *Section*-1.5.1.2, they obtained some relations between torsion of the crystal connection and the elastic and plastic distortions. The induced material

manifold is Weizenböck. Later, Yavari and Goriely, 2012a was inspired by this approach and had introduced the slightly different method where they identified the plastic deformation gradients as Cartan's moving frames to construct the appropriate material manifolds. Nevertheless, the requirement that the material manifold with an evolving connection (compatible with the metric) yielding that the frame field is everywhere parallel is not apparent.

The present model seems to be an alternative to the multiplicative decomposition. It is clear that the total gradient is Θ which controls the stretch of microelement from the initial to the final state. Elastic part is then the derivative of ϕ and hence $\mathbb{F}_p \sim F^{-1}\Theta$. This last expression obscures a crucial point: in the present model, the intermediate configuration is not present. This concept is replaced by the consideration of vertical and horizontal tangent spaces that are the support for map linearization on vector field related to distinct quantities: $H(\mathscr{M})$ is related to macroscopic vector field whereas $V(\mathscr{M})$ is related to vector field associated with the microstructure (orientation of grain in a lattice for example).
Such interpretation avoids the intermediate configuration. More crucially, it is an alternative to the homogenization process recently introduced Reina, Schlömerkemper, and Conti, 2016. In this latter work, as in the present chapter, a scaling effect is introduced in order to replace the intermediate configuration. The point of view exposed in *Section*-5.2 suffices to introduce several types of microstructural processes and defect in a unified geometrical formalism and with a reduce the number of kinematical variables (in practice, the class of defect is wider than in Reina et al.'s approach).

5.4.5 The solder form and moving frame

If we cut the continuum into many small pieces (dV), each piece will be individually deformed using the solder form (it defines a new piece $\delta V = \vartheta(dV)$). After that, each piece will be driven by the embedding ϕ that defines its position while its stretch is controlled by the elastic deformation $F = d\phi$. Mathematically, this process can be formalized as a mapping

$$\mathscr{M} \to T\mathbb{E}^3,\ (X, V) = (\phi(X), F\vartheta(V))$$

Therefore, $F\vartheta$ may be considered as the total gradient, and the solder form naturally defines a moving frame for the material manifold. Such interpretation also avoids the standard-intermediate configuration.

5.5 Explicit transformations producing curvature, torsion and metricity tensor

This section presents the applications of the proposed theory. Special attention is paid to the simulation of each process (transformation, parallel transport) in dedicated spaces (tangent space, body, etc.) in order to compare the properties of the material transformations Υ^v and the derived connection generated by Υ. Accordingly, several examples of material transformation with distributed defects are proposed and discussed. Mainly, we will find explicit material transformations producing curvature, torsion and metricity tensor separately.

5.5.1 Parallel and rolling transport

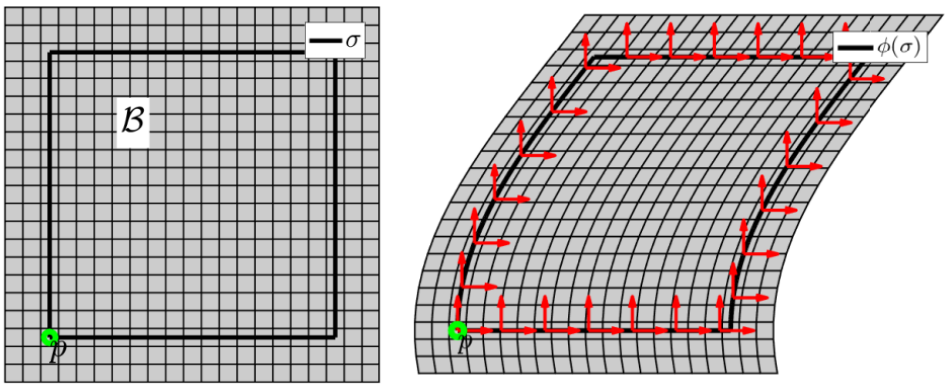

FIGURE 5.2: Left: representation of the body $\mathscr{B}$. Cells are a representation of $V_m T\mathscr{B}$. A closed material loop $\sigma(t)$ is specified. This loop σ will be used all along Section 5.5. Right: a defect-free current state in the ambient space $\mathbb{E}^2$.

In order to present the application of the *scaled material model*, illustrations are restricted to in-plane motion in the Euclidean ambient space endowed with $\mathrm{g} = \delta$ and the trivial Levi-Civita connection $n = 0$. Hence, the body $\mathscr{B}$ is labeled by two Cartesian coordinates (X^1, X^2) with respect to an affine frame (O, e_1, e_2) on the plane, see Figure 5.2-left.

A current state related to a defect-free transformation is represented in the ambient space $\mathbb{E}^2$ (Figure 5.2-right). As no defect are present, the parallel transport of a normal frame (red arrows) along a path $\phi(\sigma(t))$ do not change its ambient properties. However, material components of a parallel transported vector change along the path. On the other hand, the dragging of material vectors by the transformation is depicted by the change of size and form of the cells. This shape reveals the material metrics.

In Figure 5.3 another point of view is proposed where the transformation is presented in $\mathscr{B}$ by a pull-back operation. Here, the non-uniformity of the parallel transported frames is the manifestation of the material transformation.

For a more general transformation, for which the body contains defects, Υ^v is defined by (5.2.4)

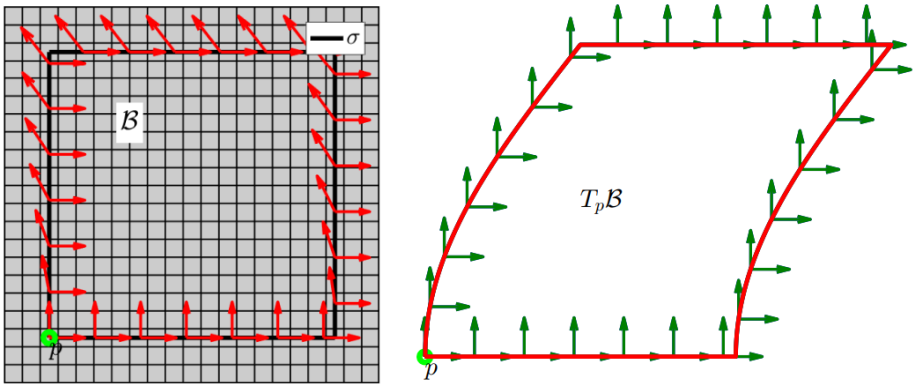

FIGURE 5.3: Left: The same defect-free current state than in Figure 5.2 but represented in $\mathscr{B}$. Right: developing curve $\widetilde{\sigma}$ of σ on $T_p\mathscr{B}$.

and with condition (5.3.8). The prescribed map ϕ, $F = \phi_*$ and Θ are smooth, invertible and orientation preserving. Hence, for a given ζ, these ingredients are used to define G, Γ, T, R and Q (see (5.3.6), (5.3.10), (5.3.11), (5.3.12), (5.3.13) respectively). These Lagrangian tensors depend on the reference coordinates and are associated with fiber bundles on the body $\mathscr{B}$. In order to illustrate the various types of defect, the parallel and rolling transports are complementary tools revealing the geometrical properties of the manifold (*Section*-4.2.3). However, their manifestations differ according to the chosen representation as it was already observed by comparing Figure 5.2 and 5.3. Here are presented briefly how such transports may be computed and illustrated.

Let us first consider a point $p \in \mathscr{B}$ and a path $\sigma(t) = (X^A(t))$ on $\mathscr{B}$ parameterized by $t \in [0,1]$ with $\sigma(0) = p$. The parameterization $\sigma(t)$ generates a tangent vector field $\dot{\sigma}(t) = \dot{X}^A(t)\partial/\partial X^A$, last $dX^A = \dot{X}^A(t)\,dt$ is defined for numerical purpose.

1. The *parallel transport* of a vector $Y^I e_I \in T_p\mathscr{B}$ along σ is the point $\sigma(t) + Y^I(t)e_I \in \mathscr{M}_{\sigma(t)}$ obtained by solving (4.2.2):

$$Y^I(t+dt) = Y^I(t) - \Gamma^I_{AJ}(\sigma(t))Y^J dX^A \qquad \text{with} \qquad Y^I(0) = Y^I. \tag{5.5.1}$$

   A vector $Y^I(t)$ belongs to $T_{\sigma(t)}\mathscr{B}$. For illustration on $\mathbb{E}^2$, $F(\sigma(t))Y(t)$ is presented at $\phi(\sigma(t))$.

2. The *rolling transport* of the point $p + \widetilde{Y}^I e_I \in T_p\mathscr{B}$ along σ is obtained by determining $Y(t) = (Y^I(t))$ solving (4.2.3) :

$$Y^I(t+dt) = Y^I(t) - \Gamma^I_{AJ}(\sigma(t))Y^J dX^A - \delta^I_A dX^A \qquad \text{with} \qquad Y^I(0) = \widetilde{Y}^I \tag{5.5.2}$$

   Such a vector gives the coordinates of a point in the frame $(\sigma(t), e_1, \dots e_n)$ of $T_{\sigma(t)}\mathscr{B}$. Remember that $\mathscr{M}_p$ is $T_p\mathscr{B}$ which is viewed as an abstract affine space tangent to $\mathscr{B}$ at p. In particular $\mathscr{M}_p \cap \mathscr{B} = \{p\}$.

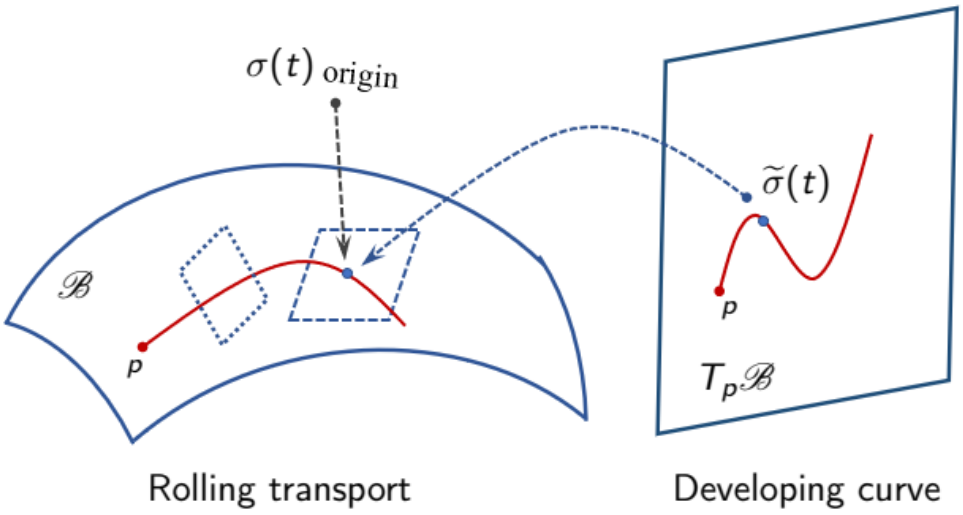

FIGURE 5.4: A pictorial representation of the developing curve.

This last transport is used to defines two reciprocal transports of curves:

1. For a path σ on $\mathscr{B}$, the *developing curve* is the curve $\widetilde{\sigma}$ on $T_p\mathscr{B}$ such that the rolling transport of $\widetilde{\sigma}(t) = p + \widetilde{Y}^I(t)e_I$ in $T_{\sigma(t)}\mathscr{B}$ is the origin of this tangent space, namely $\sigma(t)$ (a pictorial representation is given by Figure (5.4)). This curve is the curve drawn by the contact point of tangency of an affine space that rolls without slipping along σ, staying tangent to $\mathscr{B}$. It can be computed by searching the successive initial conditions $\widetilde{Y}(t)$ such that the coordinates of the rolling transport on $T_{\sigma(t)}\mathscr{B}$ is null. The procedures is the following:
Let $A(t)$ be the matrix solving $dA = -\mathcal{O}A$ along σ with initial condition $A(0) = Id$ and $B(t)$ be the solution of $dB = -\mathcal{O}B - J$ along σ with initial condition $B(0) = 0$. Then the solution of (4.2.3) along σ with initial condition $Y(0)$ is $Y(t) = A(t)Y(0) + B(t)$. Now the developing curve is $\sigma(0) + \widetilde{Y}^I(t)e_I$ with $\widetilde{Y}(t)$ satisfying $0 = A(t)\widetilde{Y}(t) + B(t)$ *i.e.* $\widetilde{Y}(t) = -A^{-1}(t)B(t)$. Technically one solves the equations on A and B by a numerical Euler scheme:

$$A^I_K(t+dt) = A^I_K(t) - \Gamma^I_{AJ}(\sigma(t))A^J_K(t)dX^A(t) \qquad \text{with} \quad A(0) = Id, \tag{5.5.3}$$

$$B^I(t+dt) = B^I(t) - \Gamma^I_{AJ}(\sigma(t))B^J(t)dX^A(t) - \delta^I_A dX^A(t) \qquad \text{with} \quad B(0) = 0. \tag{5.5.4}$$

Then $\widetilde{Y}(t) = -A^{-1}(t)B(t)$ is plotted on $T_p\mathscr{B}$. The developing curve $\widetilde{\sigma}$ of σ is presented on $T_p\mathscr{B}$ in Figure 5.3-right. On $T_p\mathscr{B}$ all the frames parallel-transported along σ are equal (this holds true even for defective transformations).

2. The *driven curve* is the curve σ on $\mathscr{B}$ whose developping curve is a given curve $\widetilde{\sigma}$ in $T_p\mathscr{B}$. The driven curve is unique if the initial point of $\widetilde{\sigma}$ is p. Indeed, comparison of two deformations could be done by fixing a curve $\widetilde{\sigma}$ in $T_p\mathscr{B}$ and compare the two driven curves on $\mathscr{B}$.
This curve is obtained by solving a non linear system of ODE. Let Γ^I_{AJ} be the coefficients of the connection and $\widetilde{\sigma}(t) = p + \widetilde{Y}^I(t)e_I$ be a path in $T_p\mathscr{B}$ satisfying $\widetilde{Y}^I(0) = 0$. The driven curve $\sigma(t) = (X^A(t))$ and the matrix of the parallel transport $A(t)$ along σ have to be computed simultaneously:

$$X^A(t+dt) - X^A(t) = \delta^A_I A^I_J(t)\Big(\widetilde{Y}^J(t+dt) - \widetilde{Y}^J(t)\Big) \tag{5.5.5}$$

$$A^I_J(t+dt) - A^I_J(t) = -\Gamma^I_{AK}(\sigma(t))A^K_J(t)(X^A(t+dt) - X^A(t)) \tag{5.5.6}$$

where $\Gamma^K_{AJ}(\sigma(t))$ is nothing else than $\Gamma^K_{AJ}(X^A(t))$. Initial conditions are $X^A(0) = 0$ and $A(0) = Id$. The driven curve can be plotted either on $\mathscr{B}$ or on $\phi(\mathscr{B})$.

Let us denote $\mathcal{D} : (p, \sigma(t)) \to (p, \widetilde{\sigma}(t))$ the application defining a developing curve. If $\widetilde{\sigma}$ is the developing curve of σ on $\mathscr{B}$, then σ is the driven curve of $\widetilde{\sigma}$. In other words, the application $(p, \widetilde{\sigma}(t)) \to (p, \sigma(t))$ defining a driven curve is $\mathcal{D}^{-1}$. Hence, the presence of defect may be characterized on $T_p\mathscr{B}$ (by fixing a loop σ and analysing the properties of $\widetilde{\sigma}$) or in $\mathscr{B}$ (by fixing a $\widetilde{\sigma}$ and checking the properties of the corresponding driven curve). These two methods are equivalent.

For a defect-free transformation, the image of the transformation given by the driven curve (Figure 5.3-right) and by the embedding in the Euclidean space (Figure 5.2-right) are the same

up to a rigid motion. It is no more true for a defective transformation as it would be seen in the next examples.

5.5.2 Pure-non-metric transformation

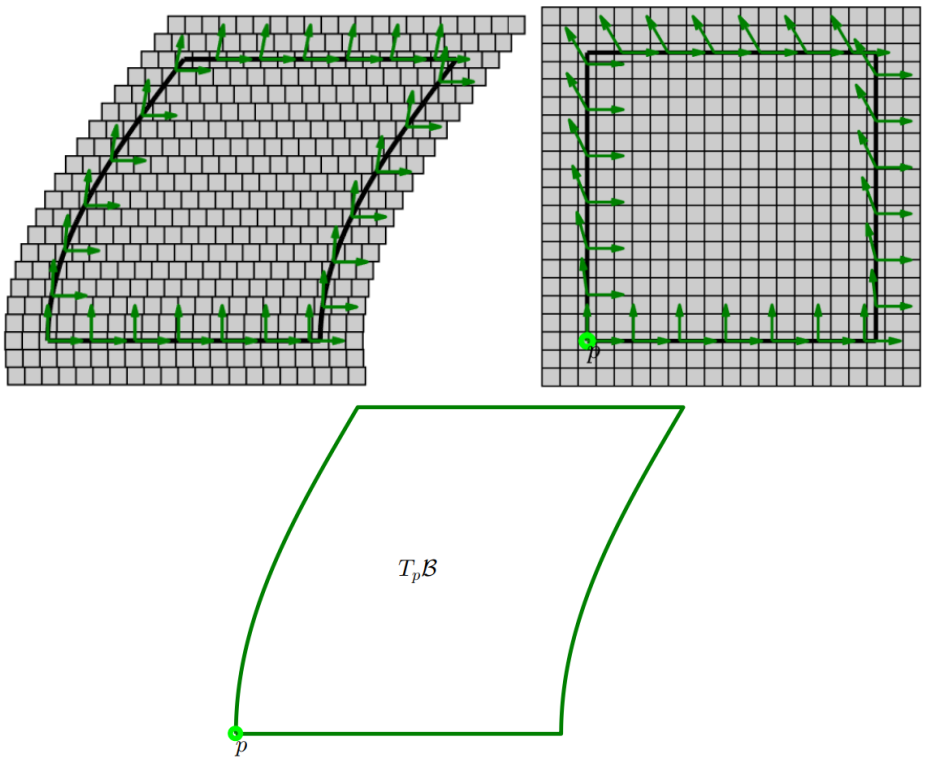

FIGURE 5.5: Numerical simulations of the transformation (5.5.7). The current state has no torsion and no curvature but the metric is not compatible with the induced connection. Top representation in $\mathbb{E}^3$ (right) and in $\mathscr{B}$ (left). The frame at p is parallel-transported along σ. Bottom developing curve of σ on $T_p\mathscr{B}$ obtained.

Let us consider the map ϕ and its derivative F as follows:

$$\begin{array}{cccc} \phi & X^1 & \to & x^1 = X^1 + h(X^2) \\ & X^2 & \to & x^2 = X^2 \end{array} \qquad F = \begin{pmatrix} 1 & f(X_2) \\ 0 & 1 \end{pmatrix}. \tag{5.5.7}$$

where h is a C^2-function $\mathscr{B} \to \mathbb{R}$ and of course $f(X^2) = \partial_2 h$. Suppose that Θ is identity, and then $\mathsf{G} = \delta$. The only non-zero connection coefficient is $\Gamma^1_{22} = (1-\zeta)\,\partial_2 f$ and consequently, $\mathsf{T} = 0$. Direct computation shows that $\mathsf{R} = 0$. However, the connection is not metric-compatible as:

$$\nabla_2 \mathsf{G}_{12} = \nabla_2 \mathsf{G}_{21} = -(1-\zeta)\frac{\partial f}{\partial X^2}. \tag{5.5.8}$$

The other components of Q are zero.

This situation is illustrated in Figure 5.6 with

$$f(X^A) = \frac{\pi}{4}\sin\left(\frac{X^A}{8L}\pi\right) \tag{5.5.9}$$

of course $X^A = X^2$. Each cell is related to a microelement. As relative placement of micro-cell is controlled by F the superposition of macro and micro-stretch is graphically interpretable. The identity $\mathsf{G} = \delta$ supported by the local metric is clearly highlighted as shape and size of cells are unchanged. This lattice representation is not sensitive to ζ. A rigid translation of each microscopic layer is observed in the current configuration. In practice, no-void or overlap appear, no defect is created during such transformation. In addition, the incompatibility of the gliding of macro-cell with the metric of microelement is clearly quantified by $\nabla_2 \mathsf{G}_{12} \neq 0$.

Geometrically, the parallel-transport along σ of a vector-frame initially placed at p is obtained by solving (5.5.1). It is observed that the vectors change along the loop even if no torsion and no-curvature are present in the induced manifold. This phenomena is a direct repercussion of the non-standard connection which takes into consideration the transformation at both scales. After transportation along the closed loop the final vector coincides with the initial vector as no curvature is present Figure 5.6. However, the closure of the developing curve assures that the connection has vanishing torsion and vanishing curvature Figure 5.6.

Last, from an energetic point of view it is clear that the reference and current state share the same internal energy. This is quantified by the preservation of metric, torsion and curvature between the two states. One may consider that in such infinite domain, the current state is obtained by a re-labeling of reference state. But in a mechanical point of view such re-organisation of material points involves some energy to cut inter-atomic interaction, even if the total energy involved for both cutting and re-connecting all atoms is null. Hence from a physical point of view, this process is associated with a shift of energetic interaction but is time-consuming too. The non-metricity tensor Q is a geometric candidate for measuring such non-elastoplastic process.

5.5.3 Length-scale dependence

Theoretically, the parallel-transport is highly sensitive to the scaling factor ζ. If $\zeta = 0$, the effect of the micro-stretch is absent on the parallel transport. If $\zeta = 1$ the connection is compatible with the micro-metric, the parallel transport does not change locally the frame as $\Theta = Id$; however vectors are converted by F if the transformation is presented in the ambient space, see Figure 5.6.

In practice, the metric-incompatibility of the connection can be illustrated by the observation from the developing curve if defects are absent. If the factor $\zeta = 0$, the developing curve coincide with $\phi(\sigma)$ up to a rigid motion. For $\zeta = 1$, the connection is metric-compatible and the developing curve coincides with σ as $\mathsf{G} = \delta$. In all these processes, the developing curves are closed, see Figure 5.6. The scaling factor effects for the torsion and curvature (or observation of dislocations and disclinations) is presented in the following subsections.

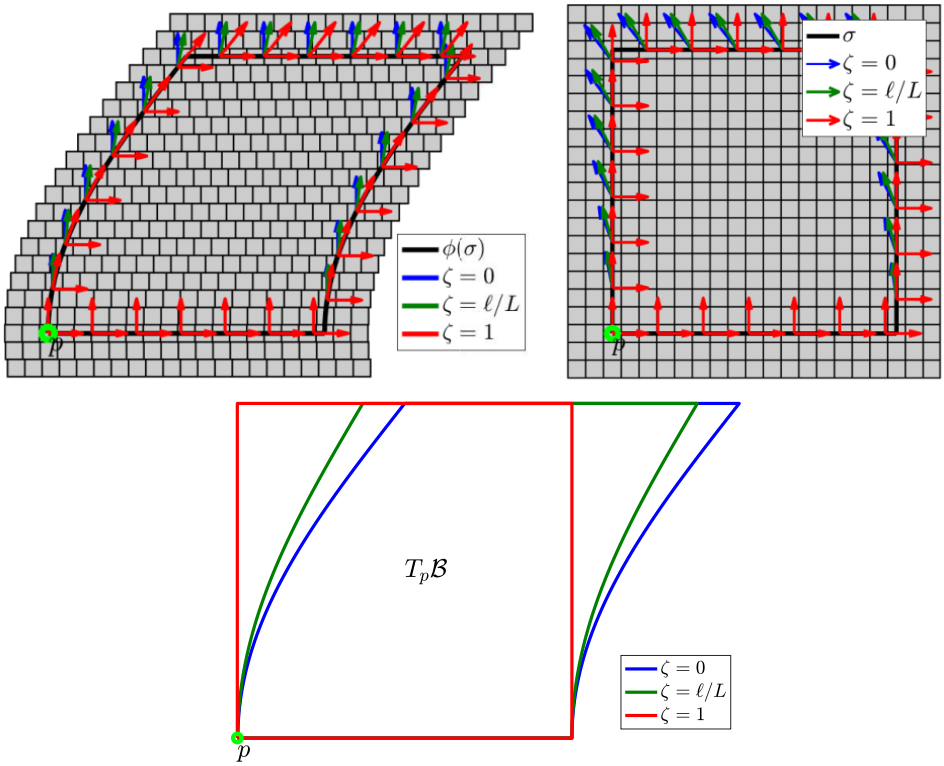

FIGURE 5.6: Numerical simulations of the transformation (5.5.7). The current state has no torsion and no curvature but the metric is not compatible with the induced connection. Top representation in $\mathbb{E}^3$ (right) and in $\mathscr{B}$ (left). The frame at p is parallel-transported along σ. Bottom developing curve of σ on $T_p\mathscr{B}$ obtained for various ζ.

5.5.4 Torsion with no curvature

The first example is already mentioned in *subsection*-1.6.3.2. For such transformation, the metric tensor becomes

$$\mathsf{G} = \begin{pmatrix} 1 & \theta \\ \theta & 1+\theta^2 \end{pmatrix}. \tag{5.5.10}$$

The non-zero connection coefficient is now $\Gamma^1_{12} = \zeta\,\partial_1\theta$ and the torsion is no more null. More precisely the non-zero components of the torsion are

$$\mathsf{T}^1_{12} = -\mathsf{T}^1_{21} = \zeta\frac{\partial\theta}{\partial X^1}. \tag{5.5.11}$$

The curvature is zero, but the non-metricity tensor indicates:

$$\nabla_1\mathsf{G}_{22} = 2(1-\zeta)\theta\,\frac{\partial\,\theta}{\partial X^1} \qquad \nabla_1\mathsf{G}_{12} = \nabla_1\mathsf{G}_{21} = (1-\zeta)\frac{\partial\,\theta}{\partial X^1}. \tag{5.5.12}$$

Illustration is given in Figure 1.14-left with $\theta(X^1)$ as follows:

$$\theta(X^A) = \frac{\pi}{4}\cos\left(\frac{X^A}{4L}\pi\right). \tag{5.5.13}$$

The presence of edge dislocation with defect along X^1 is clearly observed. Other type of disloca-

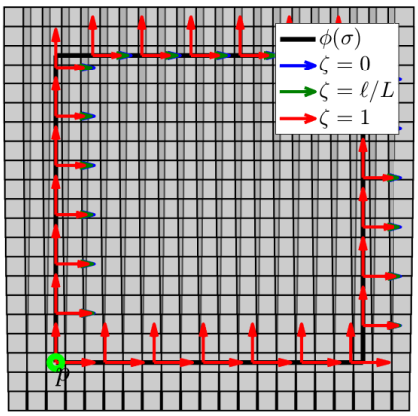

FIGURE 5.7: Representation in the ambient space of the current configuration for the transformation (5.5.14). There is no curvature but the non-zero components of the torsion are $\mathsf{T}^1_{12} = -\mathsf{T}^1_{21}$, last the metric is not compatible with the induced connection.

tions may be obtained, with still $F = \mathbb{I}$ but:

$$\Theta = \begin{pmatrix} 1+\theta(X^2) & 0 \\ 0 & 1 \end{pmatrix}. \tag{5.5.14}$$

Here

$$\mathsf{G} = \begin{pmatrix} (1+\theta)^2 & 0 \\ 0 & 1 \end{pmatrix}. \tag{5.5.15}$$

and the only non zero connection coefficient is $\Gamma^1_{21} = \zeta\,(\partial_2\theta)/(1+\theta)$ leading to a non zero torsion:

$$\mathsf{T}^1_{21} = -\mathsf{T}^1_{12} = \zeta \frac{1}{1+\theta}\frac{\partial\theta}{\partial X^2}$$

what looks qualitatively similar to (5.5.11). The non-metricity has a unique non-zero component:

$$\nabla_2 \mathsf{G}_{11} = 2(1-\zeta)(1+\theta)\,\frac{\partial\,\theta}{\partial X^2}.$$

Last the curvature is still zero. Illustration is given in Figure 5.7 with θ still specified by Figure 1.14 (with $X^A = X^2$). The pattern is clearly different to Figure 1.14. The two simulations show that several processes may be involved in order to create material with no-curvature but Burger vector along X^1. The first one is related to a non-uniform gliding of the microelement whereas the second one is obtained by a non-uniform extension of these latter. However, even if the value of the torsion T^1_{12} is the same at a fixed point, for the two processes, the non-metricity tensor Q differs and provides information on the process involved.

Geometrically, since ϕ is smooth and σ is closed, $\phi(\sigma)$ is closed whatever the transformation (1.6.12) or (5.5.14). If a vector is parallel transported along this close loop (arrow in Figure 1.15

and Figure 5.7) the final vector recovers its initial properties as it returns to the initial point (as the curvature is absent). Such procedure is not suitable for highlighting torsion of the manifold and hence revealing a distribution of dislocation in the defected material. But the presence of dislocation is predicted as follows: In Figure 1.17 and Figure 5.8 the developing curve $\widetilde{\sigma}$ of σ on $T_p\mathscr{B}$ is given. In that case the curve $\widetilde{\sigma}$ is no more closed if $\mathsf{T} \neq 0$ ($\zeta \neq 0$) and presents a gap along X^1 direction. Further discussion follows in the next subsection.

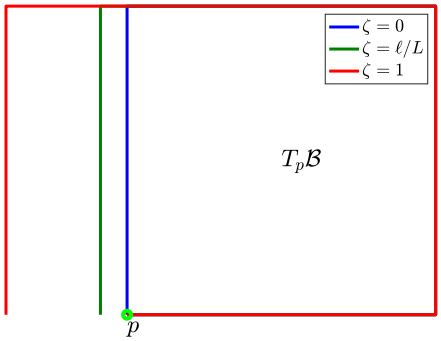

FIGURE 5.8: Representation in the ambient space of the current configuration for the transformation (5.5.14) (left) and developing curve $\widetilde{\sigma}$ obtained for various ζ (right). There is no curvature but the non-zero components of the torsion are $\mathsf{T}^1{}_{12} = -\mathsf{T}^1{}_{21}$, last the metric is not compatible with the induced connection.

5.5.5 Discussion on Burger vector

We continue the discussion on the developing curve in Figure 1.17 and Figure 5.8. If computation is performed around p along an infinitesimal material loop of size $\delta x^1 \times \delta x^2$ this gap coincides with $\mathsf{T}^1{}_{12}\delta x^1 \delta x^2$. For such infinitesimal loop, it is a quantifier of dislocation density. Here the computation is performed on a finite domain and this gap on $\widetilde{\sigma}$ does not coincide with $\mathsf{T}^1{}_{12}\Delta x^1 \Delta x^2$ (where Δx^i are size of the loop σ) as the torsion is not uniform in these simulations. It must be highlighted that even for such finite loop, the directions $\dot{\sigma}$ at p are unchanged. The developing curve preserves this signature if curvature is null as it is commonly observed for infinitesimal domain. It can be seen as a characterisation of the absence of curvature in a finite domain.

It must be emphasized that the developing curve $\widetilde{\sigma}$ of a material curve σ does not correspond to

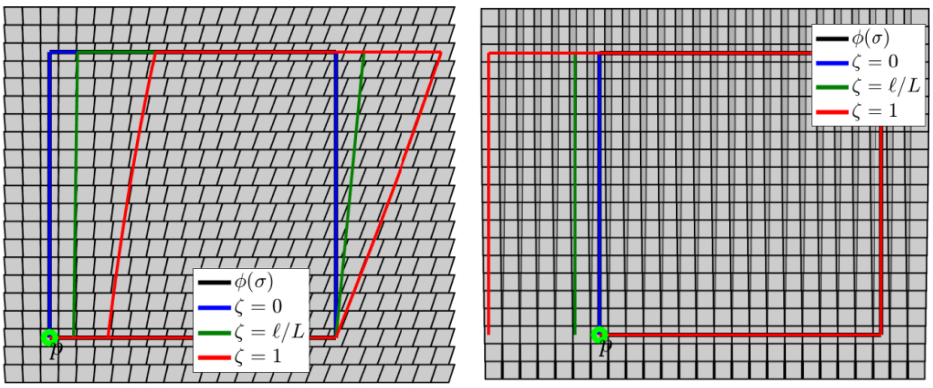

FIGURE 5.9: Burger's circuit $\underline{\sigma}$ obtained for various ζ and for the transformations (1.6.12) (left) and (5.5.14) (right) represented in the ambient space.

the heuristic process consisting to following, along with the microstructure, the directions prescribed by a macroscopic loop. This principle is commonly presented as a methodology to define the Burger vector over an infinitesimal material loop. It can be obtained by searching the path $\underline{\sigma}(t)$ (hereafter called the Burger's circuit) in $\mathscr{B}$ associated with coordinates $\underline{X}^A(t)$. The unknown $\underline{X}^A(t)$ is obtained by solving iteratively the process

$$(p, \sigma(t)) \xrightarrow{\mathcal{D}} (p, \tilde{\tilde{\sigma}}(t)) \xrightarrow{\mathsf{D}^{-1}} (p, \underline{\sigma}(t)) \tag{5.5.16}$$

where D is the application defining the developing curve with connection of the base manifold $(\mathscr{B}, \mathsf{G}^h, \mathsf{L})$. As $\mathsf{D} \neq \mathcal{D}$, the Burger's circuit $\underline{\sigma}(t)$ is not $\sigma(t)$. In practice the following explicit Euler numerical scheme is used to solve (5.5.16):

$$A^I_J(t+dt) = A^I_J(t) - \Gamma^I_{AK}(\underline{\sigma}(t)) A^K_J(t) d\underline{X}^A(t) \qquad \text{with} \quad A(0) = Id, \tag{5.5.17}$$

$$d\tilde{\tilde{Y}}(t) = A(t)^{-1} dX(t) \qquad \text{with} \quad d\tilde{Y}(0) = dX(0), \tag{5.5.18}$$

$$\mathsf{A}^I_J(t+dt) = \mathsf{A}^I_J(t) - \mathsf{L}^I_{AK}(\underline{\sigma}(t)) \mathsf{A}^K_J(t) d\underline{X}^A(t) \qquad \text{with} \quad \mathsf{A}(0) = Id, \tag{5.5.19}$$

$$d\underline{X}(t) = \mathsf{A}(t) d\tilde{\tilde{Y}}(t) \qquad \text{with} \quad d\underline{X}(0) = dX(0), \tag{5.5.20}$$

$$\underline{X}(t+dt) = \underline{X}(t) + d\underline{X}(t) \qquad \text{with} \quad \underline{X}(0) = X(0), \tag{5.5.21}$$

Illustration is given in Figure 5.9 for the two transformations. If $\zeta = 1$, the result is equivalent to the standard illustration of Burgers-circuit on Riemann-Cartan manifold (2.1) (with $\zeta = 0$ and for zero-curvature $\underline{\sigma}(t) = \sigma(t)$). The present *scaled material model* weight this effect if $\zeta \neq 1$.
In Figure 5.9, the orientation $\dot{\underline{\sigma}}$ is not preserved after the finite loop: $\Delta\dot{\underline{\sigma}} = \dot{\underline{\sigma}}(1) - \dot{\underline{\sigma}}(0) \neq 0$ as opposed to what was observed on the developing-curve. In other words, on a finite Burger-circuit $\Delta\dot{\underline{\sigma}} = 0$ is not a signature of absence of curvature. It must be also observed that the gap between initial and final point of the path $\Delta\underline{\sigma} = \underline{\sigma}(1) - \underline{\sigma}(0)$ is different to $\Delta\tilde{\sigma} = \tilde{\sigma}(1) - \tilde{\sigma}(0)$. Last numerical simulations show that $\Delta\underline{\sigma}$ changes if traveling along σ is performed clockwise or counterclockwise. This confirms that Burger-circuit is not a topologically invariant measure of defect density. In contrary $\Delta\tilde{\sigma}$ is unchanged and looks more robust for a quantification of the defect density.

5.5.6 Curvature with no torsion

Let us consider a kinematic transformation specified by the following tensors:

$$F = \begin{pmatrix} 1 & f(X^2) \\ 0 & 1 \end{pmatrix} \qquad \Theta = \begin{pmatrix} 1+\theta(X^1) & 0 \\ 0 & 1 \end{pmatrix} \tag{5.5.22}$$

Note that both of them may be defined as a total derivative of a $\mathscr{B} \to \mathbb{E}^3$ map. The metric is of the form (5.5.15). The non-null connection coefficients are

$$\Gamma^1_{11} = \frac{\zeta}{1+\theta} \frac{\partial \theta}{\partial X^1} \qquad \Gamma^1_{22} = \frac{1-\zeta}{1+\theta} \frac{\partial f}{\partial X^2} \tag{5.5.23}$$

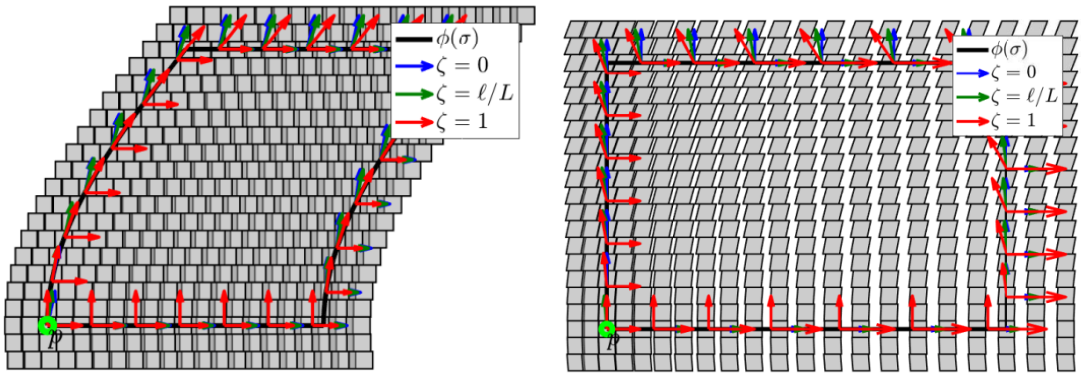

FIGURE 5.10: Representation in the ambient space of the transformation (5.5.22) (left) and (5.5.26) (right). There is no torsion but the non-zero components of the curvature are $\mathsf{R}^1{}_{212} = -\mathsf{R}^1{}_{221}$ and the metric is not compatible with the induced connection.

then the torsion is null. The non-zero components of the curvature are

$$\mathsf{R}^1{}_{212} = -\mathsf{R}^1{}_{221} = -\left(\frac{1-\zeta}{1+\theta}\right)^2 \frac{\partial f}{\partial X^2}\frac{\partial \theta}{\partial X^1}. \tag{5.5.24}$$

The non-metricity tensor has the following non-null components:

$$\nabla_1 \mathsf{G}_{11} = 2(1-\zeta)(1+\theta)\frac{\partial \theta}{\partial X^1}, \qquad \nabla_2 \mathsf{G}_{12} = \nabla_2 \mathsf{G}_{21} = -(1-\zeta)(1+\theta)\frac{\partial f}{\partial X^2}. \tag{5.5.25}$$

Numerical simulation is given in Figure 5.10-(left) with $f(X^2)$ and $\theta(X^1)$ specified by (5.5.9) and (5.5.13) respectively.

As for the example related to torsion, some other processes may be involved in order to obtain the same type of curvature. Indeed, consider the transformation

$$F = \begin{pmatrix} 1+f(X^1) & 0 \\ 0 & 1 \end{pmatrix} \qquad \Theta = \begin{pmatrix} 1 & \theta(X^2) \\ 0 & 1 \end{pmatrix}. \tag{5.5.26}$$

for which the metric is of the same form than (5.5.10). The non-null connection coefficients are

$$\Gamma^1_{11} = (1-\zeta)\frac{\partial f}{\partial X^1} \qquad \Gamma^1_{22} = \zeta\frac{\partial \theta}{\partial X^2} \tag{5.5.27}$$

then the torsion is null. The non-zero components of the curvature are

$$\mathsf{R}^1{}_{212} = -\mathsf{R}^1{}_{221} = (1-\zeta)\zeta\frac{\partial f}{\partial X^1}\frac{\partial \theta}{\partial X^2}. \tag{5.5.28}$$

The non-metricity has the following non-null components:

$$\nabla_1 \mathsf{G}_{11} = -2(1-\zeta)\frac{\partial f}{\partial X^1}, \qquad \nabla_1 \mathsf{G}_{12} = \nabla_1 \mathsf{G}_{21} = -(1-\zeta)\,\theta\,\frac{\partial f}{\partial X^1}$$
$$\nabla_2 \mathsf{G}_{22} = 2(1-\zeta)\theta\frac{\partial \theta}{\partial X^2}, \qquad \nabla_2 \mathsf{G}_{12} = \nabla_2 \mathsf{G}_{21} = (1-\zeta)\frac{\partial \theta}{\partial X^2}.$$

The corresponding illustration Figure 5.10-(right) exhibits pattern highly different from Figure 5.10-(left) even if the same components of the curvature are involved. For both simulations a frame initially placed at p is parallel transported along σ by solving (5.5.1). For both transformations the initial (vertical) vector $Y(0)$ and last vector $Y(1)$ differ if the curvature is not zero. Indeed, for infinitesimal loop of side $\delta x^1 \times \delta x^2$ the horizontal gap of $\Delta Y = Y(0) - Y(1)$ is measured by $\mathsf{R}^1_{212} Y^2 \delta x^1 \delta x^2$. For infinitesimal domain, it is a signature of the curvature and then of disclination's densities. At a macroscopic point of view, it is still measurable by such gap. The

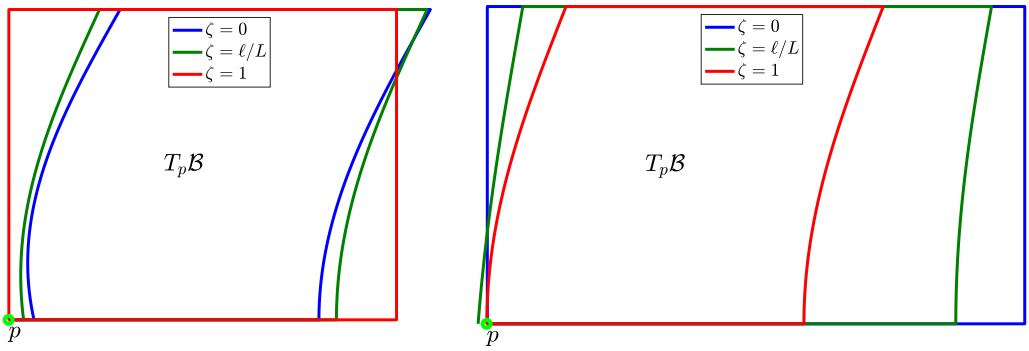

FIGURE 5.11: Developing curve $\widetilde{\sigma}$ obtained for various ζ and for the transformations (5.5.22) (left) and (5.5.22) (right).

developing curve $\widetilde{\sigma}$ is presented for the two transformations in Figure 5.11. Here the computation is performed for finite loop and $\widetilde{\sigma}$ is no more closed as if the manifold presents non-null curvature. For infinitesimal loop the computation of such gap $\Delta\widetilde{\sigma} = \widetilde{\sigma}(1) - \widetilde{\sigma}(0)$ shows that $\Delta\widetilde{\sigma} = \mathcal{O}(\delta x^3)$ in the presence of curvature. In other words, for an infinitesimal loop ΔY is predominant to $\Delta\widetilde{\sigma}$. However for an finite loop, this hierarchy is broken as both ΔY and $\Delta\widetilde{\sigma}$ are not negligible. As $\Delta\widetilde{\sigma}$ is of the same order of magnitude in presence of curvature or torsion (Figure 1.17 and Figure 5.8), it is impossible to confirm that no torsion is present in such finite domain. In other words, $\Delta\widetilde{\sigma}$-observation on a finite domain is not able to detect the density of dislocations if some disclinations are present.

The Burger's circuits $\underline{\sigma}$ obtained by (5.5.16) are presented in Figure 5.12. As in the previous

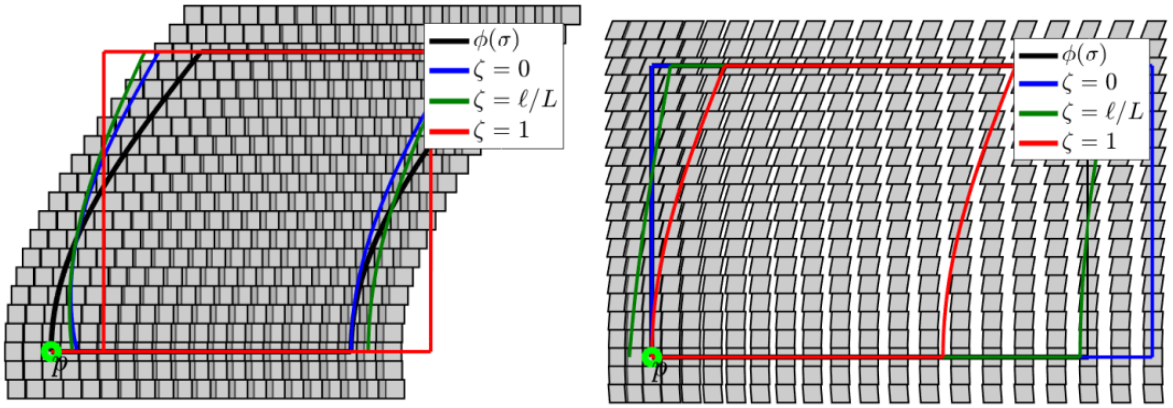

FIGURE 5.12: Burger's circuit $\underline{\sigma}$ obtained for various ζ and for the transformations (5.5.22) (left) and (5.5.26) (right) represented in the ambient space.

example (i) the gap of Burger's circuit differs quantitatively from the gap observed for the developing curve (ii) the vectors $\underline{\dot{\sigma}}(1)$ and $\underline{\dot{\sigma}}(0)$ are distinct. Hence this Burger's circuit associated with finite loop is not able to detect if defects are associated with torsion only, curvature only or both of them together. From this point of view the analysis of the developing curve has the advantage to detect the presence of curvature or not by considering $\Delta\tilde{\dot{\sigma}}$.

5.6 Conclusion

In order to model a material transformation that takes into consideration the change and possibly creations of defects, a geometrical approach has been introduced. In this context, such transformation is considered as a fiber morphism - or so-called bundle map - from the appropriate fiber bundle of the material manifold to the Euclidean space. The method is based on the concepts of Ehresmann connection and solder form. The induced connection N and metric G are first described, then curvature, torsion and non-metricity of the connection may be obtained. The more straightforward method consists in studying $\mathscr{M} \rightarrow T\mathbb{E}^3$. It has been proven that this approach is not able to introduce curvature, even in the case of non-linear maps.

The main idea to introduce rich enough transformations consists in considering that the bundle supporting the transformation is $V\mathscr{M}$, which is the vertical tangent bundle of $\mathscr{M}$. In this article, the transformations $\Upsilon^v : V\mathscr{M} \rightarrow VT\mathbb{E}^3$ are restricted to the case of linear microstructure, meaning that $\mathscr{M}$ is isomorphic to $T\mathscr{B}$.

This assertion does not constraint entirely $T\mathscr{M}$ and is a geometrical modeling of the misfit between the microscopic and macroscopic states of the material, it is a *scaled material model*. Technically this misfit is taken into account by the connections that illustrate - through its torsion, curvature and non-metricity - the presence of various material defects. Here the material is described by a body $\mathscr{B}$ having a microstructure $\mathscr{M}$. In such a way, each geometrical quantity may be measured or computed on the same material support: the body $\mathscr{B}$. In all the cases, the current state is obtained by a pull-back operation that prescribed an *induced* geometry on $\mathscr{B}$.

As the *scaled material model* embraces various underlying points of view (microscopic, macroscopic and macroscopic interpretation of a microscopic phenomena) the standard parallel transport is not sufficient. For this purpose, various interpretations, including the rolling without slipping transport and the developing curve, have been exhibited and illustrated in order to link the mathematical tools to the mechanical processes.

Such *scaled material model* is parameterized by single-valued and smooth fields. It is the case for the induced (linear) connection Γ and metric G (then for torsion or curvature) but also for the point and vector maps ϕ and Θ. This feature distinguishes the present model from other known theories referring to the nonholonomic principle. It allows mathematical analysis and numerical simulation taking into account both scales.

The non-metricity of the connection can be considered as *the price to paid* by the *scaled material model* to overcome multivalued fields. However, through this modeling, the non-metricity reveals the process involved to obtain a defective media. Analysing more deeply this mechanical interpretation is among the possible objectives of future works.

The restriction of the bundle map Υ to any element of $V\mathscr{M}$ is imposed by the transformation Υ^v. Accordingly, specifying the completed bundle map Υ is somehow free. In the present work,

a family of bundle map Υ is considered by introducing just an unique scalar ζ. This choice is sufficient to illustrate the presence of various defect types and avoids adding new unknown fields in the theory. In the present example, ζ gives a weight of macro and micro effect in a linear way, but other formulations (leading, for instance, to non-linear connection) are possible. It must be noticed that the choice of such completion may reveal some interesting physical interpretations that are beyond the scope of the chapter (in particular for multi-physical problems).

Numerical simulations are presented and show how bridges are built between microscopic defects and macroscopic observations. It is the occasion to underline that for a given density of disclinations, the characterisation of a possible presence of dislocations is not attainable by macroscopic observations (at least with the ζ-family of bundle map Υ chosen in the present case).

Up to now, the present model is purely kinematic. However, this first step was indispensable to consider full mechanical problems afterwards. (1) Staying on this kinematic approach, other possible extensions Υ (than the ζ-family) may be explored in order to take into account specific microstructured materials such as nano-material; (2) Study of the solder form turns out to be another interesting subject; (3) Another possible step consists in considering an energetic counterpart in order to define the equilibrium laws of such model. (4) Note that the present *scaled material model* is kinematically non-linear, and a linearization may be the occasion to find some meaningful explicit solutions. (5) Another possible issue consists in introducing time in the Galilean or in the Lorentzian framework.

Conclusion

There is no doubt that geometry plays a fundamental role in the understanding of physics. As a typical example, the continuum theory of dislocations and disclinations could be formulated in the Riemann–Cartan geometry framework. Once again, this statement has been confirmed by the development of fiber geometry throughout this dissertation. We pay attention to enriching the differential material manifold by metrics and connections derived from material transformations. The resulting geometry can describe and investigate the behaviour of microscopic defects in the continuum. The proposed theories allow, in many aspects, to better understand the observed phenomena. Several examples given for different types of defects distributed in the medium have thus been made to highlight the consistency between theoretical analysis and numerical simulations and to link the mathematical tools to the mechanical processes. Since our approaches involve single-valued and smooth fields, both theoretical and numerical analyses are easily treated.

The new framework yields consistent geometric backgrounds for the microcontinuum framework. It could be helpful to formulate the field theories in a universal language of differential geometry. Our ideas open a lot of interesting problems for the future. Notably, the geometrical nature of our approach suggests that it would be not difficult to obtain the relativistic version of the theory, which should fit impressively to the geometrical settings of general relativity theories. In what follows, we will summarize our contribution to the current state of understanding of defects.

Contributions

This thesis concerns a geometric model of mechanical transformations of material media with a microstructure. This type of material is common in nature. Modeling the behavior of these media is a broad subject. It encompasses homogenization, influential media theories, and multiscale theories. These approaches are often effective for infinitesimal transformations, but geometric difficulties appear for large transformations.

An alternative consists in interpreting the continuum as a fiber bundle manifold $\mathscr{M}$ over the base manifold $\mathscr{B}$. The latter is immersed in the Euclidean ambient space. In this case, the type of manifold illustrates some characteristics of the material. In continuum mechanics, the base manifold $\mathscr{B}$ makes it possible to model the macroscopic behavior of material domains. Its microstructure is modeled by choosing a connection and a metric on the bundle $\mathscr{M}$.

Our study only considers mechanical type defects arising from inconsistency in the placements and orientations of the microelements. Such a process is convincingly captured by a smooth embedding represented by a fiber morphism Υ from $\mathscr{M}$ into $T\mathbb{E}^3$. The embedding induces a connection and a metric on the material manifold by pulling back from the geometry of Euclidean space. Defects are then measured through the torsion, curvature and nonmetricity of the connection. Therefore, the choice of the kinematics of the embeddings is a crucial element for the construction of the model. In addition, the numerical and theoretical analyses are easier to handle since the geometric quantities are derived from the smooth maps rather than the existing methods.

We first specify how the linear transformation $\Upsilon : T\mathscr{B} \to T\mathbb{E}^3$, $(X, V) \mapsto (\phi(X), \Psi(X)V)$ changes the intrinsic geometry of the continuum in the RC framework. Using this kind of map, the pull-back of the Levi-Civita connection and the Euclidean metric enrich $\mathscr{B}$ in the form of a special type of RC geometry called Weitzenböck manifold. This latter is not efficient to deal with all topological defects since it is impossible to introduce curvature (the geometric quantities measuring disclinations densities). Finally, we gave the formalism of Eringen theory based on geometry. Notably, it reduces the number of material parameters compared to classical microscopic theories.

The breakthroughs of this thesis consist of the second approach - the scaled material model. This study answered nicely and in an elegant way the drawback just before. It was initially motivated by reproducing the previous research on another geometrical background - fiber geometry - that more effectively describes the microcontinuum. It turns out that if we consider the embedding of the manifold $\mathscr{B}$ and its tangent space, the induced manifold has characteristics of an RC manifold already exploited for the study of materials with crystalline defects or with dislocations.

Instead, the scaled material model deals with the material transformation that is described by the bundle map $\Upsilon^v : V\mathscr{M} \to VT\mathbb{E}^3$. To construct an Ehresmann connection pulling back from the Euclidean space, one needs to enrich the transformation Υ^v to the fiber morphism Υ defined on the whole space $T\mathscr{M}$. The extension Υ is completely constructed by just introducing a scalar field. It is sufficient to illustrate the presence of various defect types and avoids adding new unknown fields in the theory. Moreover, it recovers to give a weight of macro and micro effect in a linear way. This interpretation also has the advantage of recovering some standard behaviors: it recovers a case where the micro and macro universes behave in the same way. Recover transformation for which scaling effect is absent. The induced manifold is richer because it has a connection provided with torsion and curvature, and the metric is no longer necessarily compatible with the connection.

One of the main contributions of this thesis is to introduce a new approach to the transformations of microstructured materials. The transformations are defined on a space tangent to the material manifold $T\mathscr{M}$. The induced manifold has very rich properties distinguished from a classical Riemann manifold that can model a large class of microstructural defects. This approach allows great freedom in the description of the induced structure on the material manifold $\mathscr{M}$. It is possible to distinguish the notions of connection and metric at various scales. It gives to the model the possibility of having a physical interpretation of the results. Applications in continuum mechanics are broad: from fluid mechanics to work hardening through plasticity, but this thesis will not approach these topics.

The second significant contribution consists in the choice of this fiber morphism Υ. The present work is obtained by introducing only a new scalar quantity - the scaling factor ζ. The other ingredients (degrees of freedom of the model) used are associated with the kinematics of the microelement and have existed for a long time in other models. We, therefore, have controllable modeling by a reduced number of independent variables, which allows an exhaustive and rigorous discussion. In particular, the notion of the scale factor is relatively explicit on reading the results.

The third contribution of this thesis relates to the practical application of these models through

numerical simulations. These simulations illustrate the microscopic and macroscopic properties of the material after transformation. The effects of these connections are illustrated by numerically simulating the parallel transport of directors along a path of finite length. It is possible to interpret macroscopically some phenomena that are often presented only for infinitesimal paths. In the context of multiscale modeling, these infinitesimal loops provide only partial information. In order to broaden and complete this type of interpretation, other transports have been developed to provide original tools to mechanics: rolling without slipping transport, transport along a finite domain and Burger circuit. All of these simulations allow an exhaustive analysis of the properties of the model on scalar or vector variables. From our perspective, it can improve the agreement between the theoretical and numerical analysis.

Outlook

The thesis ends at this stage but the developed geometric construction in the geometrical theory of defects always raises many interesting questions. The answers to these will help us to better understand the applicability of the proposed approaches. Some of them are discussed as follows.

First, it is conspicuous that the induced manifold is richer than ones derived from the classical theories because the connection may not be compatible with the metric system. In this thesis, we have shown that it reveals the processes involved in rearranging elements in materials. From a mechanical point of view, such reorganization requires some energy. In this context, the non-metricity tensor should be treated as an argument of the strain energy function. However, a deeper understanding of this quantity needs additional works, it is of interest in future research.

Second, the extension of the bundle map Υ to the mechanical transformation Υ^v is somehow free. In this study, a family of bundle maps Υ is completed by introducing a unique scalar factor ζ. It is enough to illustrate various defect types and to avoid adding new unknown fields in theory. The present example gives a weight of macro and micro effect linearly, but other formulations (leading, for instance, to non-linear connection) are possible. The choice of such completion may reveal some interesting physical phenomena, in particular, for multi-physical problems. Besides, other possible extensions Υ may be explored to investigate specific microstructured materials such as nano-material.

Third, *the canonical soldering form ϑ is assumed throughout the manuscript.* The reason behinds this restriction is described in the following statements: In standard literature on continuum theories of defects, dislocations and disclinations are related to torsion and curvature of the affine connection of the base manifold $\mathscr{B}$, respectively. Accordingly, the application of the model focuses mainly on linear connection N (i.e., $N^I_A = \Gamma^I_{AJ} Y^J$), for which Γ well defined an affine connection on $\mathscr{B}$, and the torsion, curvature of N coincides with those of the affine connection Γ. The canonical solder form is initially introduced to emphasize these relationships. In other words, technical constraints and pedagogic reasons have motivated us to restrict the application to canonical solder form.

Nevertheless, we believe that such an assumption may contain some physical processes. The *Section*-4.2 presents the formulation with a non-canonical solder form to underline the enormous

scope of such modeling. Honestly, we have found no literature using non-canonical solder form for physical problems except in cosmology. In addition, at the moment, we have not found any physical phenomena that are enabled or omitted by the particular belief.

Fourth, the micro-state could be very complex. In particular, the fiber above each point may not have the same dimension of the body manifold. For example, the micro-state may be a point on the 2-sphere. Then the restriction imposed by using the canonical solder form is not suitable. It is understandable to start with the simplest case for which microelements are interpreted as first-order infinitesimal neighborhoods of geometrical points. For such cases, the micro-state is uniform inside the macroelement. The present work shows that this hypothesis is sufficient to illustrate various defect types and points out many interesting properties. In particular, torsion, curvature and non-metricity appeared through a synthetic kinematic model. It corresponds to the scope of the study, which is an attempt to introduce tools of fiber geometry towards the framework of a microstructured continuum with distributions of defects. Moreover, our construction has the advantage that it is not difficult to obtain the relative version of the theory regarding the complicated microcontinuum. The complex microstructure could be investigated by setting $\dim \mathscr{B} = \dim \mathscr{M}_p$ but using another solder form.

Next, the induced Ehresmann connection is generally non-linear even if the bundle map Υ^v is linear in the case of the scaled material model, see Section 5.2 or for the non-linear transformation $\mathcal{H}$ in the non-scale material modeling, see Section 5.4.1. The connection and metric are entirely independent. This construction is closed to the pseudo-Finsler space, in which exceptional cases include various types of geometries. Thus, it affords great generality for describing several phenomena in physics. It is an occasion to ask what a physical interpretation of such a non-linear connection is, at least in the framework of defects.

Up to the present, torsion, curvature and non-metricity tensors or equivalently the functions ϕ, Ψ or Θ are unknown fields in this theory. We plan to apply some mechanical processes to obtain governing equations or consider an energetic counterpart to define the equilibrium laws of such models. It helps us to solve numerical or analytic material transformations. Finally, the linearization of the present models may be the occasion to provide meaningful, explicit solutions.

Last but not least, one of the possible issues that we intend to study consists of a generalization of general relativity theory. The general relativity theory is Einstein's theory of space, time and gravitation in terms of differential geometry of curved spacetime. This theory states that most forces of nature are represented by fields defined on the spacetime manifold, while gravity is an intrinsic property of the spacetime manifold - curvature. The geometry of spacetime is derived from a Lorentzian metric and has the structure of Minkowskian space. The flat manifold may be twisted and curved using multi-valued coordinate transformations. However, our approaches emphasizes that such a twisted and curved manifold can be obtained by using smooth transformations. Obviously, for any new geometry background, one question arises: *how to modify and extend the theory in this framework?* We strongly believe that the geometrical nature of our approach also suggests that it would be not difficult to obtain the relativistic version of the current theory, which should adapt convincingly to the geometrical settings of general relativity theories.

References

Acharya, A. and J. L. Bassani (2000). "Lattice incompatibility and a gradient theory of crystal plasticity". In: *J. Mech. Phys. Solids* 48.8, pp. 1565–1595. ISSN: 0022-5096. DOI: 10.1016/S0022-5096(99)00075-7. URL: https://doi.org/10.1016/S0022-5096(99)00075-7.

Acharya, A., R. J. Knops, and J. Sivaloganathan (2019). "On the structure of linear dislocation field theory". In: *J. Mech. Phys. Solids* 130, pp. 216–244. ISSN: 0022-5096. DOI: 10.1016/j.jmps.2019.06.002. URL: https://doi.org/10.1016/j.jmps.2019.06.002.

Bao, D., S.-S. Chern, and Z. Shen (2000). *An introduction to Riemann-Finsler geometry*. Vol. 200. Graduate Texts in Mathematics. Springer-Verlag, New York, pp. xx+431. ISBN: 0-387-98948-X. DOI: 10.1007/978-1-4612-1268-3. URL: https://doi.org/10.1007/978-1-4612-1268-3.

Bejancu, Aurel (1990). *Finsler geometry and applications*. Ellis Horwood Series: Mathematics and its Applications. Ellis Horwood, New York, p. 198. ISBN: 0-13-317975-3.

Bilby, B. A., R. Bullough, and E. Smith (1955). "Continuous distributions of dislocations: a new application of the methods of non-Riemannian geometry". In: *Proc. Roy. Soc. London Ser. A* 231, pp. 263–273. ISSN: 0962-8444. DOI: 10.1098/rspa.1955.0171. URL: https://doi.org/10.1098/rspa.1955.0171.

Bradlyn, Barry and N. Read (2015). "Low-energy effective theory in the bulk for transport in a topological phase". In: *Phys. Rev. B* 91 (12), p. 125303. DOI: 10.1103/PhysRevB.91.125303. URL: https://link.aps.org/doi/10.1103/PhysRevB.91.125303.

Bucataru, Ioan and Radu Miron (2007a). *Finsler-Lagrange geometry*. Applications to dynamical systems. Editura Academiei Române, Bucharest, pp. xviii+252. ISBN: 978-973-27-1527-7.

— (2007b). "Nonlinear connections for nonconservative mechanical systems". In: *Rep. Math. Phys.* 59.2, pp. 225–241. ISSN: 0034-4877. DOI: 10.1016/S0034-4877(07)00013-4. URL: https://doi.org/10.1016/S0034-4877(07)00013-4.

Capozziello, Salvatore and Mariafelicia De Laurentis (2011). "Extended theories of gravity". In: *Phys. Rep.* 509.4-5, pp. 167–320. ISSN: 0370-1573. DOI: 10.1016/j.physrep.2011.09.003. URL: https://doi.org/10.1016/j.physrep.2011.09.003.

Cartan, Élie (1922). "Sur une généralisation de la notion de courbure de Riemann et les espaces à torsion". In: *Comptes Rendus, Ac. Sc. Paris* 174, pp. 593–595.

— (1923). "Sur les variétés à connexion affine et la théorie de la relativité généralisée (première partie)". In: *Ann. Sci. École Norm. Sup. (3)* 40, pp. 325–412. ISSN: 0012-9593. URL: http://www.numdam.org/item?id=ASENS_1923_3_40__325_0.

— (1924). "Sur les variétés à connexion affine, et la théorie de la relativité généralisée (première partie) (Suite)". In: *Ann. Sci. École Norm. Sup. (3)* 41, pp. 1–25. ISSN: 0012-9593. URL: http://www.numdam.org/item?id=ASENS_1924_3_41__1_0.

— (1925). "Sur les variétés à connexion affine, et la théorie de la relativité généralisée (deuxième partie)". In: *Ann. Sci. École Norm. Sup. (3)* 42, pp. 17–88. ISSN: 0012-9593. URL: http://www.numdam.org/item?id=ASENS_1925_3_42__17_0.

— (1986). *On manifolds with an affine connection and the theory of general relativity*. Vol. 1. Monographs and Textbooks in Physical Science. Translated from the French by Anne Magnon and Abhay Ashtekar, With a foreword by Andrzej Trautman. Bibliopolis, Naples, p. 199. ISBN: 88-7088-086-9.

Choquet-Bruhat, Yvonne, Cécile DeWitt-Morette, and Margaret Dillard-Bleick (1982). *Analysis, manifolds and physics*. Second. North-Holland Publishing Co., Amsterdam-New York, pp. xx+630. ISBN: 0-444-86017-7.

Clayton, J. D. (2015). "On Finsler geometry and applications in mechanics: review and new perspectives". In: *Adv. Math. Phys.*, Art. ID 828475, 11. ISSN: 1687-9120. DOI: 10.1155/2015/828475. URL: https://doi.org/10.1155/2015/828475.

— (2017a). "Generalized Finsler geometric continuum physics with applications in fracture and phase transformations". In: *Z. Angew. Math. Phys.* 68.1, Paper No. 9, 38. ISSN: 0044-2275. DOI: 10.1007/s00033-016-0752-x. URL: https://doi.org/10.1007/s00033-016-0752-x.

Clayton, J.D. (2017b). "Finsler geometry of nonlinear elastic solids with internal structure". In: *Journal of Geometry and Physics* 112, pp. 118–146. ISSN: 0393-0440. DOI: https://doi.org/10.1016/j.geomphys.2016.11.011. URL: https://www.sciencedirect.com/science/article/pii/S0393044016302832.

Cordier, Patrick et al. (Feb. 2014). "Disclinations provide the missing mechanism for deforming olivine-rich rocks in the mantle". In: *Nature* 507. DOI: 10.1038/nature13043.

Cosserat, E. and F. Cosserat (1909). *Sur la théorie des corps déformables*. Dunod, Paris.

Dumbser, Michael, Ilya Peshkov, and Evgeniy Romenski (2018). "A unified hyperbolic formulation for viscous fluids and elastoplastic solids". In: *Theory, numerics and applications of hyperbolic problems. II*. Vol. 237. Springer Proc. Math. Stat. Springer, Cham, pp. 451–463. DOI: 10.1007/978-3-319-91548-7_34. URL: https://doi.org/10.1007/978-3-319-91548-7_34.

Epstein, M. and R. Segev (2014). "Geometric aspects of singular dislocations". In: *Mathematics and Mechanics of Solids* 19.4, pp. 337–349. DOI: 10.1177/1081286512465222. eprint: https://doi.org/10.1177/1081286512465222. URL: https://doi.org/10.1177/1081286512465222.

Epstein, Marcelo (2010). *The geometrical language of continuum mechanics*. Cambridge University Press, Cambridge, pp. xii+312. ISBN: 978-0-521-19855-4. DOI: 10.1017/CBO9780511762673. URL: https://doi.org/10.1017/CBO9780511762673.

— (2012). *The elements of continuum biomechanics*. John Wiley & Sons. ISBN: 9781118361016. DOI: 10.1002/9781118361016.

— (2014). *Differential geometry: Basic notions and physical examples*. Mathematical Engineering. Springer, Cham, pp. xii+139. ISBN: 978-3-319-06919-7; 978-3-319-06920-3. DOI: 10.1007/978-3-319-06920-3. URL: https://doi.org/10.1007/978-3-319-06920-3.

Epstein, Marcelo and Marek Elżanowski (2007). *Material inhomogeneities and their evolution: A geometric approach*. Interaction of Mechanics and Mathematics. Springer, Berlin, pp. xiv+274. ISBN: 978-3-540-72372-1.

Eringen, A. Cemal (1999). *Microcontinuum field theories. I. Foundations and solids*. Springer-Verlag, New York, pp. xvi+325. ISBN: 0-387-98620-0. DOI: 10.1007/978-1-4612-0555-5. URL: https://doi.org/10.1007/978-1-4612-0555-5.

Eringen, A. Cemal and E. S. Suhubi (1964). "Nonlinear theory of simple micro-elastic solids. I". In: *Internat. J. Engrg. Sci.* 2, pp. 189–203. ISSN: 0020-7225. DOI: 10.1016/0020-7225(64)90004-7. URL: https://doi.org/10.1016/0020-7225(64)90004-7.

Eshelby, J.D. (1956). "The Continuum Theory of Lattice Defects". In: ed. by Frederick Seitz and David Turnbull. Vol. 3. Solid State Physics. Academic Press, pp. 79–144. DOI: https://doi.

org/10.1016/S0081-1947(08)60132-0. URL: https://www.sciencedirect.com/science/article/pii/S0081194708601320.

Forest, Samuel (2009). "Micromorphic Approach for Gradient Elasticity, Viscoplasticity, and Damage". In: *Journal of Engineering Mechanics* 135.3, pp. 117–131. DOI: 10.1061/(ASCE)0733-9399(2009)135:3(117).

Frenkel, J. "Zur Theorie der Elastizitätsgrenze und der Festigkeit kristallinischer Körper". In: *Zeitschrift für Physik* 37 (), pp. 572–609.

Fu, M. F., J. Saczuk, and H. Stumpf (1998). "On fibre bundle approach to a damage analysis". In: *Internat. J. Engrg. Sci.* 36.15, pp. 1741–1762. ISSN: 0020-7225. DOI: 10.1016/S0020-7225(98)00021-4. URL: https://doi.org/10.1016/S0020-7225(98)00021-4.

Futhazar, Grégory, Loïc Le Marrec, and Lalaonirina Rakotomanana (Oct. 2014). "Covariant gradient continua applied to wave propagation within defective material". In: *Archive of Applied Mechanics*, pp. 1339–1356. DOI: 10.1007/s00419-014-0873-7. URL: https://doi.org/10.1007/s00419-014-0873-7.

Ghiba, Ionel-Dumitrel et al. (2015). "The relaxed linear micromorphic continuum: existence, uniqueness and continuous dependence in dynamics". In: *Math. Mech. Solids* 20.10, pp. 1171–1197. ISSN: 1081-2865. DOI: 10.1177/1081286513516972. URL: https://doi.org/10.1177/1081286513516972.

Gonzalez, Oscar and Andrew M. Stuart (2008). *A first course in continuum mechanics*. Cambridge Texts in Applied Mathematics. Cambridge University Press, Cambridge, pp. xviii+394. ISBN: 978-0-521-71424-2. DOI: 10.1017/CBO9780511619571. URL: https://doi.org/10.1017/CBO9780511619571.

Grammenoudis, P. and Ch. Tsakmakis (Sept. 2009). "Micromorphic continuum. Part I: Strain and stress tensors and their associated rates". In: *International Journal of Non-Linear Mechanics* 44.9, p. 943. DOI: 10.1016/j.ijnonlinmec.2009.05.005. URL: https://hal.archives-ouvertes.fr/hal-00573457.

Head, A. K. et al. (1993). "An equilibrium theory of dislocation continua". In: *SIAM Rev.* 35.4, pp. 580–609. ISSN: 0036-1445. DOI: 10.1137/1035136. URL: https://doi.org/10.1137/1035136.

Hélein, Frédéric (2009). "Manifolds obtained by soldering together points, lines, etc". In: *arXiv preprint arXiv:0904.4616*.

Iliev, Bozhidar Z. (2001). "Fibre bundle formulation of nonrelativistic quantum mechanics. I. Introduction. The evolution transport". In: *J. Phys. A* 34.23, pp. 4887–4918. ISSN: 0305-4470. DOI: 10.1088/0305-4470/34/23/308. URL: https://doi.org/10.1088/0305-4470/34/23/308.

Katanaev, M. (2005). "Geometric theory of defects". In: *Phys. Usp.* 48.7, pp. 675–701. DOI: 10.1070/PU2005v048n07ABEH002027. URL: https://ufn.ru/en/articles/2005/7/b/.

Kleinert, H (1989). *Gauge Fields in Condensed Matter*. WORLD SCIENTIFIC. DOI: 10.1142/0356. eprint: https://www.worldscientific.com/doi/pdf/10.1142/0356. URL: https://www.worldscientific.com/doi/abs/10.1142/0356.

Kleinert, H. (1992). "The Extra gauge symmetry of string deformations in electromagnetism with charges and Dirac monopoles". In: *Int. J. Mod. Phys. A* 7, pp. 4693–4705. DOI: 10.1142/S0217751X9200212X.

Kleinert, Hagen (1990). "Double gauge invariance and local quantum field theory of charges and Dirac magnetic monopoles". In: *Phys. Lett. B* 246, pp. 127–130. DOI: 10.1016/0370-2693(90)91318-6.

— (2000). "Nonholonomic mapping principle for classical and quantum mechanics in spaces with curvature and torsion". In: *Gen. Relativity Gravitation* 32.5, pp. 769–839. ISSN: 0001-7701. DOI: 10.1023/A:1001962922592. URL: https://doi.org/10.1023/A:1001962922592.

— (2008). *Multivalued fields in condensed matter, electromagnetism, and gravitation*. World Scientific Publishing Co. Pte. Ltd., Hackensack, NJ, pp. xxiv+497. ISBN: 978-981-279-171-9; 981-279-171-X. DOI: 10.1142/6742. URL: https://doi.org/10.1142/6742.

Kobayaschi, S. (1957). "Theory of connections". In: *Annali di Matematica Pura ed Applicata* 43, pp. 119–194. DOI: 10.1007/BF02411907. URL: https://doi.org/10.1007/BF02411907.

Kolev, Boris and Rodrigue Desmorat (2021). *Objective rates as covariant derivatives on the manifold of Riemannian metrics*. arXiv: 2106.01126 [math.DG].

Kondo, K (1955). *Geometry of elastic deformation and incompatibility. Memoirs of the unifying study of the basic problems in engineering sciences by means of geometry. Vol. I*. Kazuo Kondo, Chairman. Gakujutsu Bunken Fukyu-Kai, Tokyo, pp. xv+590.

— (1963). "Non-riemannian and finslerian approaches to the theory of yielding". In: *International Journal of Engineering Science* 1.1, pp. 71–88. ISSN: 0020-7225. DOI: https://doi.org/10.1016/0020-7225(63)90025-9. URL: https://www.sciencedirect.com/science/article/pii/0020722563900259.

Kröner, E. (1981). *Continuum theory of defects*. Ed. by R. Balian et al. Less Houches, Session XXXV, 1980-Physics of defects. North-Holland Publishing Company.

Kröner, Ekkehart (1960). "Allgemeine Kontinuumstheorie der Versetzungen und Eigenspannungen". In: *Arch. Rational Mech. Anal.* 4, 273–334 (1960). ISSN: 0003-9527. DOI: 10.1007/BF00281393. URL: https://doi.org/10.1007/BF00281393.

Le, K. C. and H. Stumpf (1996a). "On the determination of the crystal reference in nonlinear continuum theory of dislocations". In: *Proceedings of the Royal Society of London. Series A: Mathematical, Physical and Engineering Sciences* 452.1945, pp. 359–371. DOI: 10.1098/rspa.1996.0019. eprint: https://royalsocietypublishing.org/doi/pdf/10.1098/rspa.1996.0019. URL: https://royalsocietypublishing.org/doi/abs/10.1098/rspa.1996.0019.

Le, K.C. and H. Stumpf (1996b). "A model of elastoplastic bodies with continuously distributed dislocations". In: *International Journal of Plasticity* 12.5, pp. 611–627. ISSN: 0749-6419. DOI: https://doi.org/10.1016/S0749-6419(96)00022-8. URL: https://www.sciencedirect.com/science/article/pii/S0749641996000228.

— (1996c). "Nonlinear continuum theory of dislocations". In: *International Journal of Engineering Science* 34.3, pp. 339–358. ISSN: 0020-7225. DOI: https://doi.org/10.1016/0020-7225(95)00092-5. URL: https://www.sciencedirect.com/science/article/pii/0020722595000925.

Lee, E. and D. Liu (1967). "Finite-Strain Elastic—Plastic Theory with Application to Plane-Wave Analysis". In: *Journal of Applied Physics* 38, pp. 19–27.

Love, A. E. H. (1944). *A treatise on the Mathematical Theory of Elasticity*. Fourth Ed. Dover Publications, New York, pp. xviii+643.

Lychev, Sergei et al. (2020). "Modeling and Optimization for Oriented Growing Solids". In: *2020 15th International Conference on Stability and Oscillations of Nonlinear Control Systems (Pyatnitskiy's Conference) (STAB)*, pp. 1–4. DOI: 10.1109/STAB49150.2020.9140700.

Madeo, Angela et al. (2015). "Band gaps in the relaxed linear micromorphic continuum". In: *ZAMM Z. Angew. Math. Mech.* 95.9, pp. 880–887. ISSN: 0044-2267. DOI: 10.1002/zamm.201400036. URL: https://doi.org/10.1002/zamm.201400036.

Madeo, Angela et al. (2018). "Relaxed micromorphic modeling of the interface between a homogeneous solid and a band-gap metamaterial: new perspectives towards metastructural design". In: *Math. Mech. Solids* 23.12, pp. 1485–1506. ISSN: 1081-2865. DOI: 10.1177/1081286517728423. URL: https://doi.org/10.1177/1081286517728423.

Marsden, Jerrold E. and Thomas J. R. Hughes (1994). *Mathematical foundations of elasticity*. Corrected reprint of the 1983 original. Dover Publications, Inc., New York, pp. xviii+556. ISBN: 0-486-67865-2.

Mindlin, R. D. (1964). "Micro-structure in linear elasticity". In: *Arch. Rational Mech. Anal.* 16, pp. 51–78. ISSN: 0003-9527. DOI: 10.1007/BF00248490. URL: https://doi.org/10.1007/BF00248490.

Miron, R. (1994). "Lagrange geometry". In: vol. 20. 4-5. Lagrange geometry, Finsler spaces and noise applied in biology and physics, pp. 25–40. DOI: 10.1016/0895-7177(94)90154-6. URL: https://doi.org/10.1016/0895-7177(94)90154-6.

Nabarro (1967). *Theory of crystal dislocations*. Oxford: Clarendon Press.

Nakahara, Mikio (2003). *Geometry, topology and physics*. Second. Graduate Student Series in Physics. Institute of Physics, Bristol, pp. xxii+573. ISBN: 0-7503-0606-8. DOI: 10.1201/9781420056945. URL: https://doi.org/10.1201/9781420056945.

Noll, Walter (1967/68). "Materially uniform simple bodies with inhomogeneities". In: *Arch. Rational Mech. Anal.* 27, pp. 1–32. ISSN: 0003-9527. DOI: 10.1007/BF00276433. URL: https://doi.org/10.1007/BF00276433.

Nye, J.F (1953). "Some geometrical relations in dislocated crystals". In: *Acta Metallurgica* 1.2, pp. 153–162. ISSN: 0001-6160. DOI: https://doi.org/10.1016/0001-6160(53)90054-6. URL: https://www.sciencedirect.com/science/article/pii/0001616053900546.

Obukhov, Yu. N., V. N. Ponomariev, and V. V. Zhytnikov (1989). "Quadratic Poincaré gauge theory of gravity: a comparison with the general relativity theory". In: *Gen. Relativity Gravitation* 21.11, pp. 1107–1142. ISSN: 0001-7701. DOI: 10.1007/BF00763457. URL: https://doi.org/10.1007/BF00763457.

Peshkov, Ilya and Evgeniy Romenski (2016). "A hyperbolic model for viscous Newtonian flows". In: *Contin. Mech. Thermodyn.* 28.1-2, pp. 85–104. ISSN: 0935-1175. DOI: 10.1007/s00161-014-0401-6. URL: https://doi.org/10.1007/s00161-014-0401-6.

Pfeifer, Christian (2013). "The Finsler spacetime framework: backgrounds for physics beyond metric geometry". PhD thesis. Hamburg U.

Polizzotto, Castrenze (2013). "A second strain gradient elasticity theory with second velocity gradient inertia – Part I: Constitutive equations and quasi-static behavior". In: *International Journal of Solids and Structures* 50.24, pp. 3749–3765. ISSN: 0020-7683. DOI: https://doi.org/10.1016/j.ijsolstr.2013.06.024. URL: https://www.sciencedirect.com/science/article/pii/S0020768313002746.

Puntigam, Roland A and Harald H Soleng (1997). "Volterra distortions, spinning strings, and cosmic defects". In: *Classical and Quantum Gravity* 14.5, pp. 1129–1149. DOI: 10.1088/0264-9381/14/5/017. URL: https://doi.org/10.1088/0264-9381/14/5/017.

Rakotomanana, Lalaonirina (2005). "Some class of SG continuum models to connect various length scales in plastic deformation". In: *Mechanics of material forces*. Vol. 11. Adv. Mech. Math. Springer, New York, pp. 319–326. DOI: 10.1007/0-387-26261-X_32. URL: https://doi.org/10.1007/0-387-26261-X_32.

Rakotomanana, Lalaonirina R. (1998). "Contribution à la modélisation géométrique et thermodynamique d'une classe de milieux faiblement continus". In: *Arch. Rational Mech. Anal.* 141.3, pp. 199–236. ISSN: 0003-9527. DOI: 10.1007/s002050050076. URL: https://doi.org/10.1007/s002050050076.

— (2018). *Covariance and gauge invariance in continuum physics: Application to mechanics, gravitation, and electromagnetism*. Vol. 73. Progress in Mathematical Physics. Birkhäuser/Springer, Cham, pp. xi+325. ISBN: 978-3-319-91781-8; 978-3-319-91782-5. DOI: 10.1007/978-3-319-91782-5. URL: https://doi.org/10.1007/978-3-319-91782-5.

Reina, Celia, Anja Schlömerkemper, and Sergio Conti (2016). "Derivation of $\mathbf{F} = \mathbf{F}^{e}\mathbf{F}^{p}$ as the continuum limit of crystalline slip". In: *J. Mech. Phys. Solids* 89, pp. 231–254. ISSN: 0022-5096. DOI: 10.1016/j.jmps.2015.12.022. URL: https://doi.org/10.1016/j.jmps.2015.12.022.

Romano, Giovanni (2007). "Continuum mechanics on manifolds". In: *Lecture notes University of Naples Federico II, Naples, Italy*, pp. 1–695.

Saczuk, Jan (1997). "On the role of the Finsler geometry in the theory of elasto-plasticity". In: *Rep. Math. Phys.* 39.1, pp. 1–17. ISSN: 0034-4877. DOI: 10.1016/S0034-4877(97)81467-X. URL: https://doi.org/10.1016/S0034-4877(97)81467-X.

Stumpf, H. and J. Saczuk (2000). "A generalized model of oriented continuum with defects". In: *ZAMM Z. Angew. Math. Mech.* 80.3, pp. 147–169. ISSN: 0044-2267. DOI: 10.1002/(SICI)1521-4001(200003)80:3<147::AID-ZAMM147>3.3.CO;2-G. URL: https://doi.org/10.1002/(SICI)1521-4001(200003)80:3<147::AID-ZAMM147>3.3.CO;2-G.

Suhubi, E. S. and A. Cemal Eringen (1964). "Nonlinear theory of micro-elastic solids. II". In: *Internat. J. Engrg. Sci.* 2, pp. 389–404. ISSN: 0020-7225. DOI: 10.1016/0020-7225(64)90017-5. URL: https://doi.org/10.1016/0020-7225(64)90017-5.

Volterra, Vito (1907). "Sur l'équilibre des corps élastiques multiplement connexes". In: *Ann. Sci. École Norm. Sup. (3)* 24, pp. 401–517. ISSN: 0012-9593. URL: http://www.numdam.org/item?id=ASENS_1907_3_24__401_0.

Wang, C.-C. (1967/68). "On the geometric structures of simple bodies. A mathematical foundation for the theory of continuous distributions of dislocations". In: *Arch. Rational Mech. Anal.* 27, pp. 33–94. ISSN: 0003-9527. DOI: 10.1007/BF00276434. URL: https://doi.org/10.1007/BF00276434.

Weyl, Hermann (1918). "Reine Infinitesimalgeometrie". In: *Math. Z.* 2.3-4, pp. 384–411. ISSN: 0025-5874. DOI: 10.1007/BF01199420. URL: https://doi.org/10.1007/BF01199420.

Yajima, T. and H. Nagahama (2007). "KCC-theory and geometry of the Rikitake system". In: *J. Phys. A* 40.11, pp. 2755–2772. ISSN: 1751-8113. DOI: 10.1088/1751-8113/40/11/011. URL: https://doi.org/10.1088/1751-8113/40/11/011.

Yajima, Takahiro and Hiroyuki Nagahama (2020). "Connection structures of topological singularity in micromechanics from a viewpoint of generalized Finsler space". In: *Ann. Phys.* 532.12, pp. 2000306, 8. ISSN: 0003-3804. DOI: 10.1002/andp.202000306. URL: https://doi.org/10.1002/andp.202000306.

Yavari, Arash (2010). "A geometric theory of growth mechanics". In: *J. Nonlinear Sci.* 20.6, pp. 781–830. ISSN: 0938-8974. DOI: 10.1007/s00332-010-9073-y. URL: https://doi.org/10.1007/s00332-010-9073-y.

Yavari, Arash and Alain Goriely (2012a). "Riemann-Cartan geometry of nonlinear dislocation mechanics". In: *Arch. Ration. Mech. Anal.* 205.1, pp. 59–118. ISSN: 0003-9527. DOI: 10.1007/s00205-012-0500-0. URL: https://doi.org/10.1007/s00205-012-0500-0.

— (2012b). "Weyl geometry and the nonlinear mechanics of distributed point defects". In: *Proc. R. Soc. Lond. Ser. A Math. Phys. Eng. Sci.* 468.2148, pp. 3902–3922. ISSN: 1364-5021. DOI: 10.1098/rspa.2012.0342. URL: https://doi.org/10.1098/rspa.2012.0342.

— (2013). "Riemann-Cartan geometry of nonlinear disclination mechanics". In: *Math. Mech. Solids* 18.1, pp. 91–102. ISSN: 1081-2865. DOI: 10.1177/1081286511436137. URL: https://doi.org/10.1177/1081286511436137.

UNIVERSITÉ DE RENNES 1

Titre : Modèles géométriques et applications à des milieux matériels avec défauts.

Mots clés : Variétés de Riemann-Cartan, Structures fibrées, Connexions de Ehresmann, Milieux matériels défectueux, Micro-structures, Variétés de Weyl.

Résumé : Cette thèse porte sur l'étude de la modélisation mathématique d'un milieu matériel potentiellement défectueux dans le cadre de la géométrie différentielle. Il est couramment admis que la modélisation des milieux à défauts est étroitement en lien avec l'étude des variétés de Riemann-Cartan. Dans ce cadre, les tenseurs de torsion et de courbure sont interprétés comme des densités de dislocations et de disclinations. C'est la raison pour laquelle notre attention s'est concentrée sur la formulation de telles variétés mais aussi sur l'observation de l'évolution des défauts au cours d'une transformation.

Deux modèles sont présentés, ils sont basés sur une géométrie (de variétés) de Riemann Cartan associée à une variété de base ou à une structure de fibré. La seconde approche possède des caractéristiques plus avantageuses dans le sens ou elle permet d'inclure une large classe de matériaux en illustrant des phénomènes à plusieurs échelles. Comme, nous nous concentrons uniquement sur des transformations lisses de variétés lisses les modèles s'adaptent facilement à une exploitation numérique. C'est l'occasion d'étudier numériquement et théoriquement comment l'introduction d'un facteur d'échelle permet de tenir compte de l'influence de la micro-structure sur la macro-structure. Enfin nous montrerons comment ces théories motivent une nouvelle interaction entre les mathématiques et la mécanique.

Title : Geometric models and applications to material media with defects

Keywords : Riemann-Cartan geometries, Fiber bundles, Ehresmann connections, defective media, Microstructures, Weyl manifolds.

Abstract : This dissertation focuses on studying mathematical modeling of the material with defects in the framework of differential geometries. Since it has been recognized for a long time, the defective media closely connects with Riemann-Cartan manifolds. Torsion and curvature tensors are being interpreted as densities of dislocations and disclinations, respectively. Our attention is thus paid to establishing such manifolds and investigating the evolution of defects during a transformation.

The two proposed models are based on different geometrical backgrounds, saying Riemann-Cartan geometry and Fiber bundle geometry. These approaches concern new kinds of material transformations that encompass the microcontinuum theories. Besides we focus only on smooth fields rather than multivalued fields used in existing theories. It leads that the numerical and theoretical analyses are easier to handle. Especially, the influence of the micro and macro mechanics are taken into consideration as a whole by introducing a so-called scaling factor. Special attention is given to transport along a finite path in order to extend the standard infinitesimal analysis of torsion and curvature to a macroscopical point of view. Last, the present theories motivate several interesting problems in mathematics and mechanics.